

SYNTHESIS OF NOVEL PENDANT ARM
MACROCYCLIC LIGANDS AS
POTENTIAL MODELS FOR ENTEROBACTIN

by

BETH ROSANNE CAMERON
B.Sc., Saint Mary's University, 1988

A DISSERTATION SUBMITTED IN PARTIAL FULFILLMENT
OF THE REQUIREMENTS FOR THE DEGREE OF

ACCEPTED

FACULTY OF GRADUATE STUDIES

DOCTOR OF PHILOSOPHY

in the Department

of

Chemistry

DATE

DEAN

Sept 9/93

We accept this dissertation as conforming
to the required standard

Dr. A. McAuley

Dr. T. M. Fyles

Dr. G. A. Poulton

Dr. E. Van der Flier-Keller

Dr. R. Thompson

© BETH ROSANNE CAMERON, 1993

UNIVERSITY OF VICTORIA

All rights reserved. This dissertation may not be reproduced
in whole or in part, by mimeograph or other means,
without the permission of the author.

Supervisor: Professor Alexander McAuley

ABSTRACT

A series of pendant arm tris-catecholate macrocyclic ligands were synthesized. The first, based on 1,4,7-triaminopropyl-1,4,7-triazacyclononane, was prepared via condensation with 2,3-dimethoxybenzoyl chloride. The deprotection of the catechol moieties was achieved with boron tribromide in 80% yields. The ferric complexes were characterized by electronic absorption spectroscopy.

The second series of ligands described are based on the pendant arm macrocyclic ligand, 1,4,7-triaminoethyl-1,4,7-triazacyclononane. New routes to the preparation of this ligand were investigated; the best approach used chloroacetyl chloride as the reagent in functionalizing the nitrogen atoms of the triazacyclononane ring. The ligands, 1,4,7-tris-((2,3-dihydroxyphenethyl)aminoethyl)-1,4,7-triazacyclononane (**34**) and 1,4,7-tris-((2,3-dihydroxybenzyl)aminoethyl)-1,4,7-triazacyclononane (**36**) were prepared through a series of acid chloride condensation reactions, followed by reduction of the amides with diborane.

The mononuclear ferric complexes of compounds **34** and **36** were prepared and characterized by uv-visible spectroscopy. Mononuclear nickel, cobalt, and copper complexes of these ligands were also characterized by uv-visible spectroscopy. The binuclear complexes, $\text{Na}[\text{NiFe}(\mathbf{34})]$ and $\text{Na}[\text{NiFe}(\mathbf{36})]$, were

prepared and characterized by electronic absorption spectroscopy.

Tris-((2,3-dihydroxybenzylamino)ethyl)amine, tris-((2,3-dihydroxybenzoyl)aminoethyl)amine, and tris-((2,3-dihydroxyphenethyl)aminoethyl)amine were prepared by Schiff base condensation reactions, or acid chloride condensation of tris-(2-aminoethyl)amine and the appropriate catecholate moiety. The ferric complexes of these ligands were prepared and characterized by uv-visible spectroscopy. The Al(III) tris-((2,3-dihydroxybenzyl)aminoethyl)amine complex was examined by nmr spectroscopy. The Ni(II), Cu(II) and Co(III) complexes were investigated by electronic absorption spectroscopy.

The rates of base hydrolysis of $[\text{Co}(\text{tacn})(\text{en})\text{Cl}]^{2+}$ (tacn=1,4,7-triazacyclononane), $[\text{Co}(\text{tacn})(\text{amp})\text{Cl}]^{2+}$ (amp=2-aminomethylpyridine), $[\text{Co}(\text{tacn})(\text{tn})\text{Cl}]^{2+}$, ufac-I- $[\text{Co}(\text{dien})(\text{amp})\text{Cl}]^{2+}$ (dien=1,4,7-triazaheptane), ufac-II- $[\text{Co}(\text{dien})(\text{amp})]^{2+}$ and $[\text{Co}(\text{bicycloN}_5)\text{Cl}]^{2+}$ (bicycloN₅=1,5,8,12,15-pentaazabicyclo[10.5.2]nonadecane), were measured using stopped flow techniques. The base hydrolysis rates (k_{OH} , $\text{M}^{-1}\text{s}^{-1}$; [ionic strength (M)]) are 9.66 [0.1], 154 [0.1], 40.6 [0.1], 334 [0.1], 762 [0.1], and 3×10^3 [1.0], respectively.

The rate of $[\text{NCS}^-]$ anation of $[\text{Co}(\text{bicycloN}_5)(\text{OH}_2)]^{3+}$, and the rates of $[\text{Br}^-]$ and $[\text{NCS}^-]$ anation of $[\text{Co}(\text{tacn})(\text{en})(\text{OH}_2)]^{3+}$ were measured as a function of pH. The pK_a of the coordinated

water molecules are 3.8 ($[\text{Co}(\text{bicycloN}_5)(\text{OH}_2)]^{3+}$) and 6.5 ($[\text{Co}(\text{tacn})(\text{en})(\text{OH}_2)]^{3+}$). The anation rates increase as the pH increases, indicating a base catalysed anation reaction through the deprotonation of the coordinated amine. In the case of the $[\text{Co}(\text{tacn})(\text{en})(\text{OH}_2)]^{3+}$ complex, the rate increases as the pH increases until the pH ~ 7 , then there is no reaction after that point, suggesting some sort of blockage at the five-coordinate intermediate.

Examiners:

Dr. A. McAuley^U

Dr. T. M. Fyles

Dr. G. A. Poulton

Dr. E. Van der Flier-Keller

Dr. R. Thompson

TABLE OF CONTENTS

ABSTRACT	ii
TABLE OF CONTENTS	v
LIST OF TABLES	ix
LIST OF FIGURES	x
LIST OF SCHEMES	xii
LIST OF COMPOUNDS	xiii
LIST OF ABBREVIATIONS	xvi
ACKNOWLEDGEMENTS	xvii
DEDICATION	xviii
CHAPTER 1 INTRODUCTION	1
1.1 Coordination chemistry - history and background	2
1.2 Stability of coordination compounds	4
1.3 The chelate and macrocyclic effect	6
1.3.1 The chelate effect	6
1.3.2 The macrocyclic effect	9
1.4 Macrocyclic synthesis	12
1.5 Biological importance of macrocyclic compounds	16
1.6 Iron (III) sequestering agents	19
1.7 Synthetic analogues of enterobactin	24
1.8 Purpose	28
CHAPTER 2 EXPERIMENTAL METHODS	29
2.1 Synthesis of ligands, ligand precursors and transition metal complexes	30

	vi
2.1.1 1,4,7 - triazacyclononane	30
2.1.2 1,4,7-triaminopropyl-1,4,7- triazacyclononane	33
2.1.3 Taptacn - catecholate systems	36
2.1.4 Transition metal complexes of taptacn - catecholate systems	41
2.1.5 1,4,7-triaminoethyl-1,4,7- triazacyclononane	43
2.1.6 Taetacn - catecholate systems	48
2.1.7 Transition metal complexes of taetacn - catecholate systems	52
2.1.8 Tren - catecholate systems	56
2.1.9 Transition metal complexes of tren - catecholate systems	61
2.1.10 Macrobicycle synthesis	64
2.1.11 Co(III) pentammine complexes	69
2.2 Methods and Materials	71
2.2.1 Instrumentation	71
2.2.1.1 Spectroscopy	71
2.2.2.1 Materials	73
2.2.2.2 Kinetic methods	73
 CHAPTER 3 TAPTACN-CATECHOLATE SYSTEMS	 75
3.1 Ligand synthesis	76
3.1.1 1,4,7-Triazacyclononane	76
3.1.2 Taptacn	78

	vii
3.1.3 Taptacn-catecholate systems	80
3.2 Transition metal complexes	84
3.2.1 Ferric complexes	84
3.2.1.1 Synthesis	84
3.2.1.2 Electronic spectra	85
3.2.2 Nitrogen-coordinated metal complexes of taptacn-Me ₆ catecholates	89
3.2.3 Attempts at the preparation of taptacn- catecholate systems	92
 CHAPTER 4 TAETACN - CATECHOLATE SYSTEMS	 96
4.1 Ligand synthesis	97
4.1.1 1,4,7-triaminoethyl-1,4,7- triazacyclononane	97
4.1.2 Synthesis of taetacn - catecholates	105
4.2 Mononuclear transition metal complexes	110
4.2.1 Ferric complexes of 34 and 36	110
4.2.2 Nitrogen coordinated transition metal complexes of the taetacn - catecholates	110
4.3 Binuclear transition metal complexes	113
4.3.1 Synthesis	117
4.3.2 Electronic spectra	117
 CHAPTER 5 TREN - CATECHOLATE SYSTEMS	 119
5.1 Introduction	120
5.2 Ligand synthesis	122

5.2 Fe ^{III} and Al ^{III} complexes of tren - catecholate ligands	132
5.3.1 Electronic spectra, Fe(III) complexes	132
5.3.2 Al(44) ³⁻	133
5.4 Nitrogen coordinated transition metal complexes	135
 CHAPTER 6 BASE HYDROLYSIS AND ANATION REACTIONS OF CO ^{III} PENTAAMMINES	 138
6.1 Introduction	139
6.2 Results and discussion	146
6.2.1 Electronic absorption spectra	146
6.2.2 Stereochemical assignments	148
6.2.3 Base hydrolysis	151
6.2.4 Anation reactions	159
 CHAPTER 7 CONCLUSIONS AND SUGGESTIONS FOR FUTURE STUDIES	 170
 REFERENCES	 176

LIST OF TABLES

1.1 Thermodynamic contributions to the chelate effect	7
1.2 Calculated vs. observed $\log K_1$	9
1.3 Thermodynamic contributions to the macrocyclic effect in tetraaza macrocycles	11
3.1 Electronic spectra of ferric tris-catecholate complexes	87
3.2 Electronic absorption data for Cu(II) complexes	91
4.1 Electronic spectra of NiN_6^{2+} chromophores	113
4.2 Electronic spectra of Co and Cu taetacn-catecholates	115
4.3 Electronic absorption spectra of $[NiFe(34)]^{1-}$ and $[NiFe(36)]^{1-}$	118
5.1 1H NMR data for compounds 45 and 46	124
5.2 ^{13}C NMR data for compounds 42-44	128
5.3 1H NMR data for compounds 42-44	129
5.4 ^{13}C NMR data for compounds 47-49	131
5.5 Electronic absorption data of $Fe(44)^{3-}$, $Fe(46)^{3-}$ and $Fe(49)^{3-}$	133
5.6 Electronic absorption data of $Ni(43)^{2+}$, $Cu(43)^{2+}$ and $Co(43)^{3+}$ complexes	136
6.1 Volumes of activation for the base hydrolysis of $[Co(III)pentaammineCl]^{2+}$ complexes	141
6.2 Electronic absorption data for Co(III)pentaammine complexes	147
6.3 Observed rate constants for the base hydrolysis of some $[Co(III)chloropentaammine]^{2+}$ complexes	154
6.4 Second order rate constants for the base hydrolysis of $[Co(III)chloropentaammine]^{2+}$ complexes	158

LIST OF FIGURES

1.1 Classification of metal ions (Lewis acids)	5
1.2 Synthetic routes to the preparation of macrocycles	14
1.3 Functional groups found in siderophores	21
1.4 Ortep diagram of V(IV) (enterobactin) as viewed down the threefold axis	24
1.5 Some examples of synthetic analogues of enterobactin	26
3.1 Visible spectra of Fe(12) ³⁻	86
3.2 Visible spectra of Fe(14) ³⁻ and Fe(16) ³⁻	86
3.3 Energy level diagram for Fe(III) tris-catecholates	88
3.4 Visible spectra of compounds 17 and 18	90
3.5 ESR spectra of compounds 17 and 18	90
4.1 ¹³ C NMR of [Co(taetacn)][(ClO ₄) ₃] in D ₂ O	99
4.2 Retrosynthetic analysis of target molecule	101
4.3 Possible methods of functionalizing [9]-aneN ₃ pendant arms	104
4.4 ¹³ C NMR spectra of compounds 34 and 36	109
4.5 Electronic absorption spectra of Fe(34) ³⁻ and Fe(36) ³⁻	111
4.6 Electronic absorption spectra of Ni(33) ²⁺ and Ni(34) ²⁺	112
4.7 Definition of twist angle	114
5.1 ¹³ C NMR spectra of 45 and 46	125
5.2 ¹³ C NMR of compound 44 and Al(44) ³⁻	134
6.1 Inorganic substitution reaction mechanisms	140
6.2 Base hydrolysis rate constants (M ⁻¹ s ⁻¹) for various Co(III)pentaamines	144
6.3 Possible isomers of [Co(dien)(amp)Cl] ²⁺	149
6.4 ¹³ C NMR spectra of [Co(diammine)(triammine)Cl] ²⁺ complex ions in D ₂ O	150

6.5 Splitting of energy levels for Co(III) complexes	146
6.6 Base hydrolysis of $[\text{Co}(\text{tacn})(\text{en})\text{Cl}]^{2+}$ as a function of $[\text{OH}^-]$	153
6.7 Expected shape of the kinetic titration of the Co(III)pentaammine complexes studied	151
6.8 Kinetic titration plot of $\text{Co}(\text{bicycloN}_5)(\text{OH}_2)^{3+}$	162
6.9 Kinetic titration plot of $\text{Co}(\text{tacn})(\text{en})(\text{OH}_2)^{3+}$ + a) NCS^- and b) Br^-	162
6.10 Rate data for the azide-anation of $\text{Co}(\text{dien})(\text{dapo})(\text{OH}_2)^{3+}$	164
6.11 $[\text{SCN}^-]$ dependence on the rate of the $\text{Co}(\text{bicycloN}_5)(\text{OH}_2)^{3+}$ anation	165
6.12 $[\text{SCN}^-]$ dependence on the rate of the $\text{Co}(\text{tacn})(\text{en})(\text{OH}_2)^{3+}$ anation	167

LIST OF SCHEMES

3.1 Synthesis of 1,4,7-triazacyclononane	77
3.2 Synthesis of taptacn	79
3.3 Synthesis of compound 12	81
3.4 Synthesis of compound 14	82
3.5 Synthesis of compound 16	83
4.1 Preparation of taetacn	98
4.2 Alternate methods of preparing taetacn	100
4.3 Synthetic route to compound 34	107
4.4 Synthetic route to compound 36	108
5.1 Synthetic route to the preparation of trencam (46)	123
5.2 Synthetic route to compound 44	127
5.3 Synthetic route to compound 49	130
6.2 Reaction mechanism for azide anation of Co(dien)(dapo)(OH ₂) ³⁺	164
6.3 Reaction mechanism for the [NCS ⁻] anation of Co(bicycloN ₅)(OH ₂) ³⁺	166
6.4 Possible reaction mechanism for the [NCS ⁻] anation of Co(tacn)(en)(OH ₂) ³⁺	168

LIST OF COMPOUNDS

- (1) Diethylene-1,4,7-triaminetritosylate
- (2) Ethylene glycol ditosylate
- (3) 1,4,7-Triazacyclononanetritosylate
- (4) 1,4,7-Triazacyclononane.3HCl
- (5) 1,4,7-Triazacyclononane
- (6) 1,4,7-Tricyanoethyl-1,4,7-triazacyclononane
- (7) 1,4,7-Triaminopropyl-1,4,7-triazacyclononane
- (8) Nickel 1,4,7-triaminopropyl-1,4,7-triazacyclononane perchlorate
- (9) 1,4,7-Triaminopropyl-1,4,7-triazacyclononane
- (10) 2,3-Dimethoxybenzoyl chloride
- (11) 1,4,7-Tris-((2,3-dimethoxybenzoyl)aminopropyl)-1,4,7-triazacyclononane
- (12) 1,4,7-Tris-((2,3-dihydroxybenzoyl)aminopropyl)-1,4,7-triazacyclononane.6HBr
- (13) 1,4,7-Tris-((2,3-dimethoxybenzyl)aminopropyl)-1,4,7-triazacyclononane
- (14) 1,4,7-Tris-((2,3-dihydroxybenzyl)aminopropyl)-1,4,7-triazacyclononane.6HBr
- (15) 3,4-Dioxosulfonophenylacetyl chloride
- (16) 1,4,7-Tris-((3,4-dihydroxyphenylacetyl)aminopropyl)-1,4,7-triazacyclononane
- (17,18) [Cu(13)][(ClO₄)₂]
- (19) [Ni(13)][(ClO₄)₂]
- (20) [Co(13)][(OAc)₂]
- (21) K₃[Fe(12)]
- (22) K₃[Fe(14)]
- (23) K₃[Fe(16)]

- (24) Phthalimidoacetaldehyde
- (25) 1,4,7-Tris-(phthalimidoacetyl)-1,4,7-triazacyclononane
- (26) 1,4,7-Triaminoethyl-1,4,7-triazacyclononane.6HBr
- (27) [Co(26)][(ClO₄)₃]
- (28) 1,4,7-triazacyclononane-1,4,7-triacetic acid
- (29) 1,4,7-trioxoethylchloro-1,4,7-triazacyclononane
- (30) 1,4,7-trioxoaminoethyl-1,4,7-triazacyclononane
- (31) Tris-1,4,7-((2,3-dimethoxyphenylacetyl)oxoaminoethyl)-1,4,7-triazacyclononane
- (32) Tris-1,4,7-((2,3-dimethoxybenzoyl)oxoaminoethyl)-1,4,7-triazacyclononane
- (33) 1,4,7-Tris-((2,3-dimethoxyphenethyl)aminoethyl)-1,4,7-triazacyclononane
- (34) 1,4,7-Tris-((2,3-dihydroxyphenethyl)aminoethyl)-1,4,7-triazacyclononane.6HBr
- (35) 1,4,7-Tris-((2,3-dimethoxybenzyl)aminoethyl)-1,4,7-triazacyclononane
- (36) 1,4,7-Tris-((2,3-dihydroxybenzyl)aminoethyl)-1,4,7-triazacyclononane
- (37) [Cu(33)][(ClO₄)₂]
- (38) Na[CuFe(34)]
- (39) Na[NiFe(34)]
- (40) [CoFe(34)]
- (41) Na₃[Fe(34)]
- (42) Tris-((2,3-dimethoxybenzylideneamino)ethyl)amine
- (43) Tris((2,3-dimethoxybenzylamino)ethyl)amine
- (44) Tris((2,3-dihydroxybenzylamino)ethyl)amine
- (45) Tris-((2,3-dimethoxybenzoylamino)ethyl)amine
- (46) Tris-((2,3-dihydroxybenzoylamino)ethyl)amine.4HBr

- (47) Tris-((2,3-dimethoxyphenylacetyl amino) ethyl) amine
- (48) Tris-((2,3-dimethoxyphenethyl amino) ethyl) amine
- (49) Tris-((2,3-dihydroxyphenethyl amino) ethyl) amine. 4HBr
- (50) [Co(43)] [(ClO₄)₃]
- (51) [Ni(43)] [(ClO₄)₂]
- (52) [Cu(43)] [(ClO₄)₂]
- (53) K₃[Fe(44)]
- (54) K₃[Al(44)]
- (55) K₃[Fe(46)]
- (56) K₃[Al(46)]
- (57) K₃[Fe(49)]
- (58) 1,4-Diaminopropyl-1,4,7-triazacyclononane
- (59) [Cu(58)] [(ClO₄)₂]
- (60) [Cu(61)] [(ClO₄)₂]
- (61) 1,5,8,12,15-Pentaazabicyclo[10.5.2]nonadecane
- (62) [Cu(9)] [(ClO₄)₂]
- (63) [Cu(64)] [(ClO₄)₂]
- (64) 15-Aminopropylaza-1,5,8,12-tetraazabicyclo[10.5.2]nonadecane
- (65) [CoCl(tacn)(en)] [ZnCl₄]
- (66) [CoCl(tacn)(tn)] [ZnCl₄]
- (67) [CoCl(tacn)(amp)] [ZnCl₄]
- (68,69,70) [CoCl(dien)(amp)] [ZnCl₄]
- (71) [CoCl(bicycloN₅)] [ZnCl₄]

LIST OF ABBREVIATIONS

[9]-aneN ₃	1,4,7-triazacyclononane
taen	1,4,7-triazacyclononane
cyclam	1,4,8,11-tetraazacyclotetradecane
taptacn	1,4,7-triaminopropyl-1,4,7-triazacyclononane
trén	tris-(2-aminoethyl) amine
trenam	tris-((2,3-dihydroxybenzoyl) aminoethyl) amine
bicyclon ₅	1,5,8,12,15-pentaazabicyclo[10.5.2]nonadecane
bicyclon ₆	15-aminoazapropyl-1,5,8,12-tetraazabicyclo [10.5.2]nonadecane
dien	1,4,7-triazaheptane
en	1,2-diaminoethane
tn	1,3-diaminopropane
amp	2-aminomethylpyridine
sar	3,6,10,13,16,19-hexaazabicyclo[6.6.6]- eicosane
sep	1,3,6,8,10,13,16-octaazabicyclo[6.6.6]- eicosane
dtne	1,2-bis(1,4,7-triaza-1-cyclononyl)-ethane
LAH	lithium aluminum hydride
NEt ₃	triethylamine
mNBA	meta-nitrobenzylalcohol
FAB	fast atom bombardment
TLC	thin layer chromatography

ACKNOWLEDGEMENTS

I would like to thank my supervisor, Dr. McAuley, for his encouragement, patience, and guidance throughout the course of this project. The members of the group are acknowledged, S. Chandrasekhar, B. Chak, K. Coulter, S. Subramanian, T. Whitcombe, and C. Xu. Their assistance was extremely helpful. I would like to thank Dr. Don House for his help with the kinetic studies. Mrs. C. Greenwood is acknowledged for her help with the nmr spectroscopy. The receipt of funding through a University of Victoria fellowship and through a post-graduate scholarship from NSERC is also acknowledged.

I would like to thank my family for their support, especially my sister, Lynn Cameron, whose help is greatly appreciated.

To the memory of my late brother,

Donald Raymond Cameron

CHAPTER 1
INTRODUCTION

1.1 Coordination chemistry - history and background

The modern study of coordination compounds begins with two men, Alfred Werner (1866-1919) and S. M. Jørgensen (1837-1914)¹. Although the two had completely different fundamental views of their observations, they served as protagonists; pursuing independently extensive studies to augment their ideas. Albeit, they were not the first chemists to observe these coordination "complexes". As early as 1597, Libavius noted the formation of a deep blue ion now known as $\text{Cu}(\text{NH}_3)_4\text{X}_2^{2-}$. In 1798 Tasselt observed the formation of an orange compound on the reaction of a cobalt salt with ammonia³, $(\text{Co}(\text{NH}_3)_6\text{X}_3)$.

It was Alfred Werner, however, who first established the structural basis for coordination chemistry. His contributions were two-fold; he first noted that the bonds to the ligands were fixed in space and could therefore be treated by structural principles. He also noted that there exists a constant coordination number of six for the series of cobalt compounds;

	<u>color</u>	<u>early name</u>
$\text{CoCl}_3 \cdot 6\text{NH}_3$	yellow	Luteo
$\text{CoCl}_3 \cdot 5\text{NH}_3$	purple	purpureo
$\text{CoCl}_3 \cdot 4\text{NH}_3$	green	praseo

This led to his suggestion of an octahedral geometry (now accepted for nearly all six coordinate complexes), and that anions or neutral molecules occupy the coordination sites at

the corners of the octahedron. The complexes can properly be formulated as $[\text{Co}(\text{NH}_3)_6]^{3+}[\text{Cl}_3]^-$, $[\text{Co}(\text{NH}_3)_5(\text{Cl})]^{2+}[\text{Cl}_2]^-$, $[\text{Co}(\text{NH}_3)_4(\text{Cl}_2)]^+[\text{Cl}]^-$.

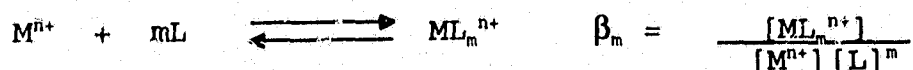
Following Werner's stereochemical studies were the bonding theories. The fact that a chemical bond required a shared pair of electrons led to the idea that a Lewis base (ligand) could donate its electron pair to a Lewis acid (the metal ion). The valence bond theory of Linus Pauling⁴, related to the hybridization and geometry of non-complex compounds, was the first successful application of bonding theory to coordination compounds. Previous to Pauling's valence bond theory, Bethe⁵ and Van Vleck⁶ proposed the crystal field theory (CFT), although the pioneering work of these physicists was not utilized by chemists until some twenty years later.

Just as the CFT replaced the valence bond theory in treating coordination compounds, the molecular orbital theory has largely replaced CFT. It was pointed out as early as 1935⁶ that the CFT and the valence bond theory were simplified approaches to the molecular orbital theory of Mülliken⁷. Ligand field theory, the most comprehensive approach to coordination compounds is a combination of the ideas of Bethe and Van Vleck and Mülliken - it is the same as pure crystal field theory except that covalent character is considered when necessary².

1.2 Stability of coordination compounds

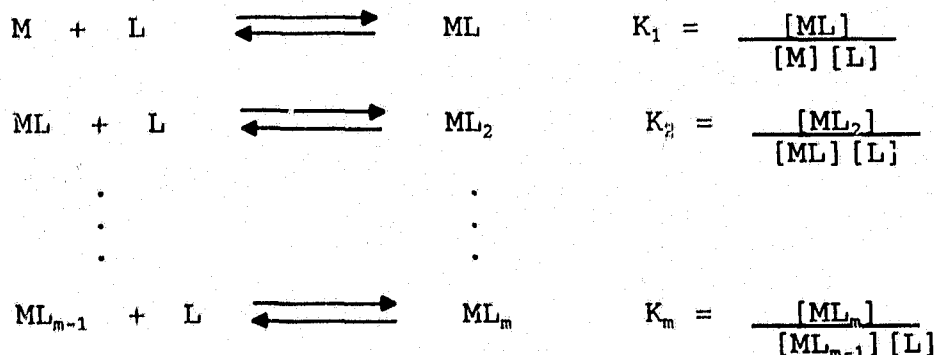
The general properties of metal ions and ligands that contribute to their stability are identified most clearly by the ligand field approach.

The stability of a metal complex is generally expressed in terms of a formation constant, β_m , for the reaction;



This is an expression of the thermodynamic stability since it is an equilibrium constant from which a free energy change for the formation of the complex can be calculated.

A series of stepwise equilibrium constants describes the formation of a complex with unidentate ligands;



where the overall formation constant is related to the stepwise formation constant by,

$$\beta_m = K_1 K_2 \dots K_m$$

In general, an increase in the basicity of a ligand or in

the most stable complexes with ligands in the second period (N,O) whereas class (b) acceptors form the most stable complexes with ligands from a third period or later. It is important to point out that the borderline regions are not well defined, as Cu(I) is a class (b) acceptor but Cu(II) remains in the borderline region.

An analogous classification of ligands (donors) and metals (acceptors) was proposed as the Pearson hard-soft-acid-base (HSAB) model⁹, where he coined the class (a) acceptors as "hard" and the class (b) acceptors are termed "soft". As a general rule, hard acids prefer to complex hard bases and soft acids prefer to bind soft bases.

1.3 The chelate and macrocyclic effect

The chelate¹⁰, macrocyclic¹¹ and cryptand¹² effects play an important role in coordination chemistry in that they permit the design of ligands with enhanced complex stability and metal ion selectivity. When considering the stabilities of complexes, it is in general the change in free energy;

$$\Delta G = -RT \log \beta_n$$

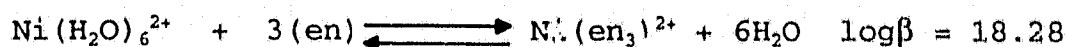
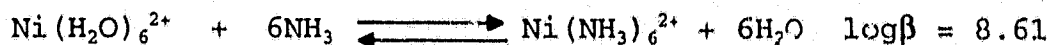
$$\Delta G = \Delta H - T\Delta S$$

The thermodynamic stabilities may arise from enthalpy effects, entropy effects or a combination of both.

1.3.1 The chelate effect

The term "chelate effect" refers to the enhanced stability of a complex containing chelate rings when compared

to the stability of a system with unidentate ligands (no chelate rings). A useful comparison is that of the Ni(II) complexes of NH_3 and ethylenediamine (en);



The thermodynamic contributions to the chelate effect are given in Table 1.1¹³. It is shown that there is both a favorable enthalpy contribution and a favorable entropic contribution.

Table 1.1 Thermodynamic contributions to the chelate effect.

Complex	ΔG	ΔH	ΔS
$[\text{Ni}(\text{NH}_3)_6]^{2+}$	-12.39	-24	-39
$[\text{Ni}(\text{en})_3]^{2+}$	-24.16	-28.0	-10
chelate effect ^a	$\Delta G^* = -11.77$	$\Delta H^* = -4$	$\Delta S^* = 29$

a. The thermodynamic manifestation of the chelate effect, such that $\Delta G^* = \Delta G(\text{en complex}) - \Delta G(\text{NH}_3 \text{ complex})$.

The origins of the enthalpic contributions to the chelate effect are manifested in the ligand field stabilization energy (LFSE), although it does not account for the whole of the

chelate enthalpy. Perhaps this is only because $10D_q$ does not account for all of the overlap in the metal-nitrogen bonds but only those from the t_{2g} and e_g energy levels¹³.

Schwarzenbach¹⁰ considers the entropic origins of the chelate effect to arise since once one donor atom of a chelating ligand has been attached to a metal ion, the second donor atom is constrained to move in a reduced volume compared to that for the unidentate system. The chelate effect is largely due to an increase in translational entropy.

A simple approach to the chelate effect, by Adamson¹⁴, is expressed for an n-dentate polydentate ligand as,

$$\log K_1(\text{polydentate}) = \log \beta_n(\text{unidentate}) + (n-1)\log 55.5$$

This equation leads to values of K_1 that are too low for the polyamines. Hancock and Martell¹³ have corrected for the "intrinsic basicity factor" ($1.152 = pK_a(\text{CH}_3\text{NH}_2)/pK_a(\text{NH}_3)$) leading to the equation,

$$\log K_1(\text{polyamine}) = 1.152 \log \beta_n(\text{NH}_3) + (n-1)\log 55.5$$

which is a very good prediction of the formation constants for polyamine ligands as shown in Table 1.2.

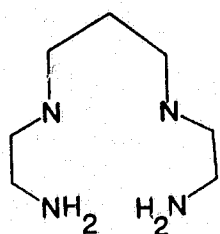
Table 1.2 Calculated vs. Observed $\log K_1$

	Ni(en)	Ni(dien)	Ni(trien)	Ni(tetren)
$\log K_1(\text{calc})$	7.6	11.0	14.1	17.3
$\log K_1(\text{obs})$	7.4	11.0	14.0	17.4

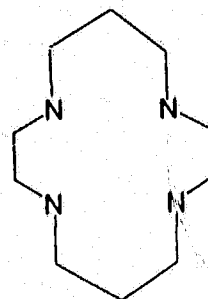
1.3.2 The macrocyclic effect

The consideration of the macrocyclic effect compares the complex stability of a metal ion with a macrocyclic ligand and that of the open chain analogue. The term was first introduced by Cabbiness and Margerum¹¹, since their results could not be explained completely by the chelate effect. Since there are the same number of molecules on both sides of the equilibrium there are no translational entropic effects.

A typical comparison of stability constants of metal complexes with 2,3,2-tet and cyclam is a good representation of the macrocyclic effect.



2,3,2-tet



cyclam

In Table 1.3 the thermodynamic contributions to the macrocyclic effect are presented.

In general, enthalpy makes the major contribution to the macrocyclic effect. Important contributions to the macrocyclic effect are listed as;

- (1) preorganization of the ligand
- (2) desolvation of the donor atoms in the confined space of the macrocyclic cavity
- (3) intrinsic basicity effects
- (4) dipole-dipole repulsion in the cavity of the ligand

The first contribution, namely preorganization of the ligand as suggested by Cram¹⁵, groups the effects of prestraining, preorienting and multiple juxtapositional fixedness (first suggested by Busch¹⁶). Only in the simplest sense does preorganization refer to the ligand being in a suitable conformation for complexation.

The three effects, namely preorganization, solvation and dipole-dipole repulsion, lead to a high energy state of the macrocycle which is relieved on complex formation.

The "intrinsic basicity effects" arise from the greater basicity of the donor atoms along the series, zeroth (NH_3) < primary (RNH_2) < secondary (R_2NH) < tertiary (R_3N). The electron donating properties of the alkyl groups, R, lead to a greater basicity of the donor atoms. In a cyclic ring, the effect is enhanced with the ethylene bridges between the donor atoms. If the amines are changed from primary to secondary in

the open chain analogue there is a steric penalty incurred by the ligand, whereas the macrocyclic structure can employ the effect. If, however, the macrocyclic donor atoms are made tertiary in nature, there is steric repulsion between the bulky alkyl groups which is reflected in the lower formation constants.

Table 1.3 Thermodynamic contributions to the macrocyclic effect in tetra-aza macrocycles¹³

		Cu(II)	Ni(II)	Zn(II)
log	cyclam	26.5	19.4	15.5
K ₁	2,3,2-tet	<u>23.2</u>	<u>15.9</u>	<u>12.6</u>
	logK (mac)	3.3	3.5	2.9
ΔH	cyclam	-32.4	-24.1	-14.8
kcal	2,3,2-tet	<u>-27.7</u>	<u>-18.6</u>	<u>-11.9</u>
mol ⁻¹	ΔH (mac)	-4.7	-5.5	-2.9
ΔS	cyclam	13	8	21
caldeg	2,3,2-tet	<u>13</u>	<u>10</u>	<u>18</u>
mol ⁻¹	ΔS (mac)	0	-2	3

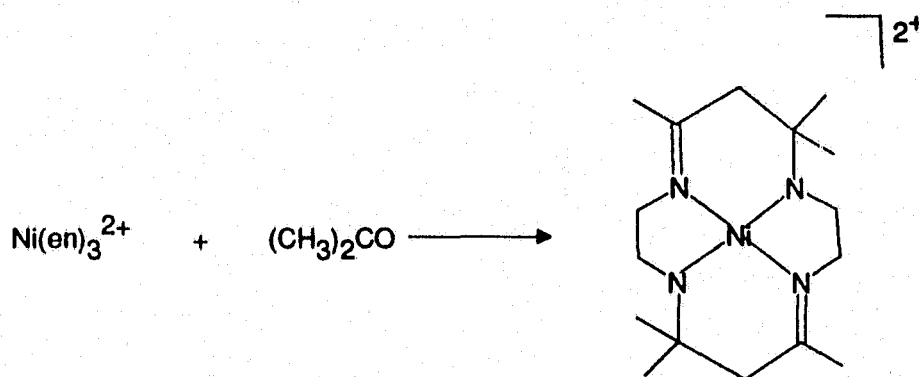
In summary, it is evident that the macrocyclic effect is predominately enthalpic in origin, with entropic effects

contributing to a minor extent - sometimes making an unfavorable contribution.

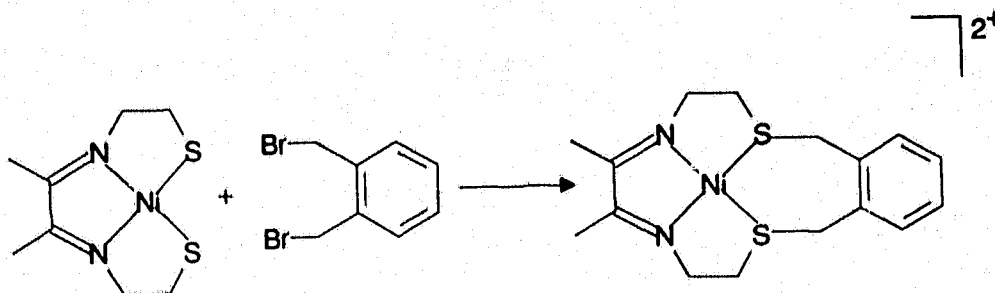
1.4 Macrocyclic synthesis

A macrocyclic compound has been defined¹⁷ as "a cyclic compound with nine or more members (including all hetero atoms) and with three or more donor (ligating) atoms".

The first macrocyclic compound was prepared serendipitously by Curtis¹⁸ when he attempted to recrystallize $[\text{Ni}(\text{en})_3][(\text{ClO}_4)_2]$ from acetone. The result was the formation of a macrocyclic complex;



The first rational synthesis was reported by Thompson and Busch¹⁹, who prepared the mixed donor macrocyclic complex;



In general, the synthetic route to preparing macrocycles is in one of three ways:

- (1) conventional organic synthesis (high dilution method)
- (2) template method
- (3) Richman-Atkins method

These are compared in Figure 1.2 for the synthesis of cyclam.

The high dilution method usually results in low yields and is dependent not on the amount of solvent used, but on the rate of addition of the reactants. The optimum rate is such that a steady concentration of the reactants is established so that the rate of introduction is the same as the rate of reaction to result in the optimum yield of the target molecule.

The template method (a metal ion mediated reaction) results in higher yields, however, it is usually specific for only one reaction. The origins of the template effect may be either thermodynamic or kinetic. If it is the directive influence of the metal ion which controls the steric course of a sequence of stepwise reactions, then the kinetic template effect is operative. In the thermodynamic template effect, the metal ion perturbs an existing equilibrium in an organic system and the macrocycle is produced¹⁷.

The tosylate method of Richman and Atkins²² generally results in reasonable yields for the synthesis of macrocycles. A series of N-tosylated macrocycles has been prepared by this

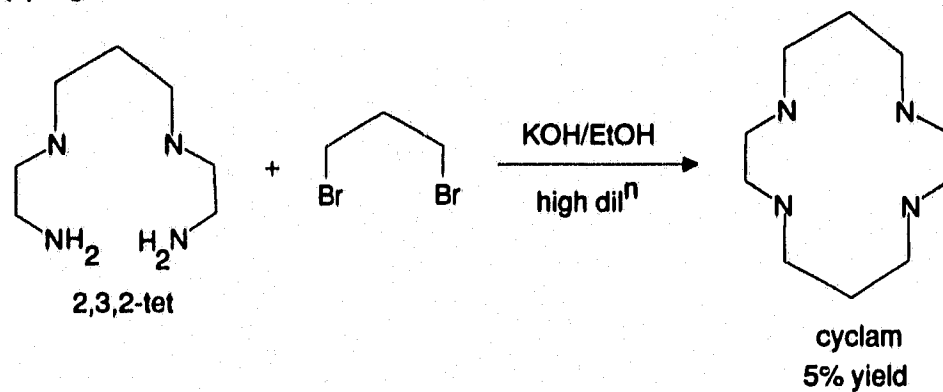
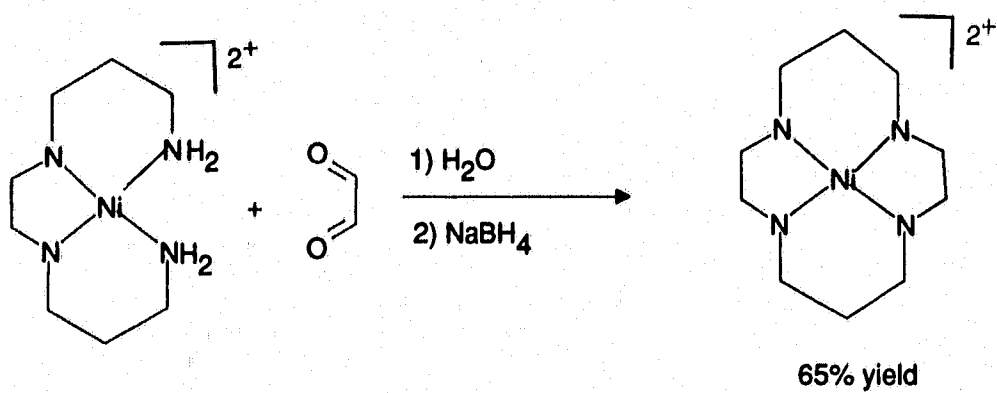
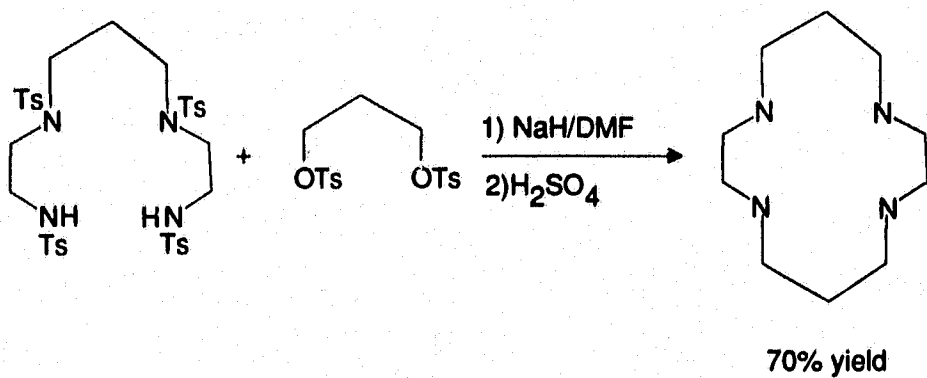
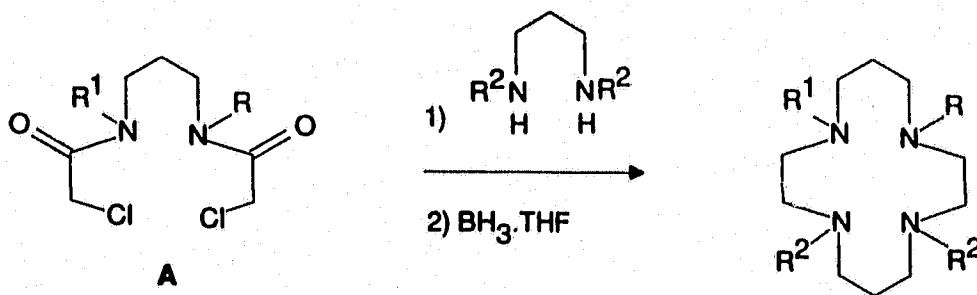
(1) High dilution method²⁰(2) Template synthesis²¹(3) Richman/Atkins method²²

Figure 1.2 Synthetic routes to the preparation of macrocycles.

method. Problems may arise, however, in the desosylation step, especially when the macrocycle contains mixed donor atoms.

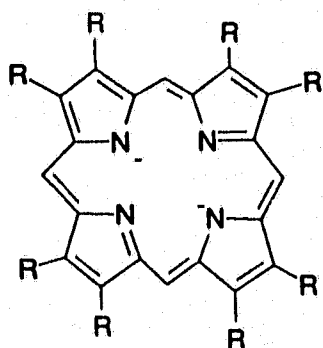
A fourth method of macrocyclization which deserves mention is that of Bradshaw et al.²⁴⁻²⁷ The authors have successfully prepared several poly-aza crowns and substituted cyclams using a "crab-like" cyclization procedure²⁵;



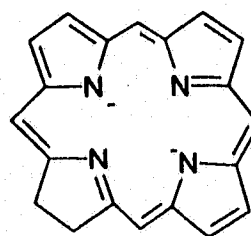
The starting material, **A**, is prepared from the reaction of chloroacetyl chloride with the appropriate amine to form the α -chloroamide. These are very reactive and poised in the proper position for cyclization, resembling a crab - hence the term "crab-like". These cyclization reactions eliminate the need for high dilution conditions and generally result in yields of 40-60%.

1.5 Biological importance of macrocyclic compounds

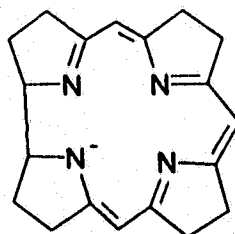
Perhaps the most common biological macrocyclic compound is the porphyrin ring of the iron containing haemoglobin. These compounds provide the fundamental basis for O_2 transport in mammalian respiratory systems and are related to the chlorin magnesium complexes of chlorophyll and the cobalt corrin complexes in vitamin B_{12} ²⁸.



porphyrin ring

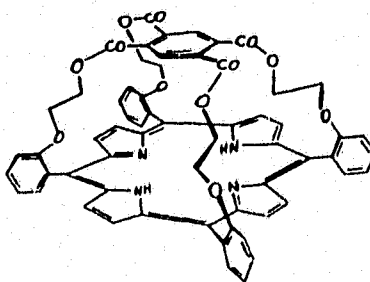
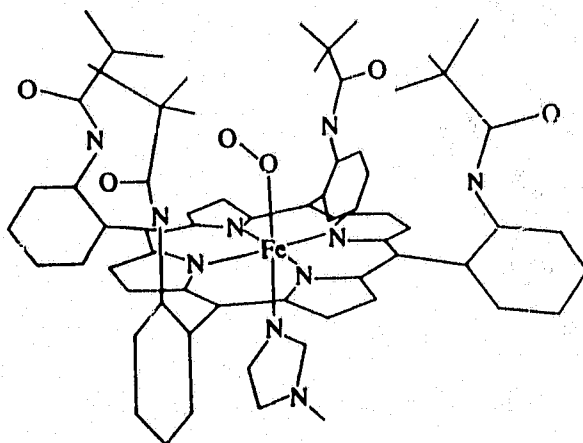


chlorin



corrin

The study of metal complexes of these compounds has provided insight into the structural requirements and mechanistic aspects of these biologically important compounds. For instance, several synthetic porphyrins such as the picket fence²⁹ and capped³⁰ porphyrins (shown below) have been prepared to examine both the structural aspects and to provide information on the reversible binding to O₂.



These model compounds eliminate the extraneous factors in the natural haemoglobin and allow investigation of the important features of the molecule.

It is not surprising that nature has chosen macrocycles as the basis of important biological functions. They provide kinetic and thermodynamic stability, stabilize less common oxidation states and effectively result in greater ligand field strengths when compared with the open chain analogues.

The stabilities of macrocyclic complexes have been discussed previously (section 1.3).

It has long been recognized that macrocycles can stabilize unusual oxidation states of metal ions. For example, in 1967, Curtis³¹ discovered that Ni(II) complexes of cyclic tetramines were oxidized in nitric acid to give Ni(III) complexes. Since then, the generation of a number of complexes exhibiting different oxidation states have been prepared. For instance, Ni(I) and Ni(III)³², Cu(I) and Cu(III)³³, and Co(I)³⁴ have all been electrochemically generated. Pt(III)³⁵ and Pd(III)³⁶ complexes of the bis [9]-aneS₃ or [9]-aneN₃ have been reported.

The high formation constant lowers the $E_{1/2}$ value;

$$E_{1/2} = E^{\circ} - \frac{RT \ln K}{nF}$$

and the increased ligand field strength raises the energy of the electrons in the antibonding orbitals, facilitating their

removal thus lowering the potential of higher oxidation states. Kinetically, the metal ion is trapped in the macrocyclic framework, so that reaction with reducing agents (in the case of higher oxidation states) or oxidizing agents (in the case of lower oxidation states) is reduced, resulting in a longer lifetime of the less common oxidation state.

The geometry of the macrocyclic complexes is also an important feature relative to their use as models for biological compounds. The "entatic"³⁷ state of metalloenzymes reflects the importance of structure in their functions. The constrictive geometry of some macrocycles enforced on the metal ion centre contributes to the stabilization of unusual oxidation states by lowering the necessary reorganization energy for these changes.

1.6 Iron (III) sequestering agents

Iron is an essential element for virtually all living organisms, thus it is probably considered the most important transition metal in biological systems. Associated with a variety of metabolic processes, its key functions involve oxidation/reduction and interactions with O₂.

A fact that is somewhat less appreciated by the public and scientific communities is that in excess, iron is toxic. Acute iron overload is a major form of poisoning in children, and chronic iron overload (hemachromatosis) is a condition developed in the transfusional treatment of Cooley's anemia³⁸.

The continuous buildup of iron in the body leads to death due to hemosiderosis.

In general there are two ways to treat metal ion toxicity. The first involves the administration of a similar but less toxic metal, leading to excretion of the toxic one. Essentially, this is a metal ion exchange reaction and has not had much clinical success. The second method is a ligand exchange reaction where a chelating agent is administered *in vivo*, which binds to the toxic metal ion and ultimately results in its excretion. The important factors governing the effectiveness of a chelating agent in removing the toxic metal ions have been reviewed^{39,40}, and will not be discussed further here.

Although iron is a vital element to living organisms, and despite the fact that it is one of the most abundant elements on the earth, it exists solely as the $\text{Fe}_2\text{O}_3 \cdot n\text{H}_2\text{O}$ insoluble salt in our oxidizing atmosphere. The amount of soluble iron in this polymeric species is only about 10^{-18}M , making its uptake extremely difficult.

Microorganisms respond to this challenge with the excretion of low molecular weight ferric ion chelating agents, which have been termed as siderophores after the Greek term meaning "iron carrier"⁴¹. First discovered over forty years ago⁴², there are now over eighty siderophores isolated. Essentially they are classic coordination compounds containing polydentate groups. Examples of the types of chelating

moieties are shown in Figure 1.3.

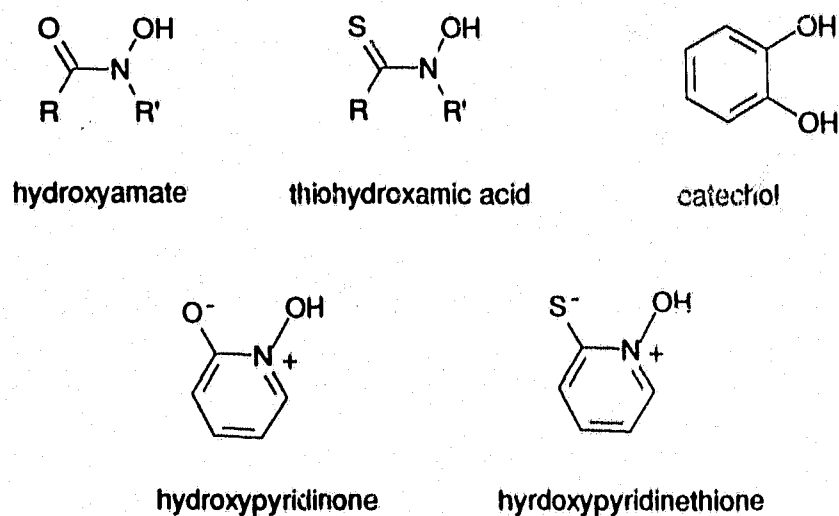
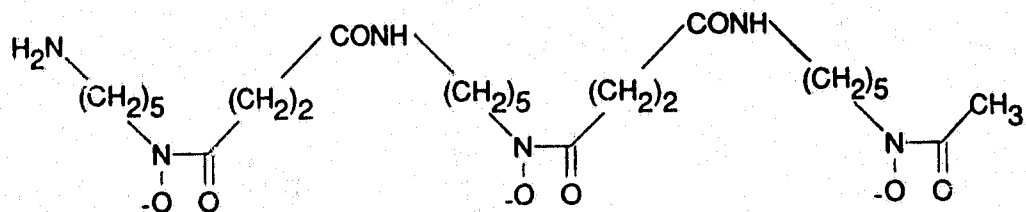


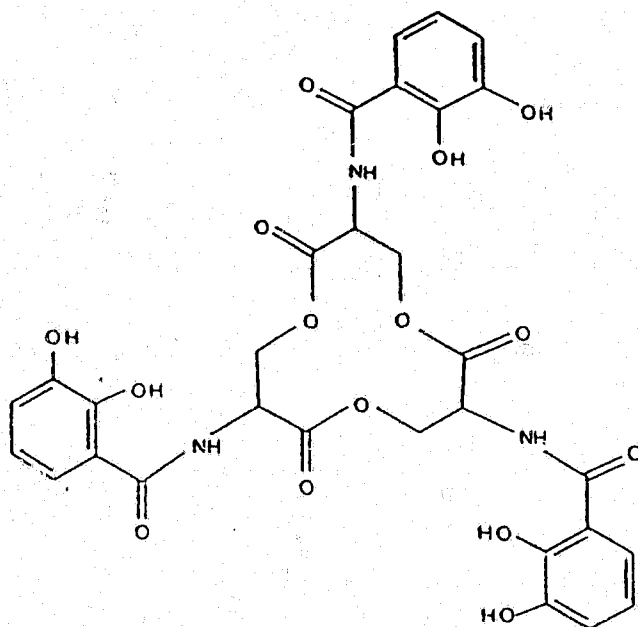
Figure 1.3 Functional groups found in siderophores.

The most commonly encountered functional groups are the hydroxamate and the catecholate, while the thiohydroxamic acid and the hydroxypyridinones are less common. Hydroxypyridinethione is not found in nature, but is considered a thio derivative of the hydroxypyridonate.

Naturally occurring siderophores include deferriferrioxamine B, shown below;



and enterobactin:



On deprotonation, the chelating groups contain hard oxygen anions which form stable complexes with hard Lewis acids such as Fe(III), Al(III), and Pu(IV).

Enterobactin is the most powerful Fe(III) sequestering agent ($K \sim 10^{49}$). The important structural features of enterobactin are the cyclic triester backbone, the amide linkage and the three catecholate groups. The three catecholate moieties form five membered chelate rings with Fe(III) resulting in a six coordinate complex. The cyclic triester backbone is hydrolytically unstable and this instability is linked to the iron release mechanism. The amide linkage is an important structural feature owing to hydrogen bonding between the amide hydrogen and the catecholate oxygen which contributes to the high thermodynamic stability⁴⁴.

Although enterobactin was first isolated over twenty years ago⁴⁵, the first structural characterization of a metal complex only appeared within the last year^{46,47}. The vanadium (IV) enterobactin complex, shown in Figure 1.4⁴⁷, was found to have approximate C_3 symmetry with the geometry being intermediate between octahedral and trigonal prismatic (twist angle = 28°). The authors indicate the importance of the backbone and the hydrogen bonding of the catecholamides in enhancing the stability constant when compared to synthetic analogues.

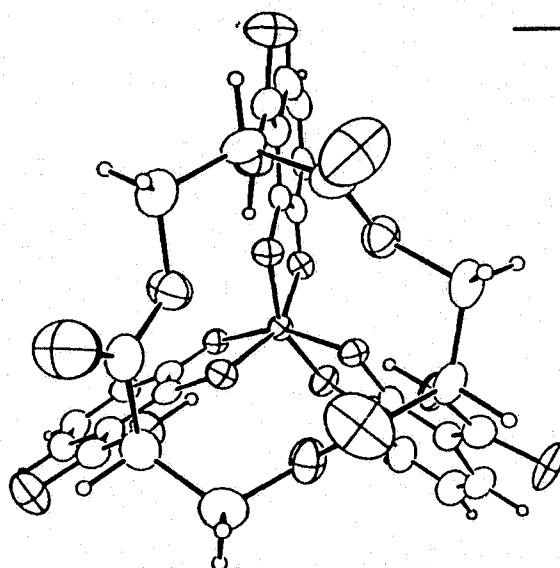


Figure 1.4⁴⁷ Ortep diagram of V(IV) enterobactin as viewed down the threefold axis.

1.7 Synthetic analogues of enterobactin

The discovery of enterobactin has prompted research in the design of artificial sequestering agents. The potential clinical uses of such analogues are numerous. Fe(III) sequestering agents can aid in the treatment of Cooley's anemia⁴⁸ or other related iron overload diseases. If four catecholate groups are incorporated into the ligand, it has potential use of plutonium removal⁴⁹⁻⁵¹ in patients with toxic levels of plutonium from exposure to nuclear reactors. The association of aluminum with Alzheimer's disease reflects the need for aluminum specific chelating agents⁴⁰. Also, with the onset of nuclear magnetic resonance imaging, chelators for ⁶⁷Ga, ¹¹¹In, and ^{99m}Tc are necessary to transport the

radionucleotide to the target organ.

The enterobactin analogues and derivatives are good candidates for these purposes since they form highly stable complexes with the cations.

Since its discovery, a number of synthetic analogues of enterobactin have been prepared^{38,41,52-54}. These include the podand⁵⁶ type ligands and the macrobicycles⁵⁵ based on tren of Raymond and coworkers, the mesitylate based macrobicycles of Vögtle *et al.*^{54,57}, the cyclodextrin based Fe(III) chelator of Coleman *et al.*⁵³ and the chiral derivatives of Shanzer *et al.*⁵². A representation of these analogues is given in Figure 1.5.

Enterobactin is still the best known ferric ion chelator ($K \sim 10^{49}$)⁵⁸, the closest synthetic sequestering agent being 1,3,5-tris-(2,3-dihydroxybenzoylaminomethyl)benzene (MECAM), with a formation constant of $K \sim 10^{45.8,59}$. Since the high stability constant is not the only concern in the design of therapeutic chelating agents, other analogues, such as the TRENCAMS, are still being prepared.

Raymond and coworkers have undertaken detailed solution⁵⁸ and structural^{60,61} analysis of enterobactin and synthetic analogues to provide insight on the important features for iron uptake. Interestingly, they have found that the geometry

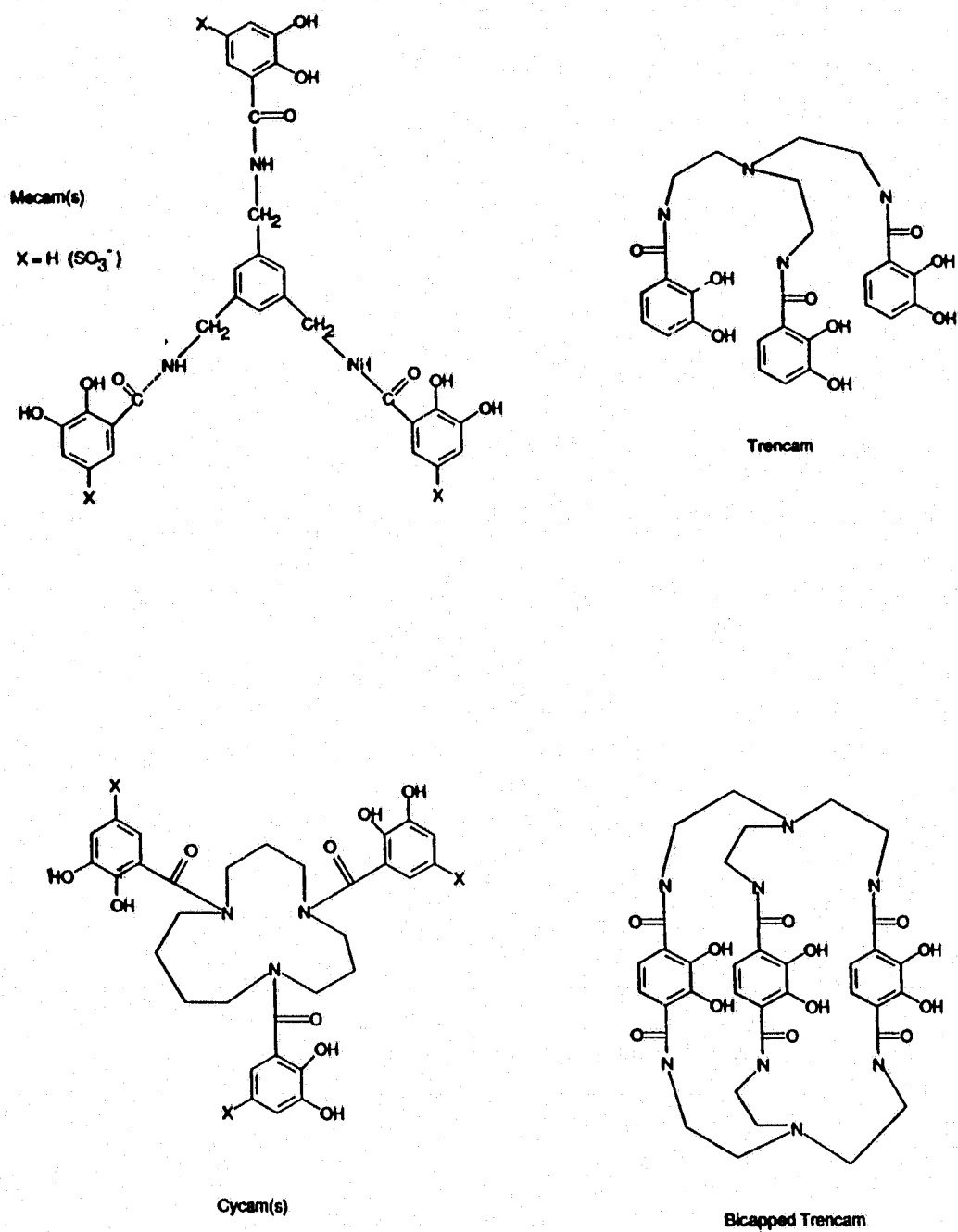


Figure 1.5 Some examples of synthetic analogues of enterobactin.

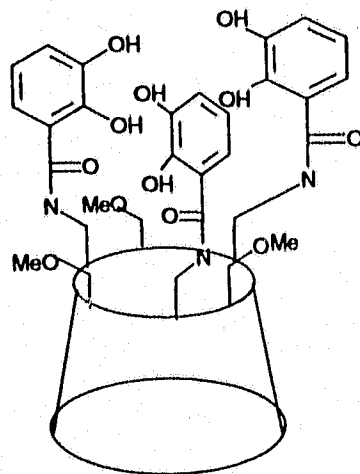
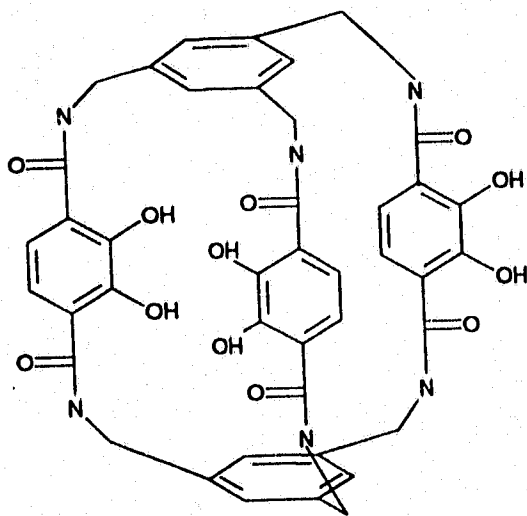
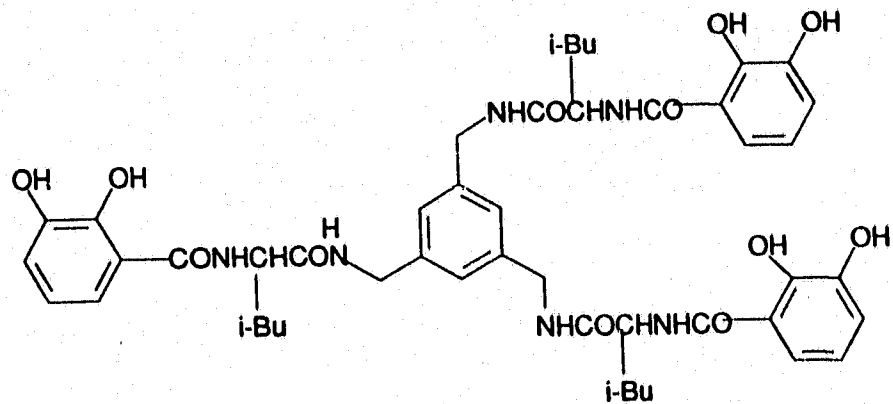


Figure 1.5 continued.

for the $\text{Na}_3[\text{Fe}(\text{bicappedTRENCAm})]$ is perfectly trigonal prismatic, the first and only example of trigonal prismatic geometry for $\text{Fe}(\text{III})$ ⁶².

1.8 Purpose

The intended goals of this project are two-fold. The first is to prepare enterobactin analogues with a cyclic amine backbone containing pendant catecholate moieties, and secondly to use these compounds as potentially binucleating pendant arm macrocycles where one metal ion will coordinate in an N_6 environment and the other metal ion binds to the catecholate functionalities. This thesis is concerned mainly with the synthetic aspects of the preparation of such ligands and metal complexes. The measurement of formation constants and other physical data is to be considered in future studies.

Chapter two describes the experimental details used in the synthesis. Chapter three concerns the synthesis and characterization of taptacn-triscatecholate systems and their metal complexes. In chapter four, the preparation of taetacn-triscatecholate ligands and the transition metal complexes are described. Chapter five describes the preparation of some tren-triscatecholates as well as their metal complexes.

Chapter six is a kinetic study on the base hydrolysis and anation reactions of $\text{Co}(\text{III})$ pentammines. An introduction to this field of study is given there.

CHAPTER 2
EXPERIMENTAL METHODS

2.1 Synthesis of ligands, ligand precursors, and transition metal complexes

2.1.1 Synthesis of 1,4,7-triazacyclononane (tacn) (5)⁶³

Diethylene-1,4,7-triaminetritosylate (1)

Diethylenetriamine (41.3g, 0.4 mol) and NaOH (48g, 1.2 mol) were dissolved in deionized H₂O (400 mL). This solution was added dropwise to *p*-toluenesulfonyl chloride (228g, 1.2 mol) in diethyl ether (1200 mL). The reaction mixture was stirred for 2 hours at room temperature. The product was filtered off, washed with water then diethyl ether. Recrystallization from methanol yielded a white solid.

yield: 181g (80%) m.p. 157-159°C

¹H nmr 90 MHz (d₆-acetone): δ 7.5 (d, 6H), 7.15 (d, 6H), 2.88 (s, 4H), 2.55 (s, 4H), 2.2 (s, 9H)

¹³C nmr 250 MHz (CDCl₃): δ 144.4, 143.9, 137.1, 135.1, 130.3, 130.1, 127.6, 127.4, 50.6, 42.8, 21.6

mass spec: M+1, 566; M+29, 594

Ethyleneglycol ditosylate (2)

Ethylene glycol (18.6g, 0.3 mol) was dissolved in dry CH₂Cl₂ (1000 mL) in a three-necked 2L round bottomed flask. This was cooled to 0°C and kept under a N₂ atmosphere. Triethylamine (150 mL) was added through a dropping funnel. *p*-Toluenesulfonyl chloride (114g, 0.6 mol) in dry CH₂Cl₂ (500

mL) was added over a 45 minute period, and the reaction mixture was stirred at 0°C for 12 hours. At this time the triethylammonium chloride was filtered off and the filtrate was washed with HCl (2M, 750 mL). The organic layer was washed with H₂O (3 x 250 mL) and saturated Na₂CO₃ (1 x 250 mL). This layer was then dried over anhydrous sodium sulphate, filtered, and the solvent was removed on the rotovap to yield a white crystalline solid. This was recrystallized from methanol if necessary.

yield: 102g (92%) m.p. 120-122°C

¹H nmr 90 MHz (CDCl₃): δ 7.7 (d, 4H), 7.2 (d, 4H), 4.15 (s, 4H), 2.4 (s, 6H)

¹³C nmr 250 MHz (CDCl₃): δ 145.5, 132.7, 130.2, 128.1, 66.9, 21.6

mass spec: M+1, 371; M+29, 399; M+41, 411

1,4,7-Triazacyclononane tritosylate (3)

Compound 1 (241g, 0.427 mol) was dissolved in dry DMF (5L) to which was added NaH (20g, 0.852 mol). A solution of 2 (158g, 0.427 mol) in dry DMF (2L) was added dropwise over a 30 hour period at 70°C. Once addition was complete, the volume was reduced to ~ 1.2 L and added slowly, with stirring, to 12 L ice and water. The product was filtered, washed with water, 100% EtOH, and diethyl ether. The crude product was dried in air for 2 days and then dried under vacuum. It was used in the next step without further purification.

yield: 235g (94%)

^1H nmr 90MHz (CDCl_3): δ 7.75 (d, 6H), 7.35 (d, 6H), 3.41 (s, 12H), 2.41 (s, 9H)

^{13}C nmr 250 MHz (CDCl_3): 143.9, 134.7, 129.9, 127.5, 51.8, 21.5

mass spec: M+1, 592

1,4,7-Triazacyclononane.3HCl (4)

Compound 3 (50g, 85mmol) was added to concentrated H_2SO_4 (75 mL) at 160°C over 30 minutes. The reaction mixture was allowed to cool to room temperature before dropwise addition to cold 100% EtOH (400 mL). Diethyl ether (700 mL) was also added during the addition, and the brown precipitate was removed by filtration. This precipitate was dissolved in H_2O and activated charcoal was added. The solution was boiled for 15-20 minutes, filtered, and the solvent removed on the rotovap. Concentrated HCl (50 mL) was added followed by 100% EtOH (300 mL). The crude salt was filtered and recrystallized from a H_2O /EtOH mixture.

yield: 17g (85%)

^1H nmr 90 MHz (D_2O): δ 3.65 (s)

^{13}C nmr 250 MHz (D_2O): δ 41.8

1,4,7-Triazacyclononane (5)

Compound 4 (47g, 0.2 mol) was dissolved in deionized H_2O (100 mL) and brought to pH ~ 13 with the addition of NaOH pellets. This was extracted into chloroform with a continuous

extractor for 48 hours. The layers were separated and the organic layer was dried over anhydrous sodium sulphate, and subsequently filtered. The solvent was removed to yield either a pale yellow oil or colorless crystals. The product was recrystallized from CH_2Cl_2 if necessary.

yield: 16g (62%)

^1H nmr 90 MHz (CDCl_3): δ 2.75 (s, 12H), 2.02 (s, 3H)

^{13}C nmr 250 MHz (CDCl_3): δ 47.0

mass spec: M+1, 130; M+29, 158; M+41, 170

2.1.2 Synthesis of 1,4,7-triaminopropyl-1,4,7-triazacyclononane (9)⁶⁴

1,4,7-Tricyanoethyl-1,4,7-triazacyclononane (6)

Compound 5 (5g, 38.8 mmol) was dissolved in a minimum amount of dry CH_2Cl_2 . Acrylonitrile (100 mL) was added and the reaction mixture refluxed for 1 hour under N_2 . The solution was stirred and gently heated overnight while maintaining an inert atmosphere. The solvent and excess acrylonitrile were removed under vacuum to leave a yellow oil. The crude product was not purified further.

yield: 8.1g (74%)

^1H nmr 250 MHz (CD_3CN): δ 3.15 (t, 6H), 3.07 (s, 12H), 2.8 (t, 6H)

^{13}C nmr 250 MHz (CD_3CN): δ 120.48, 53.36, 53.11, 16.75

IR: 2240cm^{-1} (-CN)

mass spec: M+1, 289; M+29, 317; M+41, 329

1,4,7-Triaminopropyl-1,4,7-triazacyclononane (7)

BH₃.THF (150 mL) was added to 6 (8.1g, 28 mmol) via syringe and septum. The reaction mixture was kept under an inert atmosphere and refluxed for 2 hours. The solution was cooled to room temperature and stirring was continued overnight. Excess BH₃ was quenched with the slow dropwise addition of MeOH at 0°C. The solvent was removed under reduced pressure and the residue dissolved in HCl (4M, MeOH) and refluxed for 1 hour. Upon cooling the solution was made basic (pH ~ 12) by the addition of NaOH pellets and extracted into CHCl₃ (8 X 100 mL).

yield: 6.0g (71%)

¹H nmr 250 MHz (CD₃CN): δ 2.65 (s, 12H), 2.6 (t, 6H), 2.45 (t, 6H), 1.45 (q, 6H), 1.32 (s, 6H)

¹³C nmr 250 MHz (CDCl₃): δ 55.17, 51.87, 39.16, 28.19

mass spec: M+1, 301; M+29, 329; M+41, 341

The crude product obtained also contained some of the mono- and di- armed derivatives.

Nickel(II) 1,4,7-triaminopropyl-1,4,7-triazacyclononane perchlorate (8)

Compound 7 (6.0g, 20 mmol) was dissolved in 95% EtOH (500 mL) and the pH adjusted to ~ 8. This solution was heated to reflux and a solution of Ni(OAc)₂.4H₂O (4.96g, 20 mmol) in

H₂O/EtOH (20/80, 200 mL) was added. The reaction mixture turned purple almost immediately, but stirring was continued overnight at room temperature to ensure complete complexation. The solution was filtered and brought to dryness. The residue was dissolved in H₂O and loaded onto a Sephadex C-25 cation exchange column. Elution with increasing concentrations of NaCl solution yielded five distinct bands. The first three were found to be identical by uv-vis spectroscopy and were therefore combined. The combined fractions were taken to dryness and dissolved in 100% EtOH, and filtered to remove the NaCl. This procedure was repeated until no NaCl was left. The product was recrystallized from an H₂O/EtOH solution.

yield: 2.0g (17%)

λ_{\max} (nm) (ϵ , M⁻¹cm⁻¹): 340(10), 538(7.9), 815(sh, 7.7), 860(7.8)

1,4,7-Triaminopropyl-1,4,7-triazacyclononane 9

Compound 8 (5.58g, 10 mmol) was dissolved in H₂C (40 mL) and heated to reflux. NaCN (1.96g, 40 mmol) was added to the solution and refluxing continued for 3 hours. Additional NaCN (1.0g, 20 mmol) was added and refluxing continued for 1 hour. The solution was cooled to room temperature and following the addition of NaOH (1.5g), the volume was reduced to a semi-solid on the rotovap. This residue was suspended in CH₂Cl₂ and stirred overnight. After filtration the organic layer was dried over anhydrous sodium sulphate. Usual workup yielded a white hygroscopic solid.

yield: 1.7g (57%)

^1H nmr 250 MHz (CD_3CN): δ 2.65 (s, 12H), 2.6 (t, 6H), 2.45 (t, 6H), 1.45 (q, 6H), 1.32 (s, 6H)

^{13}C nmr 250 MHz (CDCl_3): δ 55.17, 51.87, 39.16, 28.19

mass spec: M+1, 301; M+29, 329; M+41, 341

2.1.3 Synthesis of taptacn - catecholate systems

2,3-Dimethoxybenzoyl chloride (**10**)⁶⁵

2,3-Dimethoxybenzoic acid (2.0g, 10 mmol) was dissolved in freshly distilled SOCl_2 (20 mL) and stirred overnight at room temperature (under N_2). Excess thionyl chloride was removed under vacuum, and the product was co-evaporated with benzene (3 X 20 mL), to yield a white crystalline solid.

yield: quantitative

IR: 1770 cm^{-1} (Ar-COCl)

^1H nmr 90 MHz (CDCl_3): δ 7.55 (m, 1H), 7.2 (m, 2H), 3.90 (s, 3H), 3.89 (s, 3H)

^{13}C nmr 250 MHz (CDCl_3): δ 164.7, 153.4, 149.0, 128.8, 123.8, 123.6, 117.8, 61.5, 56.1

mass spec: M+1, 201(203); M+29, 229(231); M+41, 241(243)

1,4,7-Tris-((2,3-dimethoxybenzoyl)aminopropyl)-1,4,7-triazacyclononane (**11**)

Compound **9** (1.0g, 3.3 mmol) was dissolved in CH_2Cl_2 (100 mL) and H_2O (100 mL) in a four-necked 1L round bottomed flask

fitted with condensor, two 500 mL dropping funnels and overhead stirrer. Simultaneous dropwise addition of NaOH (0.5M, 200 mL) and 2,3-dimethoxybenzoyl chloride (2.0g, 0.01 mol) in dry CH_2Cl_2 (200 mL) over a 2 hour period at 50°C under an inert atmosphere resulted in the desired product. The workup was as follows; the organic layer was separated and washed with H_2O (3 X 250 mL), followed by drying over anhydrous MgSO_4 . The solvent was removed under vacuum to yield a colorless oil.

yield: 1.7g (65%)

IR (CH_2Cl_2 solution): 3380 cm^{-1} (N-H stretch)
 2930 cm^{-1} (C-H stretch)
 1640 cm^{-1} (C=O amide)
 1570 cm^{-1} (N-H bend)
 1520 cm^{-1} (C=C stretch)

^1H nmr 250 MHz (CDCl_3): δ 8.02 (t, 3H), 7.56 (dd, 3H), 7.08, 6.98 (t,dd, 6H), 3.85,3.84 (s,s 18H), 3.45 (q, 6H), 2.74,2.58 (s,s 18H), 1.73 (q, 6H)

^{13}C nmr 250MHz (CDCl_3): δ 165.2, 152.5, 147.3, 127.3, 124.3, 122.6, 114.0, 61.0, 56.5, 56.0, 55.9, 38.1, 27.9

1,4,7-Tris-((2,3-dihydroxybenzoyl)aminopropyl)-1,4,7-triazacyclononane.6HBr (12)

Compound 11 (1.5g, 1.9 mmol) was dissolved in dry CH_2Cl_2 in a three-necked round bottomed flask fitted with condensor, N_2 inlet and septum. The reaction mixture was kept at 0°C and

under an inert atmosphere. BBr_3 (1M in CH_2Cl_2 , 50 mL) was added slowly via syringe and septum. The mixture was allowed to warm to room temperature and stirred for 24 hours. The reaction mixture was then cooled to 0°C and MeOH (50 mL) was added dropwise over 2 hours. The solvent was removed under vacuum and the product was coevaporated with MeOH (15 X 50 mL), followed by precipitation from hot MeOH and diethyl ether, leaving an off-white solid.

yield: 1.98g (94%)

^1H nmr 250 MHz (d_6 -dmsO): δ 8.86 (s, 3H), 7.30 (dd, 3H), 6.91 (dd, 3H), 6.66 (t, 3H), 3.35 (m, 18H), 1.96 (s, 6H), 1.07 (t, 6H)

^{13}C nmr 250 MHz (d_6 -dmsO): δ 169.9, 149.5, 146.2, 118.8, 117.9, 117.3, 115, 54, 48.7, 36.6, 23.6

1,4,7-Tris-((2,3-dimethoxybenzyl)aminopropyl)-1,4,7-triazacyclononane (**13**)

Compound **9** (0.8g, 2.67 mmol) was dissolved in reagent grade MeOH (80 mL) and this solution was saturated with N_2 . A 10% HCl (1 drop) solution in MeOH was added followed by the dropwise addition of 2,3-dimethoxybenzaldehyde (1.33g, 8 mmol) in MeOH (60 mL) (under N_2) over 1.5 hours. Stirring was continued for an additional 5 hours. NaBH_4 (3g, 81 mmol) was added to the reaction mixture and, once dissolved, the solution was refluxed for 1.5 hours. The reaction mixture was cooled to room temperature and the solvent removed on the

rotovap. The residue was dissolved in H₂O and the pH adjusted to 10 with NaOH. This solution was extracted with CH₂Cl₂ (6 X 100 mL), dried over anhydrous Na₂SO₄, filtered, and brought to dryness to yield a colorless oil.

yield: quantitative

¹³C nmr 250MHz (CDCl₃): δ 152.1, 146.8, 133.8, 123.3, 121.2, 110.9, 60.2, 56.4, 55.4, 55.2, 48.3, 47.3, 28.1

1,4,7-Tris-((2,3-dihydroxybenzyl)aminopropyl)-1,4,7-triazacyclononane.6HBr (**14**)

Compound **13** (0.7g, 0.9 mmol) was dissolved in dry CH₂Cl₂, bubbled with N₂, and cooled to 0°C. BBr₃ (1M in CH₂Cl₂, 20 mL) was added via syringe and septum. A white precipitate formed almost immediately, but stirring was continued for 48 hours at room temperature. The reaction mixture was cooled to 0°C and dropwise addition of MeOH (20 mL) quenched the excess BBr₃. The solvent was removed on the rotovap and the residue was co-evaporated with MeOH (15 X 50 mL). The brown solid was dissolved in a minimum amount of MeOH and precipitation was achieved by dropwise addition to ethyl acetate (600 mL). The white product was filtered and dried under vacuum.

yield: quantitative

¹H nmr 360 MHz (D₂O): δ 6.27, 6.15 (dd, m, 9H), 3.57 (s, 6H), 2.47 (m, 24H), 1.42 (m, 6H) *EtOAc peaks, 3.41 (q), 1.35 (s), 0.46 (t)

¹³C nmr 250 MHz (D₂O): 144.4, 143.9, 122.9, 121, 118.4, 117.7,

52.9, 49, 46.6, 44.1, 21.1

mass spec, positive ion FAB mNBA matrix: m/e 667 [M+1]

Analysis; Calc. for 14.EtOAc (found); C, 38.73% (38.63%); H, 5.53% (5.58%); N, 6.78% (6.93%)

3,4-Dioxosulfonophenylacetyl chloride (15)

3,4-Dihydroxyphenylacetic acid (1.5g, 8.9 mmol) was refluxed in freshly distilled SOCl_2 (25 mL) for 24 hours under a N_2 atmosphere. Excess thionyl chloride was removed under vacuum and the product was co-evaporated with benzene (4 X 25 mL), to leave a yellow oil.

yield: 1.8g (87%)

IR - 1790 cm^{-1} (Ar-COCl)

mass spec: M+1, 233 (235); M+29, 261 (263); M+41, 273 (275)

1,4,7-Tris-((3,4-dihydroxyphenylacetyl)aminopropyl)-1,4,7-triazacyclononane (16)

Compound 9 (0.8g, 2.7 mmol) and NEt_3 (2.2 mL) were dissolved in dry THF, and an inert atmosphere was maintained. 3,4-Dioxosulfonophenylacetyl chloride (1.8g, 8 mmol) in dry THF (50 mL) was added dropwise and the reaction mixture was stirred for 2 hours. The $\text{NEt}_3\cdot\text{HCl}$ formed was filtered off and the solvent from the filtrate was removed on the rotovap to leave a yellow oil. The sulfono group was displaced by dissolving the product in deionized H_2O and adding NaHCO_3 , to yield a cream colored solid.

yield: 0.78g (38.5%)

^{13}C nmr 250 MHz (D_2O): δ 173.6, 143.9, 143.1, 125.8, 121.3, 116.4, 115.5, 52.1, 50.2, 46.6, 40.2, 30.1

2.1.4 Synthesis of transition metal complexes of taptacn catecholate ligands.

[Cu(13)][(ClO₄)₂] (17,18)

Compound **13** (0.265g, 0.35 mmol) was dissolved in EtOH (100%, 20 mL) and Cu(ClO₄)₂.6H₂O (0.132g, 0.35 mmol) was added to the solution. The solution turned blue almost immediately, with the formation of a precipitate. The reaction mixture was refluxed for 3 hours, removed from the heat and cooled to room temperature. The solution was loaded onto a Sephadex C-25 cation exchange column and two bands were eluted. The first, yellow band, with 0.1 - 0.3 M NaCl, and the second, blue band, with 0.5 - 1.0 M NaCl.

Yellow (**17**); λ_{max} = 465 nm, g_{\parallel} = 2.23, (170G) g_{\perp} = 2.032

Blue (**18**); λ_{max} = 643 nm, g_{\parallel} = 2.22, (165G) g_{\perp} = 2.067

[Ni(13)][(ClO₄)₂] (19)

Compound **13** (0.21g, 0.28 mmol) was dissolved in EtOH (100%, 30 mL) and Ni(ClO₄)₂.4H₂O (0.092g, 0.28 mmol) in an EtOH solution (100%, 10 mL) was added. A white precipitate formed immediately, so the reaction mixture was refluxed overnight after addition of a small amount of water. The solvent was

removed on the rotovap to yield the crude brown solid (0.296g). This was dissolved in H₂O and loaded onto a Sephadex C-25 cation exchange column. Four separate yellow bands were eluted from the column with increasing NaCl concentrations.

[Co(13)][(OAc)₂] (20)

Compound 13 (0.4g, 0.5 mmol) was dissolved in MeOH (40 mL) and one equivalent Co(OAc)₂·4H₂O (0.134g, 0.5 mmol) in MeOH (10 mL) was added. A catalytic amount of activated charcoal was added to catalyze the oxidation of the cobalt. The reaction mixture was bubbled with air and stirred at room temperature overnight. The charcoal was removed by filtration to yield a pink solution. More charcoal was added and the reaction mixture was refluxed for 24 hours to yield an orange/brown solution. The MeOH was removed and the residue dissolved in H₂O and loaded onto a Sephadex C-25 cation exchange column. Owing to the high charge of the cobalt complex, all attempts at eluting it from the column were unsuccessful.

K₃[Fe(12)] (21), K₃[Fe(14)] (22), and K₃[Fe(16)] (23)

All ferric ion complexes were prepared in the following manner; the appropriate ligand.HBr salts 12, 14, or 16 (0.09 mmol) were dissolved in MeOH (200 mL) and this solution was kept under a N₂ atmosphere (to prevent oxidation to the

quinones). A solution of $\text{FeCl}_3 \cdot 6\text{H}_2\text{O}$ (0.09 mmol) in MeOH (100 mL) was added dropwise to the ligand solution. The reaction mixture turned green at first but on addition of K_2CO_3 (saturated solution) to pH ~ 9 the reaction mixture turned purple and the complex precipitated out of solution. This was filtered and dried in air. Yields were on the order of 75-80%.

2.1.5 Synthesis of 1,4,7-triaminoethyl-1,4,7-triazacyclononane

Phthalimidoacetaldehyde (24)⁶⁶

Acetamide (300g, 5 mol) was heated slowly to 80°C in a 2 L 3-necked round bottomed flask, and then heated to 140°C. Once the acetamide was melted, potassium phthalimide (235g, 1.26 mol) was added to the reaction mixture. 1-Bromo-2-dimethoxyethane (1.45 mL) was added from a dropping funnel, the reaction mixture was cooled and diluted with water (1.5 L) and left overnight. The brown precipitate was filtered, dissolved in CHCl_3 , and the acetamide was removed by filtration. The filtrate was decolorized with activated charcoal, filtered and the solvent removed on the rotovap. Yield: 60g (21%). This product was dissolved in HCO_2H (90%, 70 mL) and conc. HCl (10 mL) and heated until water soluble. The mixture was diluted with water (~ 1 L), decolorized with activated charcoal, filtered, and the solvent removed on the rotovap. The cream colored solid was dried under vacuum.

yield: 44g (88%, based on the dimethoxy derivative)

^1H nmr 90 MHz (CDCl_3): δ 9.64 (s, 1H), 7.85 (m, 2H), 7.74 (m, 2H), 4.55 (s, 2H)

^{13}C nmr 250 MHz (CDCl_3): δ 193.5, 167.5, 134.3, 123.7, 123.6, 47.4

mass spec: M+1, 190; M+29, 218; M+41, 230

1,4,7-Tris-(phthalimidoacetyl)-1,4,7-triazacyclononane (25)⁶⁷

Compound 5 (4g, 31 mmol) was dissolved in freshly distilled CH_3CN (300 mL) and placed under a N_2 atmosphere. Molecular sieves (4Å, 10g), phthalimidoacetaldehyde (24) (23.4g, 124 mmol) and NaBH_3CN (7.8g, 124 mmol) were added to the solution. The reaction mixture was stirred at room temperature for 8 hours, refluxed for 1 hour, and stirred at room temperature for an additional 10 hours. The mixture was filtered and the filtrate brought to dryness to leave a brown oil. The oil was dissolved in aqueous NaOH (pH ~ 12) and extracted into CHCl_3 . The combined extracts were dried over anhydrous Na_2SO_4 , filtered and brought to dryness. This crude product was used in the next step without any further purification.

1,4,7-Triaminoethyl-1,4,7-triazacyclononane.6HBr (26)

Compound 25 was dissolved in HBr (48%, 75 mL) and glacial acetic acid (75 mL) and refluxed for 20 hours. The volume was reduced and the residue dissolved in a minimum amount of hot

HBr solution (48%) and cooled in an ice bath. Precipitation occurred with the dropwise addition of glacial acetic acid. The solid was filtered and dried under vacuum.

yield: 22g (crude)

The purification was best achieved by preparing the cobalt complex and loading onto a Dowex cation exchange column.

[Co(26)](ClO₄), (27)

Compound 26 (22g, 30 mmol) was dissolved in deionized H₂O (100 mL). The solution was made alkaline with the addition of NaOH (6 M). A solution of Co(OAc)₂·4H₂O (7.47g, 30 mmol) in deionized H₂O (120 mL) was added to the ligand solution. A catalytic amount of activated charcoal was added and the reaction mixture was saturated with air. Stirring was continued overnight, after which the charcoal was removed by filtration and the filtrate was loaded onto a Dowex 50 X 8 cation exchange column. Three bands were eluted from the column. The first, pink band was eluted with 2 M HCl and was identified as containing CoCl₂·6H₂O. The second, magenta band was eluted with 4 M HCl and remains unidentified. The third, orange/red band was eluted with 4 - 6 M HCl and contained the desired product. The cobalt complex was recrystallized from H₂O/saturated NaClO₄ with the slow diffusion of isopropanol into the solution.

yield: 0.02g, 1.2%

¹³C nmr 250 MHz (D₂O): δ 64.6, 63.6, 62.8, 45

Analysis for [Co(26)](ClO₄)₃, Calc. (found); C 23.41% (23.47%),
H 4.91% (4.74%), N 13.65% (13.39%)

More product could be isolated as the ZnCl₅³⁻ salt prepared by the following manner. The crude oil was dissolved in warm HCl (0.1 M, 50 mL) and solid ZnCl₂ was added along with HCl (6 M). Orange crystals appeared upon cooling.

yield: 4.2g, 25%

1,4,7-triazacyclononane-1,4,7-triacetic acid (28)

Bromoacetic acid (6.84g, 42 mmol) and NaOH (1.68g, 42 mmol) were dissolved in deionized H₂O (14 mL) and stirred at room temperature. A solution of 5 (1.8g, 14 mmol) in H₂O (8 mL) was added to the reaction mixture and the temperature was raised to 80°C. Sodium hydroxide (1.68g, 42 mmol) in H₂O (14 mL) was added dropwise over a 1 hour period. The temperature was lowered to 50°C and stirring was continued for 4 hours. The pH was adjusted to 3 with HBr solution (48%) and the solvent removed on the rotoevaporator. The residue was dissolved in hot EtOH (100%) and the product removed by filtration.

yield: quantitative

¹H nmr 90 MHz (D₂O): 3.85 (s, 6H), 3.44 (s, 12H)

¹³C nmr 250 MHz (D₂O): 173.6, 59, 51.1

1,4,7-(trioxoethylchloro)-1,4,7-triazacyclononane (29)

Simultaneous addition of chloroacetyl chloride (7.4 mL,

93mmol) in CH_2Cl_2 (200 mL), under N_2 , and K_2CO_3 (12.8g, 93mmol) in H_2O (200 mL) over a 2 hour period to a vigorously stirred solution of **5** (2.0g, 15.5mmol) in $\text{CH}_2\text{Cl}_2/\text{H}_2\text{O}$ (5/1, 300 mL), followed by separation and usual workup of the organic layer resulted in the product.

yield: 5.1g (92%)

TLC (silica) $R_f=0.71$ in 4:1 $\text{CHCl}_3/\text{MeOH}$.

^1H nmr 90MHz ($\text{CDCl}_3/\text{CD}_3\text{OD}$): δ 3.9 (s, 6H), 3.45 (m, 12H)

^{13}C nmr 250MHz ($\text{CDCl}_3/\text{CD}_3\text{OD}$): δ 168.7, 50.5, 47.9, 40.7

mass spec (CI): M+1 360, M+29 388

IR: 1636 cm^{-1} (C=O amide)

m.p. 158-9°C

Analysis, Calc. for **29** (found): C 40.17% (40.20%), H 5.06% (5.00%), N 11.59% (11.72%)

1,4,7-(trioxoaminoethyl)-1,4,7-triazacyclononane (**30**)

Compound **29** (1.0g, 2.8 mmol) was refluxed in conc. NH_4OH (50 mL) for 1 hour. The reaction mixture was cooled to room temperature and taken to dryness. This was used in the next step without further purification.

yield: quantitative

^1H nmr 90MHz (D_2O): δ 3.98 (broad s, 6H), 3.65 (broad, 12H)

^{13}C nmr 250MHz (CD_3OD): δ 168.6, 49, 47.2, 40.8

mass spec (CI): M+1 301, M+29 329

2.1.6 Synthesis of taetacn - catecholate systems

Tris-1,4,7-((2,3-dimethoxyphenylacetyl)oxoaminoethyl)-1,4,7-triazacyclononane (31)

Compound 30 (0.9g, 3 mmol) was dissolved in CH₂Cl₂/H₂O (80/20, 800 mL) and to this solution was added 3 equivalents of 2,3-dimethoxyphenylacetyl chloride (1.93g, 9 mmol) in CH₂Cl₂ (100 mL) and 3 equivalents of K₂CO₃ (1.26g, 9 mmol) in H₂O (100 mL) over a period of 3 hours. Once addition was complete, the reaction mixture was stirred for 18 hours at room temperature. The organic layer was separated and washed with H₂O (2 x 150 mL). The organic layer was dried over anhydrous Na₂SO₄, filtered, and brought to dryness under reduced pressure to yield a white solid. This solid was purified by centrifugal chromatography, then eluted with a CH₂Cl₂/MeOH mixture.

yield: 1.5g (60%)

TLC silica, 4:1CHCl₃:MeOH R_f=0.57

¹H nmr 360MHz (CDCl₃): δ 6.97 (t, 3H), 6.82 (m, 9H), 5.27 (s, 6H), 3.91 (d, 6H), 3.82, 3.81 (s,s, 18H), 3.56 (s, 12H)

¹³C nmr 360MHz (CDCl₃): δ 171.51, 169.97, 152.81, 147.07, 128.89, 124.33, 122.74, 111.71, 60.66, 55.69, 51.10, 47.48, 41.75, 37.89

IR 1650cm⁻¹ C=O amide

mass spec: positive ion FAB mNBA matrix m/e 835 [M+1]

Tris-1,4,7-((2,3-dimethoxybenzoyl)oxoaminoethyl)-1,4,7-

triazacyclononane (32)

Compound **30** (0.84g, 2.8 mmol) was dissolved in CH₂Cl₂ (500 mL) and H₂O (50 mL) and to this solution was added 2,3-dimethoxybenzoyl chloride (1.67g, 8.4 mmol) in CH₂Cl₂ (100 mL) and K₂CO₃ (1.16g, 8.4 mmol) in H₂O (100 mL) over a 2 hour period. The reaction mixture was stirred at room temperature overnight. The organic layer was separated and washed with H₂O (2 X 100 mL), followed by drying with anhydrous Na₂SO₄. The solution was filtered and brought to dryness under reduced pressure to yield a white solid. Purification was achieved with centrifugal chromatography (CH₂Cl₂/MeOH was the preferred eluent).

yield: 1.5g (68%)

¹H nmr 360MHz (CDCl₃): δ 8.82 (t, 3H), 7.58 (dd, 3H), 7.05 (m, 6H), 4.26 (d, 6H), 3.93, 3.89, 3.84 (s, m, s, 30H)

¹³C nmr 360 MHz (CDCl₃): δ 170.2, 165.4, 152.7, 148.1, 126.2, 124.1, 122.7, 115.6, 61.6, 56.1, 51.2, 47.6, 42.2

mass spec: positive ion FAB in mNBA matrix m/e 793 [M+1]

1,4,7-Tris-((2,3-dimethoxyphenethyl)aminoethyl)-1,4,7-triazacyclononane (33)

Compound **31** (0.79g, 0.9 mmol) was dissolved in BH₃.THF (1 M, 40 mL) at 0°C. The reaction mixture was maintained under an inert atmosphere and refluxed for 5 hours. After cooling to 0°C, excess BH₃ was quenched with the dropwise addition of MeOH. The solvent was removed and the residue dissolved in

HCl (0.8 M in MeOH, 100 mL) and refluxed for 3 hours. The solution was cooled to room temperature and the solvent was removed. The white residue was dissolved in a minimum amount of aqueous NaOH (6 M), and extracted into CHCl₃ (5 X 50 mL). The combined extracts were dried over anhydrous sodium sulphate, filtered, and brought to dryness to yield a yellow oil. All attempts at purification were unsuccessful so the crude product was used in the next step without complete characterization.

yield: 0.32g (45%)

1,4,7-Tris-((2,3-dihydroxyphenethyl)aminoethyl)-1,4,7-triazacyclononane.6HBr (34)

BBr₃ (1 M in CH₂Cl₂, 40 mL) was added via syringe and septum to a degassed solution of 33 (0.32g, 0.427 mmol) in CH₂Cl₂ (10 mL) at 0°C. The reaction mixture was kept under N₂ and allowed to warm up to room temperature. Stirring was continued for 48 hours, at which time the solution was cooled to 0°C and excess BBr₃ was quenched with the dropwise addition of MeOH. The solvent was removed under vacuum and the residue was co-evaporated with MeOH (10 X 25 mL). The product was recrystallized from hot MeOH and EtOAc, leaving an off-white powder.

yield: 0.492g (quantitative)

¹H nmr 360 MHz (D₂O): δ 6.07 (m, 9H), 2.65, 2.56 (m, m, 18H), 2.31 (m, 18H) *EtOAc peaks, δ 3.39 (q), 1.34 (s), 0.44 (t)

^{13}C nmr 360 MHz (D_2O): δ 144.6, 142.9, 124.4, 122.4, 121.3, 115.5, 50.7, 49.8, 48.1, 43.1, 26.8 EtOAc peaks, 174.9, 61.9, 20.8, 13.5

mass spec, positive ion FAB mNBA matrix: m/e 667 [M+1]

Analysis, Calc. for 34.EtOAc (found); C 38.73% (38.99%), H 5.53% (5.49%), N 6.78% (7.27%)

1,4,7-Tris-((2,3-dimethoxybenzyl)aminoethyl)-1,4,7-triazacyclononane (35)

Compound 32 (0.75g, 0.947 mmol) was dissolved in $\text{BH}_3\cdot\text{THF}$ (1 M, 40 mL) at 0°C . The solution was refluxed for 5 hours under an inert atmosphere. Excess BH_3 was quenched with the dropwise addition of MeOH at 0°C . The solvent was removed and the residue dissolved in HCl (1.5 M in MeOH, 100 mL) and the solution refluxed for 2 hours. After cooling to room temperature the solvent was removed on the rotovap and the residue was dissolved in a minimum amount of H_2O . NaOH pellets were added until the pH reached ~ 13 . This was extracted into CHCl_3 (5 X 50 mL) and the combined organic fractions were dried over anhydrous sodium sulphate. The solution was filtered and the filtrate removed under vacuum to yield a yellow oil.

yield: 0.28g (41.8%)

The crude product was used in the next step without purification.

1,4,7-Tris-((2,3-dihydroxybenzyl)aminoethyl)-1,4,7-triazacyclononane.6HBr (36)

Compound 35 (0.28g, 0.395 mmol) was dissolved in a minimum amount of CH₂Cl₂ and de-aerated by bubbling with N₂ for 15 minutes. The N₂ atmosphere was maintained and the solution was cooled to 0°C. BBr₃ (1 M in CH₂Cl₂, 40 mL) was added via syringe and septum and the solution was stirred for 48 hours while warming to room temperature. At this time the solution was cooled to 0°C and excess BBr₃ was destroyed with the dropwise addition of MeOH. The crude product was co-evaporated with MeOH (10 X 50 mL) and precipitated from hot MeOH and EtOAc. The solid was filtered and dried under vacuum.

yield: 0.41g (93.5%)

¹H nmr 360 MHz (D₂O): δ 6.28, 6.22, 6.15 (dd, dd, t, 9H), 3.60 (s, 6H), 2.60 (m, 12H), 2.33 (s, 12H) *EtOAc peaks, 3.37 (q), 1.34 (s), 0.51 (t)

¹³C nmr 360 MHz (D₂O): δ 144.2, 143.9, 122.9, 120.9, 117.9, 117.6, 50.7, 50.0, 46.9, 42.1 *EtOAc peaks, 61.7, 20.5, 13.2 (more scans would be necessary to see the C=O peak)

mass spec, positive ion FAB mNBA matrix: m/e 625 [M+1]

Analysis, Calc. for 36.EtOAc (found); C 36.45% (36.98%), H 5.27% (5.11%), N 7.09% (7.57%)

2.1.7 Synthesis of transition metal complexes of taetacn - catecholate systems

[Cu(33)][(ClO₄)₂] (37)

Compound **33** (0.1g, 0.14 mmol) was dissolved in MeOH (50 mL) and stirred at room temperature. To this solution was added Cu(ClO₄)₂.6H₂O (0.0517g, 0.14 mmol) in MeOH (10 mL). The reaction mixture turned blue almost immediately but stirring was continued with gentle heating (40°C) for 2 hours. The solvent was removed under vacuum and the residue dissolved in CH₃CN. The purple product was recrystallized from CH₃CN/aqueous Ba(ClO₄)₂ with diffusion of diethyl ether into the solution.

yield: 0.03g (22%)

Na[CuFe(34)] (38)

Compound **34** (0.02g, 0.017 mmol) was dissolved in degassed MeOH (10 mL) containing 4 equivalents NaHCO₃ (5.7 mg, 0.068 mmol). The solution was saturated with N₂ continuously throughout the synthesis. Cu(ClO₄)₂.6H₂O (6.3 mg, 0.017 mmol) was added to the reaction mixture. The solution was refluxed for 1 hour and then cooled to room temperature. The uv-vis spectrum was run before continuing to the next step to confirm the metal ion coordination. This solution was added to degassed MeOH (800 mL) in a three necked 2 L round bottomed flask. An additional 4 equivalents of NaHCO₃ (5.7 mg, 0.068 mmol) were added. A solution of FeCl₃.6H₂O (4.63 mg, 0.017 mmol) in MeOH (600 mL) was added dropwise over a period of 12 hours. Once addition was complete another 4 equivalents of

NaHCO_3 (5.7 mg, 0.068 mmol) were added to the solution. The volume was reduced to ~ 250 mL and the solution was left to stand at room temperature, during which time a precipitate settled out of solution. This precipitate was removed by centrifugation and dried under vacuum.

yield: 5mg (36%)

Na[NiFe(34)] (39)

Compound 34 (0.02g, 0.017 mmol) was dissolved in degassed MeOH (10 mL) containing 4 equivalents NaHCO_3 (5.7 mg, 0.068 mmol). The solution was saturated with N_2 continuously throughout the synthesis. $\text{Ni}(\text{OAc})_2 \cdot 4\text{H}_2\text{O}$ (4.2 mg, 0.017 mmol) was added to the reaction mixture. The solution was refluxed for 1 hour and then cooled to room temperature. The uv-vis spectrum was run before continuing to the next step to ensure complete metal ion coordination. This solution was added to degassed MeOH (800 mL) in a three necked 2 L round bottomed flask. An additional 4 equivalents of NaHCO_3 (5.7 mg, 0.068 mmol) was added. A solution of $\text{FeCl}_3 \cdot 6\text{H}_2\text{O}$ (4.63 mg, 0.017 mmol) in MeOH (600 mL) was added dropwise over a period of 12 hours. Once addition was complete another 4 equivalents of NaHCO_3 (5.7 mg, 0.068 mmol) were added to the solution. The volume was reduced to ~ 250 mL and the solution was left to stand at room temperature, during which time a precipitate settled out of solution. This precipitate was removed by centrifugation and dried under vacuum.

yield: 6mg (44%)

Analysis, calc. (found) for (39). $2\text{H}_2\text{O}\cdot 1.5\text{NaHCO}_3$, C 48.65% (48.22%), H 5.83% (5.68%), N 9.08% (8.59%)

[CoFe(34)] (40)

Compound 34 (0.02g, 0.017 mmol) was dissolved in degassed MeOH (10 mL) containing 4 equivalents NaHCO_3 (5.7 mg, 0.068 mmol). The solution was bubbled with N_2 continuously throughout the synthesis. Dry CoCl_2 (2.2 mg, 0.017 mmol) (dried in the oven at 110°C for 2 days) was added to the reaction mixture. The solution was refluxed for 1 hour, cooled to room temperature, and opened to air for 5 minutes. The uv-vis spectrum confirmed the metal ion coordination. This solution was added to degassed MeOH (800 mL) in a three necked 2 L round bottomed flask. An additional 4 equivalents of NaHCO_3 (5.7 mg, 0.068 mmol) was added. A solution of $\text{FeCl}_3\cdot 6\text{H}_2\text{O}$ (4.63 mg, 0.017 mmol) in MeOH (600 mL) was added dropwise over a period of 12 hours. Once addition was complete another 4 equivalents of NaHCO_3 (5.7 mg, 0.068 mmol) were added to the solution. The volume was reduced to ~ 250 mL and the solution was left to stand at room temperature, during which time a precipitate settled out of solution. This precipitate was removed by centrifugation and dried under vacuum.

yield: 3mg (23%)

Na₃[Fe(34)] (41)

Compound **34** (0.02g, 0.017 mmol) was dissolved in degassed MeOH (800 mL). Eight equivalents NaHCO₃ (11.4 mg, 0.136 mmol) were added. To this solution was added dropwise FeCl₃·6H₂O (4.6 mg, 0.017 mmol) in degassed MeOH (600 mL) over 12 hours. The reaction mixture was kept under an inert atmosphere during the addition. Once addition was complete an additional 4 equivalents NaHCO₃ (5.7 mg, 0.068 mmol) was added. The volume was reduced to ~ 200 mL and a fine precipitate settled out of solution. This was centrifuged, the solvent decanted off and the solid dried under vacuum.

yield: 9mg (67%)

2.1.8 Synthesis of tren - catecholate systems**Tris-((2,3-dimethoxybenzylidene)aminoethyl)amine (42)**

Tris-(2-aminoethyl)amine (tren) (2.0g, 13.7mmol) was dissolved in 100% ethanol (50 mL) and added to a solution of 2,3-dimethoxybenzaldehyde (6.8g, 41 mmol) in ether (50 mL). The reaction mixture was stirred for one hour and taken to dryness under reduced pressure to leave a yellow solid.

yield: 7.5g (93%)

¹H nmr 360MHz (CDCl₃): δ 8.6 (s, 1H), 7.46 (dd, 1H), 6.9 (m, 2H), 3.81 (s, 3H), 3.80 (s, 3H), 3.74 (t, 2H), 2.94 (t, 2H)

¹³C nmr 360MHz (CDCl₃): δ 157.7, 152.7, 149.1, 129.8, 124.1,

118.7, 114, 61.6, 60.4, 55.7, 55.6

mass spec: positive ion FAB mNBA matrix m/e 591 [M+1]

Tris((2,3-dimethoxybenzylamino)ethyl)amine (43)

Compound **42** (6.8g, 11 mmol), and $\text{Na}_2\text{B}_4\text{O}_7 \cdot 10\text{H}_2\text{O}$ (1.86g) were dissolved in methanol (150 mL) and stirred at room temperature. NaBH_4 (0.25g) was added to the solution every 5 minutes for 1/2 hour (total, 1.5g), and stirring was continued for 3 hours at room temperature. The solution was taken to dryness under reduced pressure at which time NH_4Cl (10g) in H_2O (100 mL) was added to the residue and extracted into CHCl_3 (3 X 150 mL). The combined extracts were dried over anhydrous sodium sulphate, filtered, and taken to dryness to yield a yellow oil.

yield: 6.5g (99%)

^1H nmr 360MHz (CDCl_3): δ 6.94 (t, 1H), 6.85 (dd, 1H), 6.78 (dd, 1H), 3.79 (s, 3H), 3.77 (s, 3H), 3.73 (s, 2H), 2.55 (m, 4H)

^{13}C nmr 360MHz (CDCl_3): δ 152.47, 147.15, 133.60, 123.82, 121.53, 111.23, 60.59, 55.59, 54.26, 48.10, 46.85

mass spec: positive ion FAB mNBA matrix m/e 597 [M+1]

Tris((2,3-dihydroxybenzylamino)ethyl)amine.4HBr (44)

Compound **43** (6.5g, 11 mmol) was dissolved in dry CH_2Cl_2 (50 mL) under a N_2 atmosphere and cooled to 0°C . BBr_3 (1M, 70 mL) in CH_2Cl_2 was added via syringe and septum. The reaction mixture was stirred at room temperature for 2 days and then

cooled to 0°C. Excess BBr₃ was destroyed by the dropwise addition of methanol. The solution was brought to dryness and co-evaporated with methanol (10 X 100 mL). The product was dried under vacuum overnight to yield an off-white solid.

yield: 7.2g (79%)

¹H nmr 360MHz (D₂O): δ 6.79 (dd, 2H) 6.68 (m, 1H), 4.04 (s, 2H), 3.15 (s, 1H), 2.95 (t, 2H), 2.69 (t, 2H)

¹³C nmr 360MHz (D₂O): δ 144.19, 143.72, 122.85, 120.84, 118.01, 117.50, 48.63, 46.67, 43.35

mass spec: positive ion FAB mNBA matrix (dissolved in MeOH first) m/e 513 [M+1]

Analysis, Calc. for **44** (found): C 38.80% (39.00%), H 4.80% (4.95%), N 6.70% (6.50)

Tris-((2,3-dimethoxybenzoyl)aminoethyl)amine (**45**)⁶⁸

Tren (1.75g, 0.012 mol) was dissolved in CH₂Cl₂/H₂O (50 mL/50 mL) in a three necked round bottomed flask, set up with an overhead stirrer. Simultaneous dropwise addition of aqueous NaOH (0.4 M, 100 mL) and 2,3-dimethoxybenzoyl chloride (8.42g, 0.042 mol) in CH₂Cl₂ (100 mL) over a 1 hour period resulted in the formation of the desired product. The two layers were separated and the organic layer was washed with deionized H₂O (2 X 50 mL). The organic layer was dried over anhydrous Na₂SO₄, filtered and taken to dryness. The crude, colorless oil was recrystallized from EtOAc and cyclohexane to leave a white solid.

yield: 3.65g (48%)

^1H nmr 360 MHz (CDCl_3): δ 8.16 (t, 3H), 7.58 (dd, 3H), 7.07 (t, 3H), 6.97 (dd, 3H), 3.83, 3.82 (s,s, 18H), 3.57 (q, 6H), 2.85 (t, 6H)

^{13}C nmr 360 MHz (CDCl_3): δ 165.4, 152.4, 147.4, 126.7, 124.1, 122.5, 115.1, 61.2, 55.9, 53.4, 37.8

mass spec: M+1, 639; M+29, 667; M+41, 679

Analysis, Calc. for 45 (found): C 62.06% (62.13%), H 6.63% (6.71%), N 8.78% (8.77%)

Tris-((2,3-dihydroxybenzoyl)aminoethyl)amine.4HBr (46)

Compound 45 (2.5g, 3.9 mmol) was dissolved in a minimum amount of degassed, dry CH_2Cl_2 at 0°C . BBr_3 (1M in CH_2Cl_2 , 70 mL) was added via syringe and septum. This solution was allowed to warm to room temperature and stirring was continued for 24 hours, while maintaining an inert atmosphere. The solution was cooled to 0°C and excess BBr_3 was quenched with the dropwise addition of MeOH. The solvent was removed on the rotovap and the residue was co-evaporated with MeOH (15 X 50 mL) to leave an off-white solid.

yield: 3.2g (93.5%)

^1H nmr 360 MHz ($\text{D}_2\text{O}/\text{NaOD}$): δ 6.31 (dd, 3H), 5.89 (dd, 3H), 5.66 (t, 3H), 2.87 (t, 6H), 2.21 (t, 6H)

^{13}C nmr 360 MHz ($\text{D}_2\text{O}/\text{NaOD}$): δ 172.1, 163.1, 158.9, 118.1, 116.7, 114.6, 113.3, 52.9, 36.1

mass spec, positive ion FAB mNBA matrix: m/e 558 [M+4]

Tris-((2,3-dimethoxyphenylacetyl)aminoethyl)amine (47)

Tren (0.5g, 3.4 mmol) was dissolved in CH_2Cl_2 (150 mL) and H_2O (50 mL). To this solution was added 2,3-dimethoxyphenylacetyl chloride (2.14g, 0.01 mol) in CH_2Cl_2 (100 mL) and K_2CO_3 (1.4g, 0.01 mol) in H_2O (100 mL) dropwise over a 1/2 hour period. Stirring was continued at room temperature for 1 hour, followed by separation of the organic layer. This was washed with H_2O (2 X 100 mL), dried over anhydrous sodium sulphate, filtered and brought to dryness under reduced pressure. The solid was purified by centrifugal chromatography with a $\text{CH}_2\text{Cl}_2/\text{MeOH}$ mixture as the eluent.

yield: 2.3g (75%)

^{13}C nmr 250MHz (CDCl_3): δ 171.15, 152.72, 146.84, 129.38, 124.28, 122.58, 111.47, 60.51, 55.57, 54.01, 38.03, 37.88

mass spec: positive ion FAB mNBA matrix, m/e 681 [M+1]

Tris-((2,3-dimethoxyphenethyl)aminoethyl)amine (48)

Compound 47 (0.75g, 1.1mmol) was added to a LiAlH_4 slurry in THF (1.25g in 75 mL) at 0°C . The reaction mixture was heated to reflux and maintained at this condition for 24 hours. After cooling to 0°C the excess LiAlH_4 was destroyed by dropwise addition of H_2O . Diethyl ether (100 mL) was added, the solution was filtered and the filtrate was brought to dryness. The crude product was purified on a Sephadex gel column (LH-20) eluted with a 4:3 $\text{CHCl}_3:\text{MeOH}$ solution.

Yield 0.29g (42%)

^{13}C nmr 250MHz (CDCl_3) δ 152.77, 147.35, 133.89, 123.77, 122.20, 110.53, 60.62, 55.62, 54.57, 50.59, 47.60, 30.65

Tris-((2,3-dihydroxyphenethyl)aminoethyl)amine.5HBr (49)

Compound **48** (0.25g, 0.4mmol) was dissolved in dry CH_2Cl_2 (10 mL) and cooled to 0°C . BBr_3 (1M in CH_2Cl_2 , 15 mL) was added to the solution via syringe and septum. The reaction mixture was kept under an inert atmosphere and stirred at room temperature for 2 days. The solution was cooled to 0°C and excess BBr_3 was destroyed with the dropwise addition of MeOH. After co-evaporation with MeOH (10 X 50 mL) and recrystallization from MeOH/EtOAc, the grey solid was dried under vacuum.

yield: 0.25g (78%)

^{13}C nmr 360 MHz (D_2O): δ 155.52, 151.45, 127.96, 120.06, 119.63, 116.63, 55.68, 51.04, 47.99, 32.20

Analysis, Calc. for **49**.EtOAc (found): C 38.98% (38.49%), H 5.29% (5.10), N 5.35% (5.80%)

2.1.9 Synthesis of transition metal complexes of tren-catecholate systems

[Co(43)](ClO₄)₃ (50)

Compound **43** (0.01g, 0.017 mmol) was dissolved in MeOH (3 mL). To this solution was added $\text{Co}(\text{OAc})_2 \cdot 4\text{H}_2\text{O}$ (4.2 mg, 0.017 mmol). The solution was left to sit open to air for 1 week,

during which time a red oil formed. The oil was recrystallized from a solution of CH_3CN , EtOH , diethyl ether, and $\text{Ba}(\text{ClO}_4)_2$ by very slow cooling to yield red crystals.

yield: 9.8mg (61%)

[Ni(43)](ClO₄)₂ (51)

Compound **43** (0.01g, 0.017 mmol) was dissolved in MeOH (10 mL). $\text{Ni}(\text{OAc})_2 \cdot 4\text{H}_2\text{O}$ (4.2 mg, 0.017 mmol) was added and the solution was heated to 50°C for 1/2 an hour, at which time a pale violet solution resulted. This solution was reduced to an oil on the addition of $\text{Na}(\text{ClO}_4)$ and evaporation of solvent. All attempts at recrystallization were unsuccessful.

[Cu(43)](ClO₄)₂ (52)

Compound **43** (0.01g, 0.017 mmol) was dissolved in MeOH (10 mL). $\text{Cu}(\text{ClO}_4)_2 \cdot 6\text{H}_2\text{O}$ (6.3 mg, 0.017 mmol) was added and the solution was warmed to 50°C for 1/2 an hour. The solution turned blue and was left to evaporate to leave an oil. Attempts to recrystallize were unsuccessful.

Na₃[Fe(44)] (53)

Compound **44** (0.1g, 0.12 mmol) was dissolved in MeOH (200 mL) and this solution was degassed by bubbling with N_2 for 20 minutes. The solution was made alkaline by the addition of

Na_2CO_3 (0.5 M) until a pH of ~ 9 was reached. $\text{FeCl}_3 \cdot 6\text{H}_2\text{O}$ (32.7 mg, 0.12 mmol) in MeOH (200 mL) was added dropwise over a period of 3 hours. An inert atmosphere was maintained during the addition. The volume was reduced on the rotoevaporator to leave a purple solid.

yield: 38mg (46%)

Analysis, Calc. for **53** (found); C 51.36% (51.06%), H 4.79% (5.39%), N 8.87% (8.48%)

$\text{K}_3[\text{Al}(\mathbf{44})]$ (**54**)

Compound **44** (0.1g, 0.12 mmol) was dissolved in degassed MeOH (500 mL). The pH was adjusted to ~ 9 with the addition of K_2CO_3 (0.5 M). $\text{Al}(\text{NO}_3)_3 \cdot 6\text{H}_2\text{O}$ (38.5 mg, 0.12 mmol) in MeOH (200 mL) was added dropwise to the ligand solution over 3 hours. The volume was reduced to leave a light brown solid.

yield: 34mg (43%)

^{13}C nmr 360 MHz (d_6 -dmsO): δ 157.3, 156.1, 113.8, 112.3, 111.8, 110.6, 52.3, 51.3, 43.8

$\text{K}_3[\text{Fe}(\mathbf{46})]$ (**55**)

Compound **46** (1.0g, 1.1 mmol) was dissolved in degassed methanol (300 mL) and the pH was adjusted to ~ 12 with the addition of KOH (1 M). $\text{FeCl}_3 \cdot 6\text{H}_2\text{O}$ (0.27g, 1 mmol) in a methanol solution (100 mL) was added dropwise to the ligand solution. The complex precipitated out of solution on formation. The precipitate was filtered and dried in air.

yield: 0.5g (69%)

K₃[Al(46)] (56)

Compound **46** (1.0g, 1.1 mmol) was dissolved in degassed methanol (300 mL) and the pH was adjusted to ~12 with the addition of KOH (1 M). A methanolic solution (100 mL) of Al(NO₃)₃.6H₂O (0.32g, 1 mmol) was added dropwise to the ligand solution. The volume was reduced to ~150 mL and the complex precipitated out of solution. The solid was filtered and dried in air.

yield: 0.45g (65%)

K₃[Fe(49)] (57)

Compound **49** (50mg, 0.05 mmol) was dissolved in methanol (150 mL) and the pH was adjusted to ~12 with the addition of KOH (1 M). The ligand solution was deaerated by a continuous flow of N₂ through the solution. FeCl₃.6H₂O (13.5mg, 0.05 mmol) in methanol (100 mL) was added dropwise to the ligand solution. Once addition was complete, the complex was removed by filtration and dried in air.

yield: 11mg (30%)

2.1.10 Synthesis of Macrobicycles

1,4-Diaminopropyl-1,4,7-triazacyclononane (58)

This compound was isolated during the synthesis of

compound **7**. It was separated as the nickel complex on a Sephadex C-25 cation exchange column. The nickel was removed by boiling the complex in HCl (6 M) for 3 hours, and loading onto a Dowex 50 X 8 cation exchange column. The ligand was eluted with HCl (4 M), to yield the penta-hydrochloride salt. yield: (10%)

^{13}C nmr 250 MHz (D_2O): δ 52.7, 48.9, 48.3, 42.1, 36.7, 21.5

The solvent was removed and the residue dissolved in a minimum amount of NaOH solution (3 M) and extracted into CHCl_3 (3 X 50 mL). The combined fractions were dried over anhydrous sodium sulphate, filtered and the filtrate taken to dryness, to give the free ligand.

[Cu(**58**)](ClO_4)₂ (**59**)

Compound **58** (1.17g, 4 mmol) was dissolved in EtOH (95%, 100mL) and this solution was heated to 60°C. $\text{Cu}(\text{ClO}_4)_2 \cdot 6\text{H}_2\text{O}$ (1.88g, 4 mmol) was added to the ligand solution and the reaction mixture turned blue almost immediately. The solution was stirred overnight at room temperature to ensure complete metal coordination. The solvent was removed on the rotovap and the blue crystals were recrystallized from CH_3CN /diethyl ether.

yield: 1.6g (77%)

Analysis, Calc. for (**59**) (Found): C 28.49% (28.28%), H 5.77% (5.77%), N 13.84% (13.59%)

[Cu(61)](ClO₄)₂ (60)⁶⁹

Compound **59** (1g, 2 mmol) was dissolved in MeOH/H₂O (9/1, 1 L) in a three-necked round bottomed flask. A solution of glyoxal (40% in H₂O, 240 μL) in MeOH/H₂O (9/1, 500 mL) was added dropwise to the solution over a period of 12 hours at 50°C, under a N₂ atmosphere. After addition was complete the cyclization was checked by removing a small amount of the solution and adding HCl (50%). If the solution kept its blue color then the reaction was continued as follows. The reaction mixture was cooled to room temperature and NaBH₄ (0.19g, 5 mmol) was added. Additional NaBH₄ (0.4g, 10.5 mmol) was added and the solution refluxed for 2 hours. The solution was cooled to room temperature and the volume reduced. A purple solid appeared on cooling.

yield: 0.89g (81%)

1,5,8,12,15-Pentaazabicyclo[10.5.2]nonadecane (**61**)

Compound **60** (0.5g, 0.9 mmol) was dissolved in deionized H₂O (50 mL). An excess of Na₂S.9H₂O (3g, 12.5 mmol) was added and the reaction mixture was stirred with gentle heating (50°C) for 2 hours. The solution was cooled to room temperature and the black CuS was filtered off using a fine sintered frit. The filtrate, containing the free ligand, was extracted with CHCl₃ (4 X 75 mL) and the combined fractions were dried over anhydrous sodium sulphate. After filtration

and reduction to dryness the product was a colorless oil.

yield: 0.19g, 74%

^{13}C nmr 250 MHz (CDCl_3): δ 54.4, 53.1, 52.7, 47.3, 46.6, 45.1, 26.0

mass spec: M+1, 270; M+29, 298; M+41, 310

[Cu(9)][(ClO₄)₂] (62)

Compound **9** (1.17g, 4 mmol) was dissolved in EtOH (95%, 100mL) and this solution was heated to 60°C. $\text{Cu}(\text{ClO}_4)_2 \cdot 6\text{H}_2\text{O}$ (1.88g, 4 mmol) was added to the ligand solution and the reaction mixture turned blue almost immediately. The solution was stirred overnight at room temperature to ensure complete metal coordination. The solvent was removed on the rotovap and the blue crystals were recrystallized from CH_3CN /diethyl ether.

yield: 1.4g (62.5%)

Analysis, Calc. for $\text{Cu}(\mathbf{9})(\text{ClO}_4)_2 \cdot \text{HClO}_4$ (found): C 27.16% (27.49%); H 5.62% (5.28%); N 12.67% (12.55%)

[Cu(64)][(ClO₄)₂] (63)

Compound **62** (1.4g, 2.5 mmol) was dissolved in MeOH/ H_2O (9/1, 1 L) in a three-necked round bottomed flask. A solution of glyoxal (40% in H_2O , 250 μL) in MeOH/ H_2O (9/1, 500 mL) was added dropwise to the metal solution over a period of 12 hours

at 50°C, under a N₂ atmosphere. After addition was complete the cyclization was checked by removing a small amount of the solution and adding HCl (50%). If the solution kept its blue color then the reaction was continued as follows. The reaction mixture was cooled to room temperature and NaBH₄ (0.19g, 5 mmol) was added. Additional NaBH₄ (0.4g, 10.5 mmol) was added and the solution refluxed for 2 hours. The solution was cooled to room temperature and the volume reduced. A purple solid appeared on cooling.

yield: 1.1g (78%)

15-Aminopropylaza-1,5,8,12-tetraazabicyclo[10.5.2]nonadecane
(64)

Compound 63 (0.4g, 0.7 mmol) was dissolved in deionized H₂O (50 mL). An excess of Na₂S.9H₂O (3g, 12.5 mmol) was added and the reaction mixture was stirred with gentle heating (50°C) for 2 hours. The solution was cooled to room temperature and the black CuS was filtered off using a fine sintered frit. The filtrate, containing the free ligand, was extracted with CHCl₃ (4 X 75 mL) and the combined fractions were dried over anhydrous sodium sulphate. After filtration and reduction to dryness the product was a colorless oil.

yield: 0.14g (61%)

mass spec: M+1, 327

2.1.11 Synthesis of Co^{III} pentaammine Complexes

[CoCl(tacn)(diamine)][ZnCl₄] complexes (diamine = en (65), tn (66), amp (67))

One mole equivalent of tacn.3HCl (0.5g in 15 mL water) was reacted at room temperature with an aqueous slurry (15 mL) of Na₃Co(CO₃)₃.3H₂O (0.76g) to give a clear red solution. One mole equivalent of the appropriate diamine was then added dropwise and the solution warmed to 40°C. Upon slow addition of 3 M HCl (effervescence), a clear orange acidic solution was obtained. Solid ZnCl₂ (5g) was added and heating at 80°C was continued (1-2 hours) to give a crystalline deposit of red [CoCl(tacn)(diamine)][ZnCl₄]. Yields were about 50% based on tacn.3HCl. The salts were recrystallized quantitatively from 0.1 M HCl by the addition of 3 M HCl and solid ZnCl₂.

[CoCl(tacn)(en)][ZnCl₄] (65); λ_{\max} = 523nm (79.7), 362nm (77.7), weak shoulder at 480nm

¹³C nmr (D₂O): 51.59, 51.47, 51.14, 51.05, 44.52, 44.40.

[CoCl(tacn)(tn)][ZnCl₄] (66); λ_{\max} = 537nm, 371nm, moderate shoulder at 480nm

¹³C nmr (D₂O): 53.84, 53.55, 52.70, 40.69, 40.53, 40.42, 27.85.

[CoCl(tacn)(amp)][ZnCl₄] (67); λ_{\max} = 521nm, 361nm, weak shoulder at 470nm

¹³C nmr (D₂O): 165.19, 151.39, 140.99, 126.40, 122.86, 53.52, 53.33, 53.17, 49.99, 49.92, 49.33, 49.08.

[CoCl(dien)(amp)][ZnCl₄] (68, 69, 70)

An aqueous mixture (50 mL) of Co(NO₃)₂·6H₂O (3.0g), dien (1.0 mL), and amp (1.0 mL) was oxygenated with dioxygen gas at room temperature for 30 minutes to give a chocolate brown solution. The solution was cooled in an ice bath to yield a sticky brown-black solid. Further attempts to isolate the μ -peroxo intermediate were discontinued. However, upon addition of hydrochloric acid (50 mL, 6M) and ZnCl₂ (5g), and heating to 60°C until effervescence was complete, a pink coloured solution formed. The solution was left for about two weeks at room temperature, and the crystalline material that deposited was removed periodically. As each crop was isolated, it was recrystallized as the ZnCl₄²⁻ salt by dissolving in warm 0.1 M HCl and adding 3 M HCl and solid ZnCl₂. The yield and IR spectrum of the recrystallized material were recorded.

The first three crops (1.19g total) had identical IR spectra and were combined and further recrystallized. The ¹³C nmr spectrum of the dien region (54.34, 53.37, 49.79, 44.36, 43.16) is consistent with unsym-fac coordination¹³⁸ (68). Based upon IR information, crop 4 (1.04g) contained a new isomer and the dien fragment ¹³C nmr (54.74, 54.28, 49.77, 43.07, 42.78) again indicates unsym-fac coordination¹³⁸ (69). Likewise, crop 5 (0.21g), a third isomer, had a visible absorption spectrum indicating mer-dien coordination (70). ($\lambda_{\text{max}}=360, 483, \text{sh } 525\text{nm}$). This isomer was not used in the kinetic studies.

[CoCl(bicycloN₅)] [ZnCl₄] (71)

An aqueous solution of Co^{II}(ClO₄)₂·6H₂O (105 mg,) in ~10 mL was added to a refluxing solution of bicycloN₅ (77 mg,) in EtOH/H₂O (80/20, 50 mL). The reaction mixture turned green almost immediately, and the addition of a catalytic amount of activated charcoal yielded a pink solution. The solution was refluxed for 2 hours and saturated with air. After cooling to room temperature the charcoal was removed by filtration and one drop of HClO₄ (9 M) was added to the filtrate. Following purification by Sephadex gel filtration, the [ZnCl₄]²⁻ salt was prepared in the manner described above.

λ_{\max} =553nm(80), 377nm(106), moderate shoulder at 484nm

¹³C nmr (D₂O): 61.65, 58.95, 57.95, 52.99, 51.85, 48.04, 23.97

(Figure 6.4).

2.2 Methods and Materials**2.2.1 Instrumentation****2.2.1.1 Spectroscopy**

All ¹H nmr spectra were recorded on either a Perkin-Elmer R32 90 MHz or a Bruker WM250 MHz or AMX360 MHz spectrometer. All chemical shifts are referenced to tetramethylsilane (TMS) at 0 ppm. ¹³C nmr spectra were recorded on a Bruker WM250 MHz spectrometer or a Bruker AMX360 MHz spectrometer, and again were referenced to TMS at 0 ppm.

Infrared spectra were recorded on either a Bruker IFS25

spectrometer or a Perkin-Elmer 1330 spectrometer. Samples were studied as KBr discs, Nujol mulls, or in CH_2Cl_2 solution.

Electron spin resonance (esr) spectra were recorded on a Varian E6 spectrometer. All spectra were referenced to the standard diphenylpicrylhydrazyl radical (dpph). Samples were studied either as a solution at room temperature or as a frozen solution at 77°K.

Ultraviolet - visible (uv-vis) spectra were obtained on either a Cary 5 uv-vis-nir spectrophotometer or a Phillips PU8870 spectrophotometer. All samples were generally studied as solutions in 1 cm quartz cells at ambient temperature. The anation reactions of the Co^{III} pentaammine complexes which were measured at 50°C.

Samples for mass spectrometry were submitted to the mass spectral service at the University of Victoria. Mass spectra were recorded as CI on a Finnegan 3300 GCMS system or as liquid secondary ion mass spectra (LSIMS) on a Kratos Concept double focusing magnetic instrument.

Centrifugal chromatography was performed on a Harrison Research chromatotron, model 7924T. The plates were coated with TLC grade silica gel (Merck) with gypsum binder and fluorescent indicator.

Elemental analyses were performed by Canadian Microanalytical Services, Vancouver, B.C.

2.2.2.1 Materials

All starting materials were purchased from Aldrich Chemicals with the exception of 2,3-dimethoxyphenylacetic acid which was purchased from Trans World Chemicals. These compounds were used without further purification. Solvents were in general reagent grade. Dichloromethane was distilled, and acetonitrile was distilled over calcium hydride.

CAUTION! Perchlorate salts are explosive and care should be taken when these compounds are handled.

2.2.2.2 Kinetic Methods

Base hydrolysis rates were determined using an Applied Photophysics stopped flow apparatus with the temperature controlled to $\pm 0.1^\circ\text{C}$. One syringe was charged with a solution of the complex ($\sim 10^{-4}$ M) dissolved in aqueous NaClO_4 (1.0 M) solution, while the other contained the appropriate $\text{NaOH}/\text{NaClO}_4$ (I=1.0 M) mixture.

The rates of anation reactions were measured on a Cary 5 spectrophotometer with the temperature controlled to $\pm 0.1^\circ\text{C}$. All reactions were carried out at 50°C with the exception of the $[\text{SCN}^-]$ dependence on the rate of anation of the $[\text{Co}(\text{tacn})(\text{en})(\text{OH}_2)]^{3+}$ complex which was measured at 60°C . The concentration of complex in each case was $\sim 10^{-4}$ M and that of the anion was 0.6 M for all pH dependence measurements. The pH values of the solutions were measured with a Fisher Scientific Accumet pH meter 910 and Ingold U402-M6-S7 semi-

micro combined pH electrode. All pH values were corrected using a 0.01 M Borax/0.99 M NaClO₄ solution. The ionic strength was maintained at 1.0 M (NaClO₄).

The chloro complexes of the Co^{III}pentaammine systems were hydrolysed with 0.01 M NaOH for approximately 20 minutes at room temperature. The pH was adjusted with 0.1 M HClO₄ to ~ 6 or 7, and any Zn(OH₂) from the counter-ion was removed by millipore filtration. At this time it was mixed with the appropriate anion solution and the pH adjusted with either 0.1 M HClO₄ or 0.1 M NaOH, in the 1 cm quartz cells. The cells were placed in the spectrophotometer and allowed to equilibrate to 50°C before monitoring the reaction. The kinetic data were recorded at 300nm for [Co(tacn)(en)(OH₂)]³⁺ and at 320nm for the [Co(bicycloN₅)(OH₂)]³⁺ complex.

CHAPTER 3
TAPTACN-CATECHOLATE SYSTEMS

3.1 Ligand Synthesis

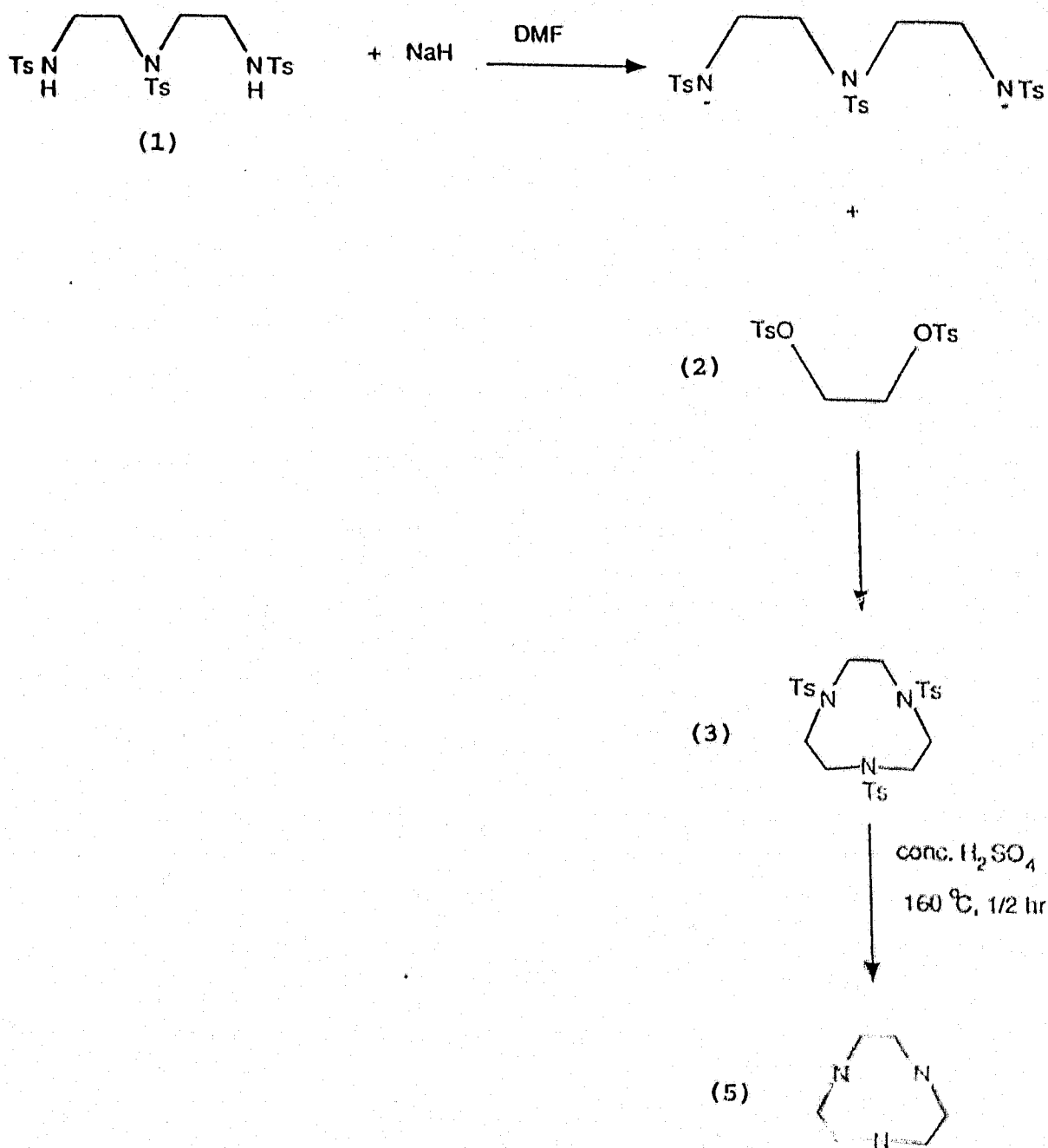
3.1.1 1,4,7-Triazacyclononane

The compound 1,4,7-triazacyclononane (5) was successfully prepared by a slight modification of the Richman/Atkins method⁷⁰. The cyclization reaction between the tri-tosylated diethylenetriamine and the ditosylate of ethylene glycol was carried out on a 0.5 molar scale with impressive yields of 90% or greater.

Detosylation of the cyclized product was carried out⁷¹ in conc. H_2SO_4 at 160°C. The yields are improved markedly when the reaction is carried out on a 50 g scale as opposed to a 75 g scale as suggested⁷², provided the initial compound is extremely dry. Yields of the HCl salt were on the order of 85% or greater.

The isolation of the free ligand, however, results in lower yields (60-65%). The reason of course is that it is difficult to extract all the free amine into organic solvents as the amines are extremely hygroscopic and water soluble, thus accounting for the lower yield. The synthesis is outlined in Scheme 3.1.

Scheme 3.1 Synthesis of 1,4,7-triazacyclononane



3.1.2 Taptacn

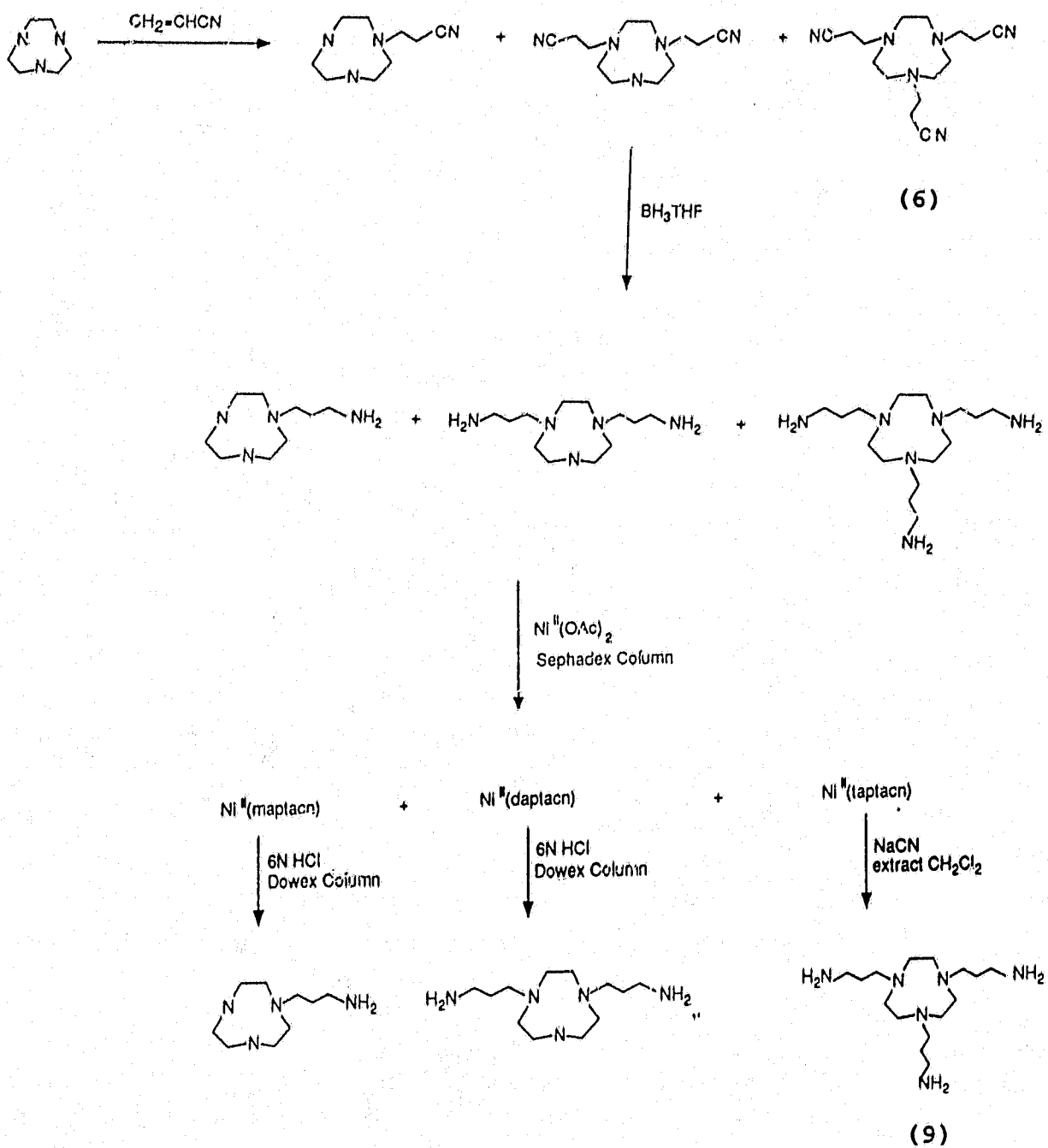
Literature procedures were followed for the preparation of 1,4,7-triaminopropyl-1,4,7-triazacyclononane (9) (taptacn)^{72,73}, and the synthesis is outlined in Scheme 3.2.

The first step involves a Michael addition of acrylonitrile to [9]ane-N₃, which is followed by the reduction of the tri-nitrile derivative to the primary amines. Although the use of sodium metal in toluene was reported⁷³, the method of choice for the reduction was to use the BH₃.THF complex. Provided that the conditions for the workup remain somewhat "mild" (i.e. reflux in 3/9/30 HCl/H₂O/MeOH for 3 hours as opposed to 4 M HCl in MeOH for 1 hour), the yields are acceptable (~75-80%).

In the preparation there was always the formation of the mono- and di-armed derivatives. The most successful separation of these three compounds was as the nickel (II) complexes on a Sephadex cation exchange column, followed by removal of the metal ion.

In the case of Ni(taptacn)²⁺, the metal ion was removed with sodium cyanide in almost quantitative yields, resulting in either a white hygroscopic solid or a colorless oil.

Scheme 3.2 Synthesis of taptacn



3.1.3 Taptacn-catecholate Systems

The first compound prepared, 1,4,7-tris-((2,3-dimethoxybenzoyl)aminopropyl)-1,4,7-triazacyclononane (11) (see Scheme 3.3), followed a procedure of Raymond *et al*⁷⁴. The process involved the reaction of three equivalents of an acyl chloride with three primary amines under modified Schotten-Baumen conditions. The overall yield was approximately 65% for the reaction.

Owing to hydrogen bonding of the catechol moieties with the reactive functional group (acid chloride or aldehyde in the preparation of compound 13) it was necessary to protect these groups as the methoxy derivatives.

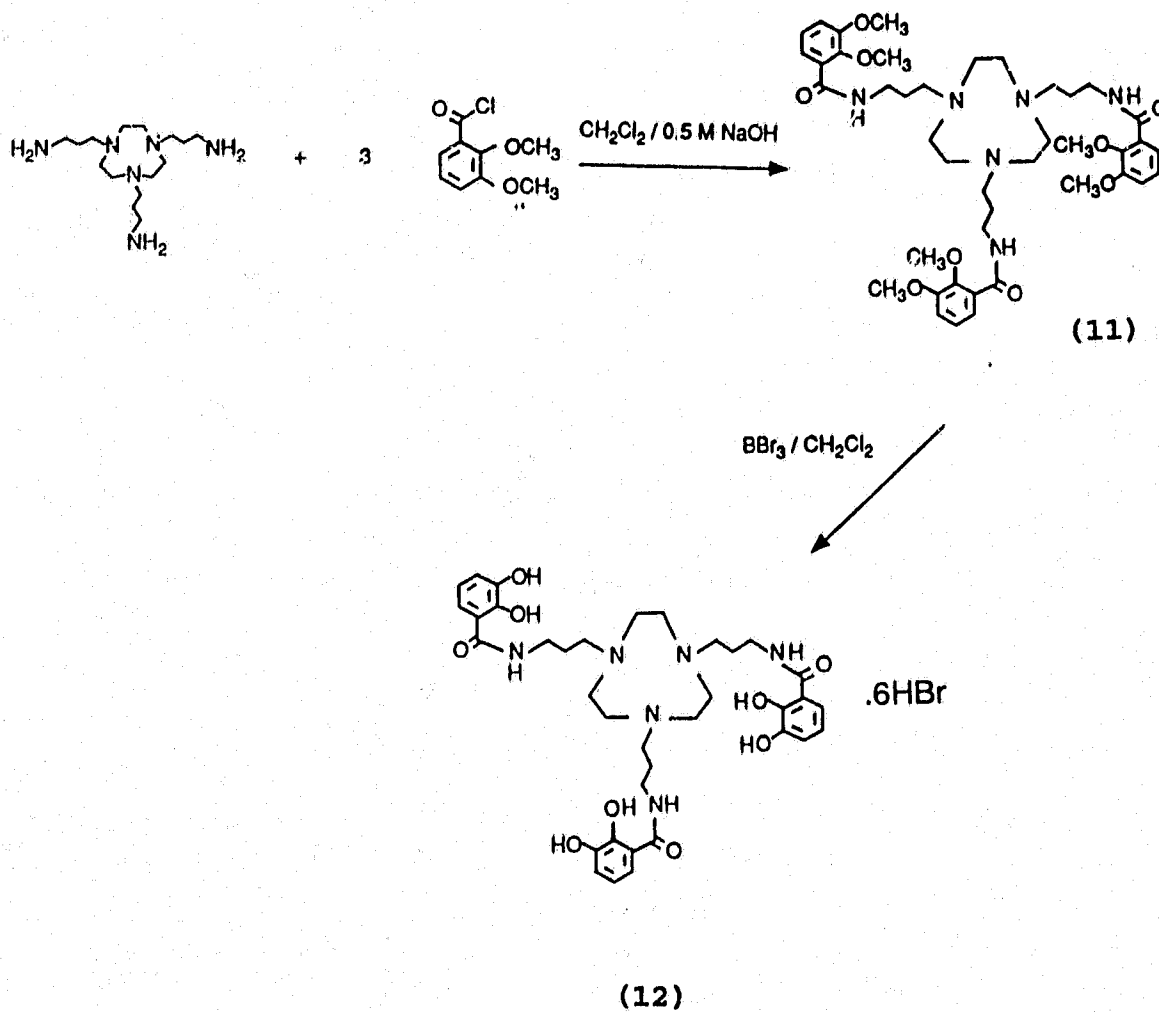
There are several reported methods of deprotection of these methoxy groups^{75,76}. However, the method of choice was by BBr_3 in dichloromethane solution, resulting in the HBr salt of the ligand in quantitative yields.

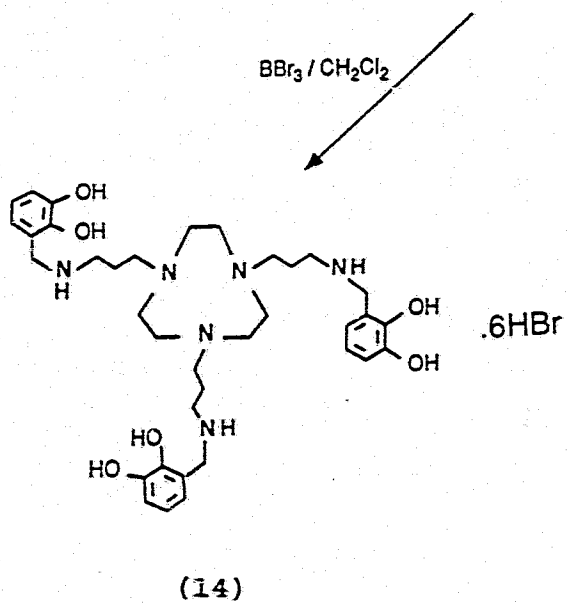
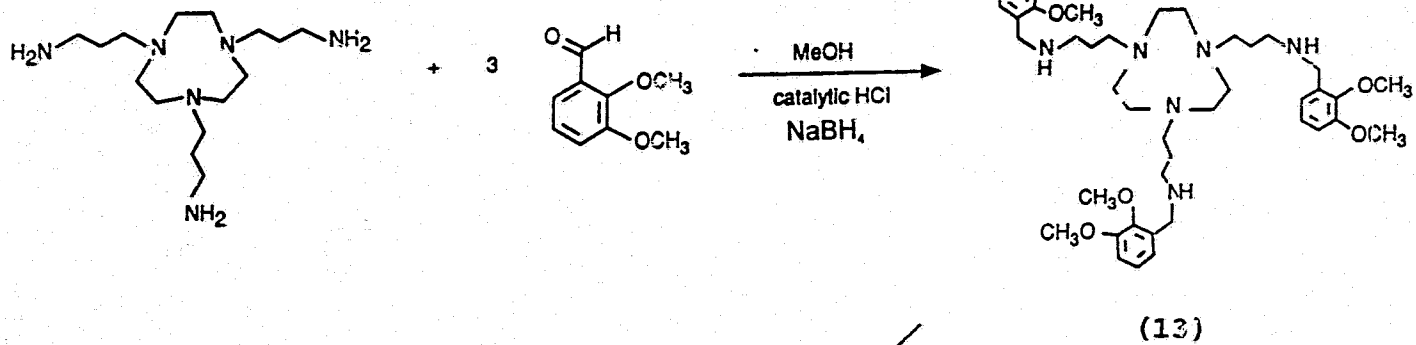
The ligand appears to be quite stable to oxidation if it is stored as the dry hexa-hydrobromide salt, but in solution it must be kept under an inert atmosphere to prevent oxidation of the unprotected catechols.

Attempts at reducing the protected amide were unsuccessful in the purification steps, therefore the reduced compound was prepared via an acid-catalysed Schiff base condensation, a reaction of the primary amines with 3 mole equivalents of the aldehyde (see Scheme 3.4). The imine formed was reduced *in situ* with the addition of sodium

borohydride. The compound was isolated in quantitative yields.

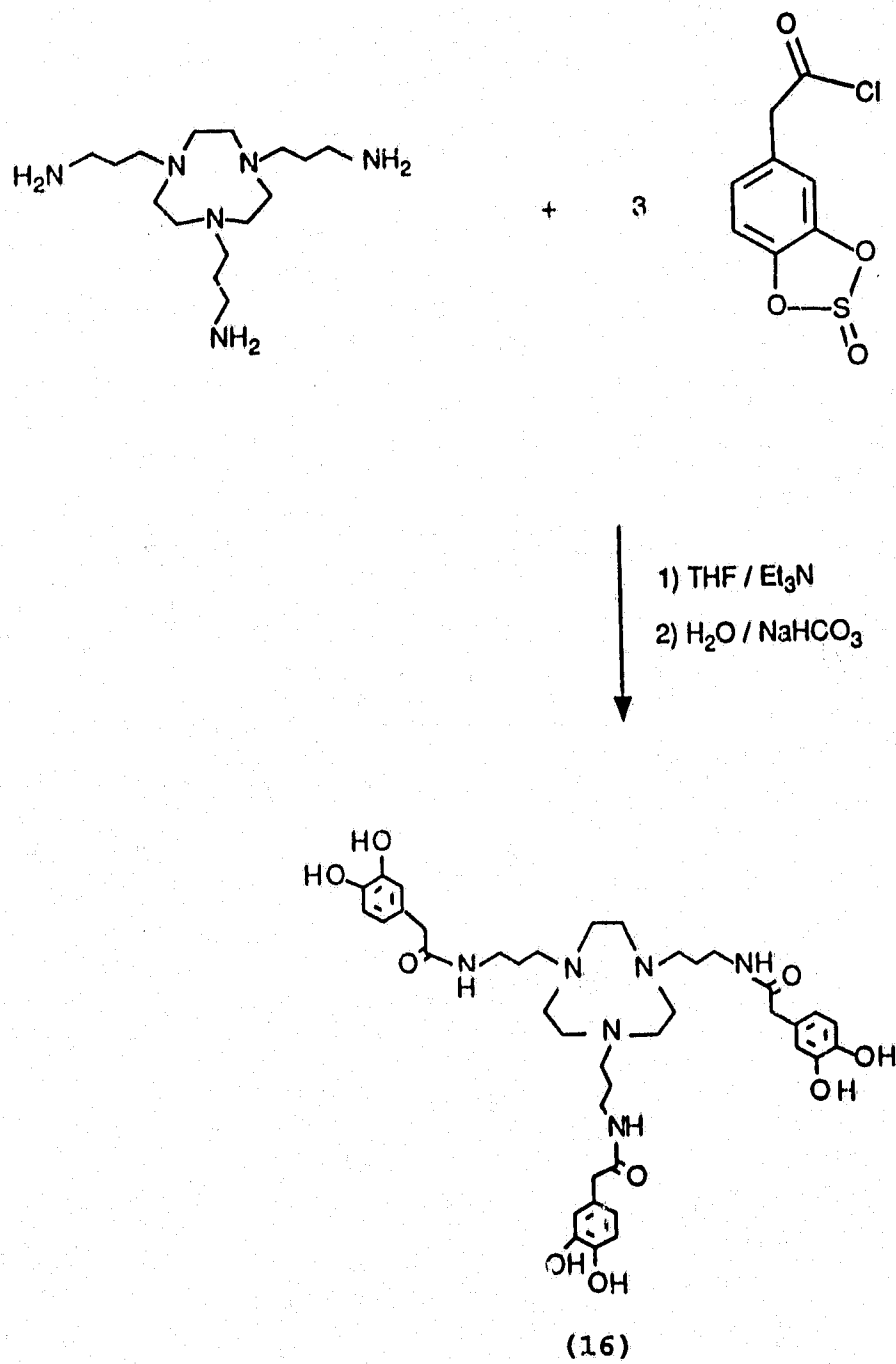
Scheme 3.3 Synthesis of compound 12





Scheme 3.4 Synthesis of compound 14

Scheme 1.5 Synthesis of compound 16



1,4,7-Tris-((3,4-dihydroxyphenylacetyl)aminopropyl)-1,4,7-triazacyclononane (16) was prepared following a procedure of Corey et al⁷⁷ where he and coworkers synthesized enterobactin.

The reaction of 3 mole equivalents of 3,4-dioxosulfonylphenylacetyl chloride with taptacn in THF resulted in the desired product upon removal of the sulfonyl groups (Scheme 3.5). The dihydroxy groups become protected during the synthesis of the acid chloride. Difficulty was found in the removal of the $\text{NEt}_3 \cdot \text{HCl}$ from the THF solution. Although it should theoretically precipitate out of the THF solution, the triethylamine is extremely hygroscopic and this prevents its removal. For this reason again the preferred method of preparing the catechol-amine systems was by using the methoxy protected catechol derivatives.

3.2 Metal Complexes of Taptacn-Catecholate Systems

3.2.1 Ferric Complexes

3.2.1.1 Synthesis

To prevent polymer formation the ferric complexes of ligands 12, 14, and 16 were prepared under anaerobic and high dilution conditions. The highly colored purple compounds precipitated out of a methanol solution upon the addition of a base (K_2CO_3). Although $\text{FeCl}_3 \cdot 6\text{H}_2\text{O}$ was used in the preparation of these compounds when the project was first

use of Fe(acac), in a metathesis reaction with the catecholate ligands is preferred. Owing to the high insolubility of these complexes, all attempts at crystallization were unsuccessful.

3.2.1.2 Electronic Spectra

The absorption spectra for the ferric complexes of compounds 12, 14, and 16 (complexes 21, 22, and 23) are shown in Figures 3.1 and 3.2. The spectral data of these complexes and other selected tris-catecholate ferric complexes are tabulated in Table 3.1.

All of the complexes, except two, exhibit a broad, intense band in the 500 nm region of the visible spectrum, characteristic of Fe(III)tris-catecholate species. $\text{Fe}(\eta^3\text{-cat})_3^{3+}$ and $\text{Fe}(\text{bicappedTrenCam})_3^{3+}$ display two absorption bands; one centered at around 430 nm and the other at approximately 520 nm. These transitions are assigned as ligand-to-metal charge transfer bands (LMCT), an assignment supported by the associated high extinction coefficients. No ligand field transitions are observed since they are weak and obscured by the intense charge transfer bands.

The tris-catecholate complex, $\text{Fe}(\text{cat})_3^{3+}$ represents a simple model of enterobactin and its synthetic analogues. Despite esr^{78} , variable temperature magnetic susceptibility⁷⁹,

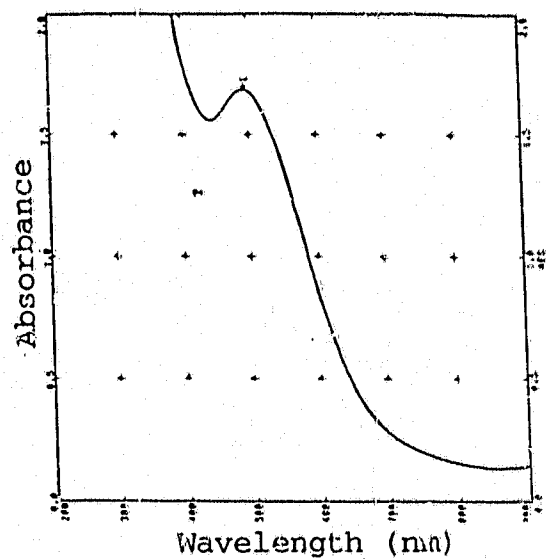
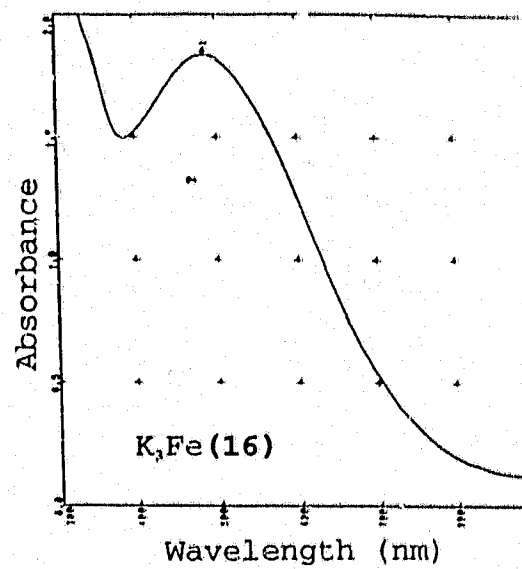
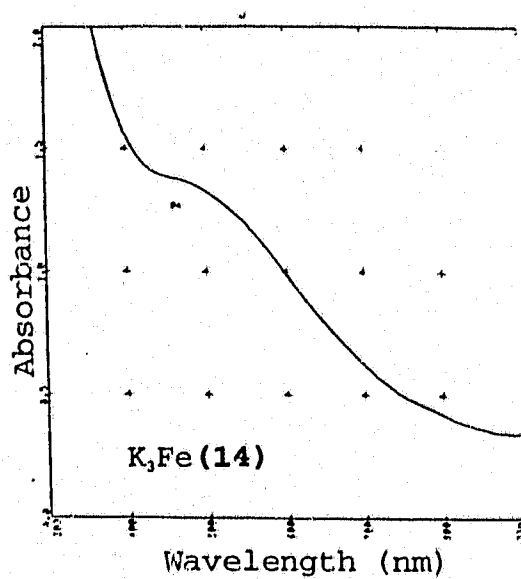
Figure 3.1 Visible spectra of Fe(12)^{3-} Figure 3.2 Visible spectra of Fe(14)^{3-} and Fe(16)^{3-} 

Table 3.1 Electronic spectra of ferric tris-catecnolate complexes

Complex	λ_{\max} , nm ($\epsilon, M^{-1}cm^{-1}$)	Ref.
Fe(enterobactin) ³⁻	495 (5600)	89
Fe(trencam) ³⁻	496 (4900)	89
Fe(bicappedTrencam) ³⁻	511 (5700) 425 (7300)	91
Fe(12) ³⁻	496 (5100)	a
Fe(14) ³⁻	481 (4700)	a
Fe(16) ³⁻	485 (4800)	a
Fe(cat) ₃ ³⁻	487	90
Fe(eta) ₃ ³⁻	538 (4600) 437 (4800)	90, b

a. this work

b. eta = 2,3 dihydroxyethylterephthalamide

and Mossbauer⁸⁰ data, illustrating that $\text{Fe}(\text{cat})_3^{3-}$ has an $S=5/2$ ground state (high spin), Gordon and Fenske⁸¹ have calculated an $S=1/2$ ground state based on Fenske-Hall molecular orbital calculations⁸². This has been disputed again by a detailed analysis of ferric tris-catecholates reported by Karpishin et al⁸³. The latter authors present evidence (based on magnetic circular dichroism and single crystal polarised absorption techniques) that the broad band in the absorption spectrum is actually composed of two overlapping x,y transitions. These transitions are, however, resolved in the $\text{Fe}(\text{eta})_3^{3-}$ and $\text{Fe}(\text{bicappedTrenCam})_3^{3-}$ spectra. The molecular orbital energy diagram for ferric tris-catecholates is depicted in Figure 3.3. The charge transfer transitions I and II are those discussed (in the 500 nm region).

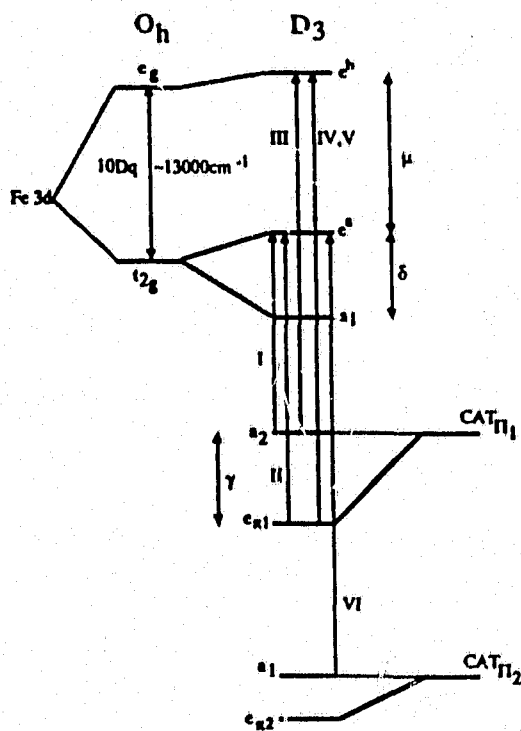


Figure 3.3 Energy level diagram for $\text{Fe}(\text{III})$ tris-catecholates

3.2.2 Nitrogen-Coordinated Metal Complexes of Taptacn-Me₆Catecholates

Metal complexes of the nitrogen-coordinated ligand (14) were prepared from the catechol protected species (13). Unsatisfactory results in the amide reduction of compound 16, allowed no investigation of the nitrogen coordinated metal complexes of this ligand.

The reaction of one mole equivalent of $\text{Cu}(\text{ClO}_4) \cdot 6\text{H}_2\text{O}$ with compound 13 resulted in the isolation of two separate compounds on a Sephadex cation exchange column. The electronic spectra are shown in Figure 3.4 and the esr are shown in Figure 3.5.

The first compound isolated was yellow in color and had λ_{max} at 463 nm and a shoulder at ~ 600 nm. The esr spectrum was characteristic of copper (II) with $g_1=2.32$ ($A_1=170$ G) and $g_2=2.032$. Superhyperfine coupling to the coordinated nitrogen atoms was either not detected or not resolved. The second, blue compound isolated showed only one absorption in the visible spectrum at 645 nm. The esr, again typical of copper (II), had $g_1=2.22$ ($A_1=165$ G) and $g_2=2.067$. Coupling to the nitrogen atoms was undetected.

For comparison to the above compounds, the simpler $\text{Cu}(\text{taptacn})^{2+}$ and $\text{Cu}(\text{bicycloN}_6)^{2+}$ were prepared, as well as the previously reported⁷² $\text{Cu}(\text{daptacn})^{2+}$ and $\text{Cu}(\text{bicycloN}_5)^{2+}$. The results of the electronic spectra are reported in Table 3.2.

The absorption data, together with micro-analyses provide

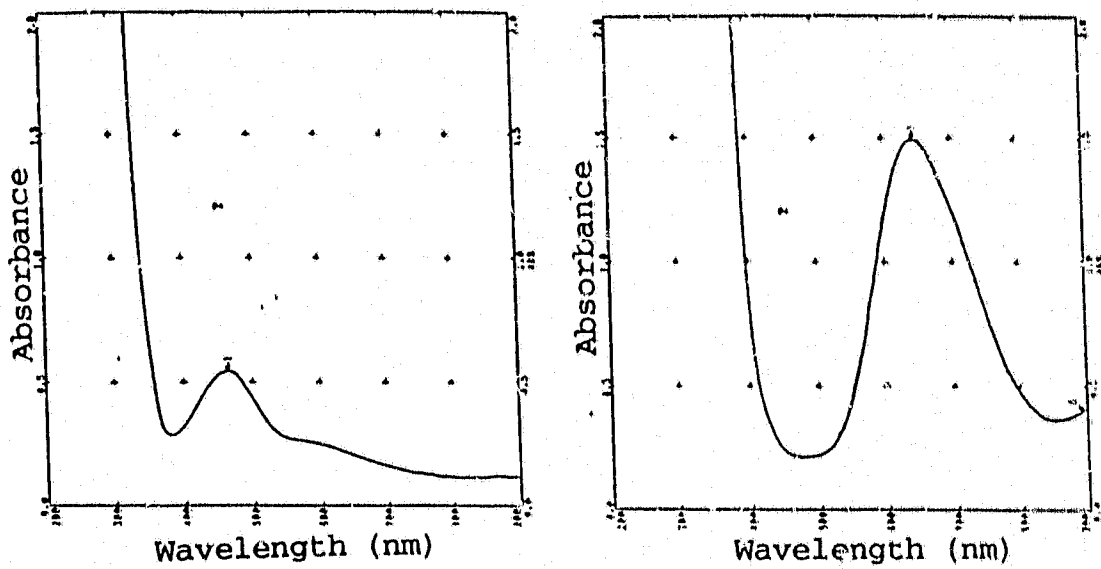
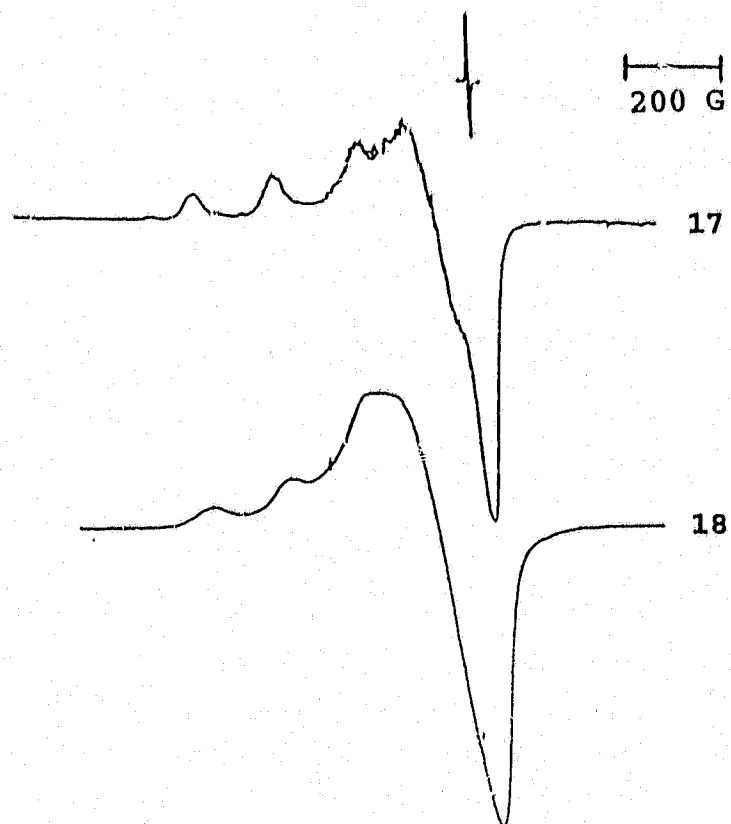
Figure 3.4 Visible spectra of compounds 17 and 18**Figure 3.5 ESR spectra of compounds 17 and 18**

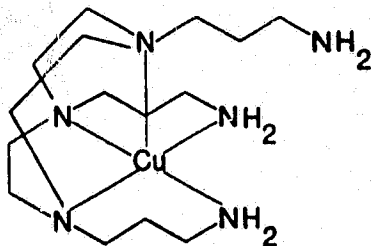
Table 3.2 Electronic absorption data for Cu(II) complexes

Complex	λ_{\max} , nm (ϵ , $M^{-1}cm^{-1}$)	Ref.
17	465 (208) 600 (sh)	a
18	645 (152)	a
Cu(daptacn) ²⁺ (59)	578 (106) 865 (39)	b
Cu(bicycloN ₅) ²⁺ (60)	276 (5700) 567 (145) 859 (42)	b
Cu(daptacn) ²⁺ (62)	278 (5300) 581 (98) 867 (39)	a
Cu(bicycloN ₆) ²⁺ (63)	280 (5500) 558 (135)	a

a. this work

b. Ref. 72

evidence that the $\text{Cu}(\text{taptacn})^{2+}$ is only five-coordinate, and the ability to synthesize the bicyclo N_6 compound via template method suggest the following structure, where the two



coordinated pendant amines are in the equatorial positions.

In the catecholate ligand systems the Cu (II) atom probably exists in a similar geometry, although the visible spectrum suggests some distortion of the square pyramidal structure. This is also demonstrated by esr spectroscopy through the change in the hyperfine coupling with the copper nucleus ($A_{\parallel}=170$ G versus $A_{\parallel}=190$ G for $\text{Cu}(\text{taptacn})^{2+}$).

The nickel or cobalt complexes of the catecholate ligands, discussed further in the next section, were not isolated.

3.2.3 Attempts at preparation of Binuclear Taptacn-Catecholate Systems

The synthesis of binuclear complexes was attempted in two ways:

- (1) first incorporate the appropriate metal into the N_6 system, followed by coordination of the ferric ion to the catecholate end of the ligand;
- (2) coordinate ferric ion first, and then react with the

appropriate metal ion for incorporation into the nitrogen donor system.

Method (1) appears to be the most promising approach for several reasons including,

(1) the metal should more easily coordinate in the N_6 position since it would not be forcing its way into a rigid cage;

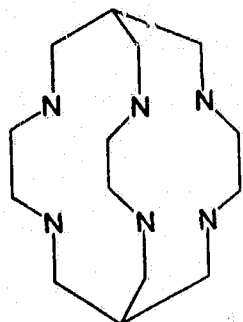
(2) by coordinating the N_6 system the three catechols would be maintained in a position suitable for coordination to ferric ion, limiting possibilities of polymer formation, and;

(3) a "preformed geometry" for the ferric ion would increase its formation constant.

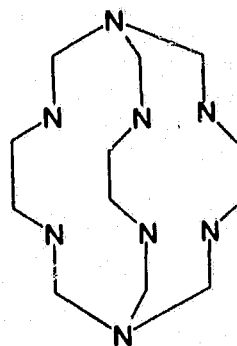
All attempts at binuclear coordination of these ligand systems were unsuccessful regardless of which metal was used in coordination to the N_6 moiety or which approach was taken in their synthesis. These results were at first surprising. However, examination of the crystal structures of the $M(\text{taptacn})^{n+}$ complexes⁷² provided an explanation.

Cage ligands such as sarcophagine⁸⁴ (sar) and sepulchrates^{85,86} (sep) have been synthesized by capping $\text{Co}(\text{en})_3^{3+}$ with formaldehyde and ammonia or with formaldehyde and nitromethane. These techniques are applicable only to those systems where the metal centre is substitution inert. $\text{Co}(\text{taetacn})^{3+}$ can also be encapsulated by the above procedures⁸⁷, but attempts at capping $\text{Co}(\text{taptacn})^{3+}$ and

$\text{Ni}(\text{taptacn})^{2+}$ were unsuccessful⁷².



sar



sep

The bite distances of the primary amines in $\text{Co}(\text{taptacn})^{3+}$ (2.749 Å)⁷² are smaller than those of the analogous $\text{Co}(\text{taetacn})^{3+}$ (2.769 Å) indicating enclosure of the metal centre and folding in of the pendant primary amine arms. This encapsulation imposes enough strain on the system such that extension of the arms (with the catechols) prevents coordination of the pendant nitrogen atoms. This is also consistent with the inability to cap $\text{Co}(\text{pn})^{3+}$ ⁸⁸.

This dilemma could be overcome by two different approaches:

- (1) choose a ligand with larger bite distances (taetacn instead of taptacn), or;
- (2) prevent encapsulation of the metal centre by coordinating a larger metal.

$\text{Pd}(\text{taptacn})^{2+}$ was synthesized, however, capping reactions were unsuccessful (with formaldehyde and nitromethane). For this

reason, the synthesis of taetacn and taetacn-catecholates was carried out as discussed in the next chapter.

CHAPTER 4
TAETACN-CATECHOLATE SYSTEMS

4.1 Ligand Synthesis

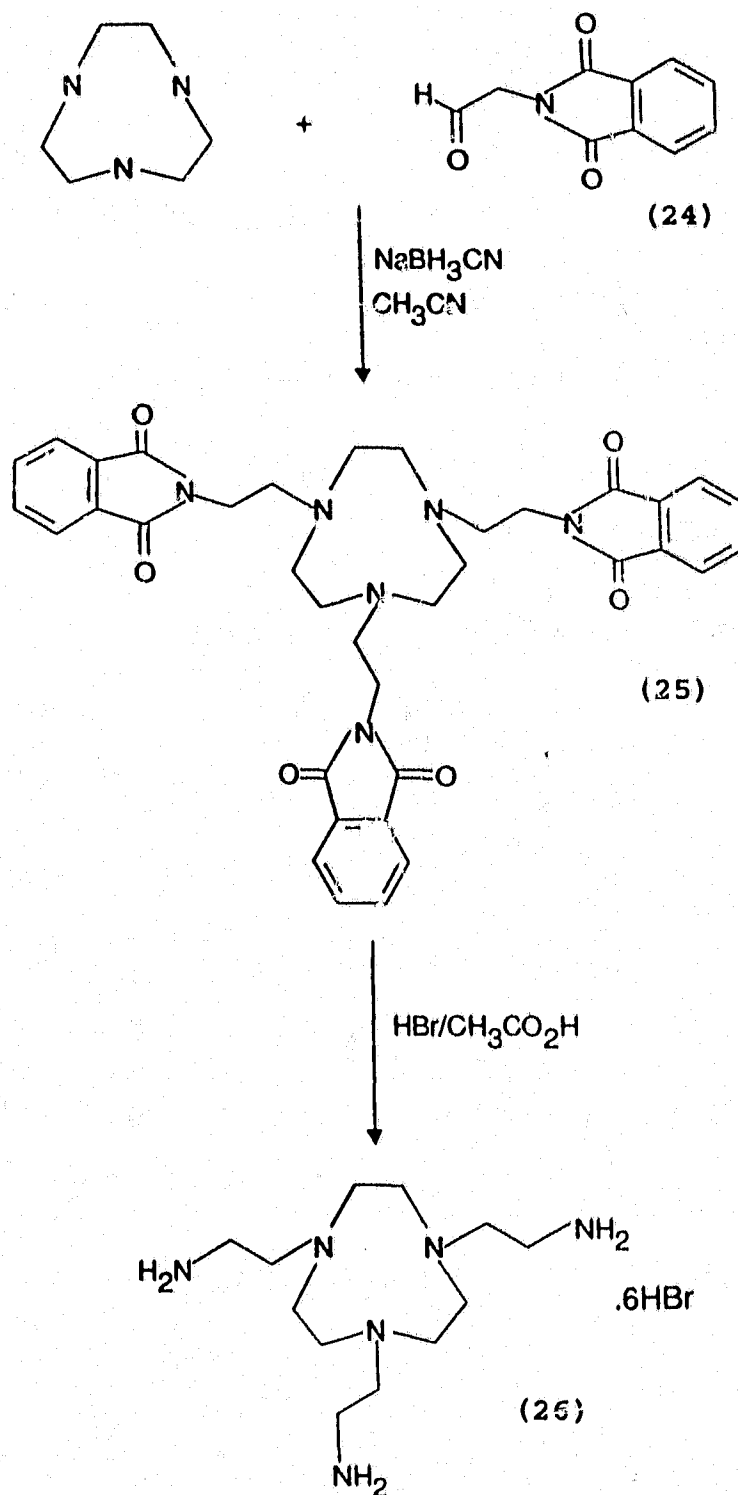
4.1.1 Synthesis of Taetacn

Successful preparation of 1,4,7-triaminoethyl-1,4,7-triazacyclononane (taetacn, 26) was achieved following the method of Sargeson *et al.*⁹² (Scheme 4.1). The procedure utilizes a Strecker synthesis in which three equivalents phthalimidoacetaldehyde are reacted with [9]-aneN₃. The imine formed in the reaction was reduced in situ, with the addition of sodium cyanoborohydride. The protecting group was cleaved as phthalic acid with a HBr/CH₃CO₂H mixture.

Purification of the crude product was carried out as the cobalt (III) complex. The complex was prepared in aqueous solution from Co(OAc)₂·4H₂O in the presence of activated charcoal to catalyze the oxidation of Co(II) to Co(III). The Co(taetacn)³⁺ species was eluted from a Dowex cation exchange column by use of 4-6 M HCl. Recrystallization from H₂O/NaClO₄ or ZnCl₂/HCl resulted in the pure complex either as the [Co(taetacn)](ClO₄)₃ complex or as the [Co(taetacn)][ZnCl₅] complex. Unfortunately the yield was not as high as expected, resulting in only 4.22g (26%) of the pure Co(taetacn)³⁺ ion. The ¹³C NMR of the complex is shown in Figure 4.1.

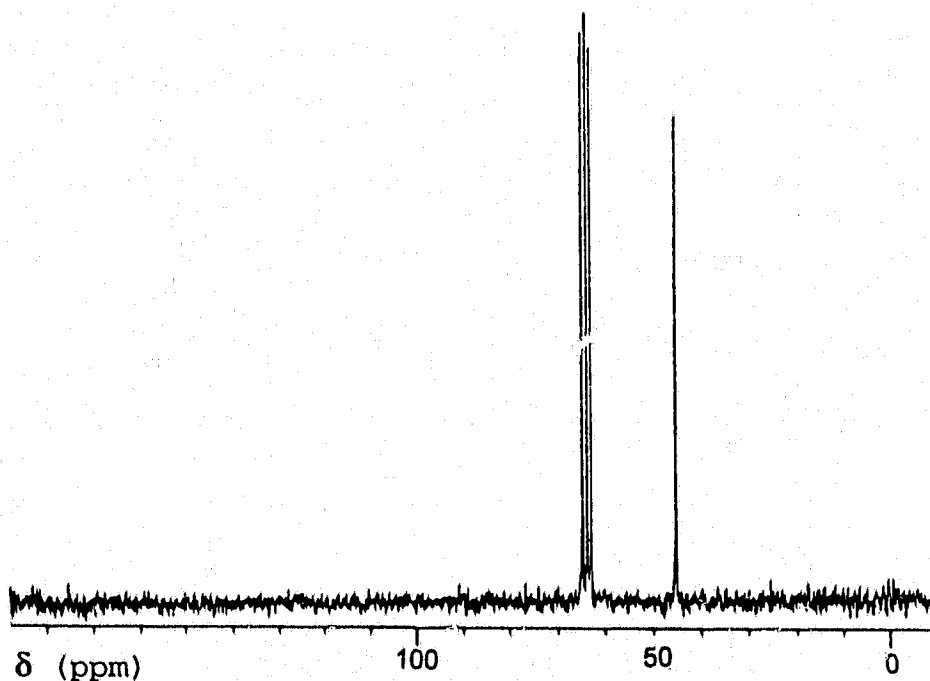
Attempts at removing the cobalt from the complex to obtain the free ligand, by various methods (H₂S or Zn/HCl), were not successful and resulted either in decomposition or isolation of the starting material. The reaction of the

Scheme 4.1 Preparation of Taetacn



complex with 2,3-dimethoxybenzaldehyde in acetonitrile resulted only in isolation of the starting materials.

Figure 4.1 ^{13}C NMR of $[\text{Co}(\text{taetacn})][\text{ClO}_4]_3$ in D_2O .



Other methods of preparing the free ligand, taetacn, were sought. These included the reaction of [9]-ane N_3 with aziridine, tosylaziridine and bromoacetonitrile (see Scheme 4.2). The first two reactions showed significant polymer formation. Purification on a Sephadex cation exchange column as the Cu^{2+} complex ion showed mostly polymer that could not be removed from the column even with 5M NaCl. The reaction with bromoacetonitrile resulted in complete decomposition with the formation of black oils that could not be characterized.

A totally different synthetic approach was required, and therefore a new perspective of the target ligand. Figure 4.2

Scheme 4.2 Alternate methods of preparing taetacn

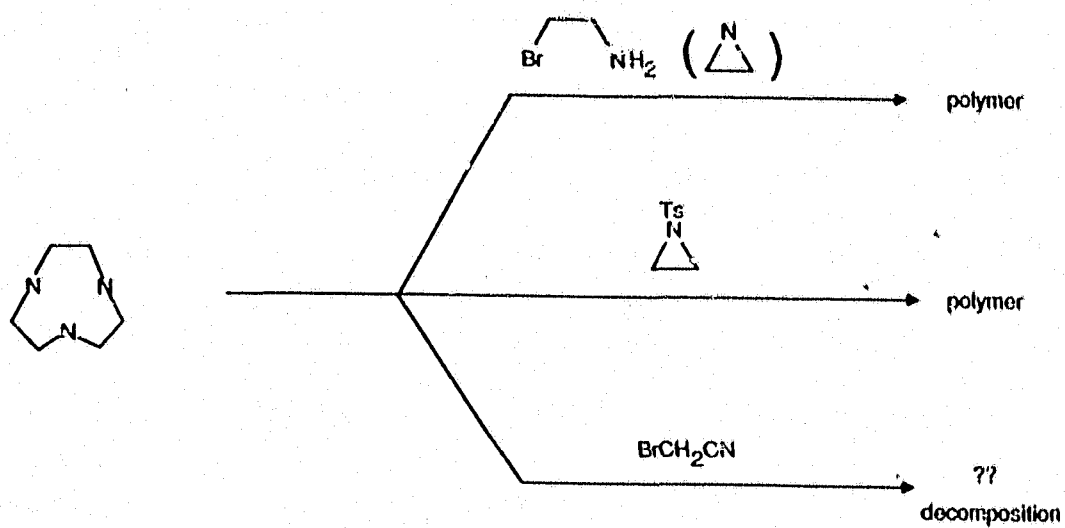
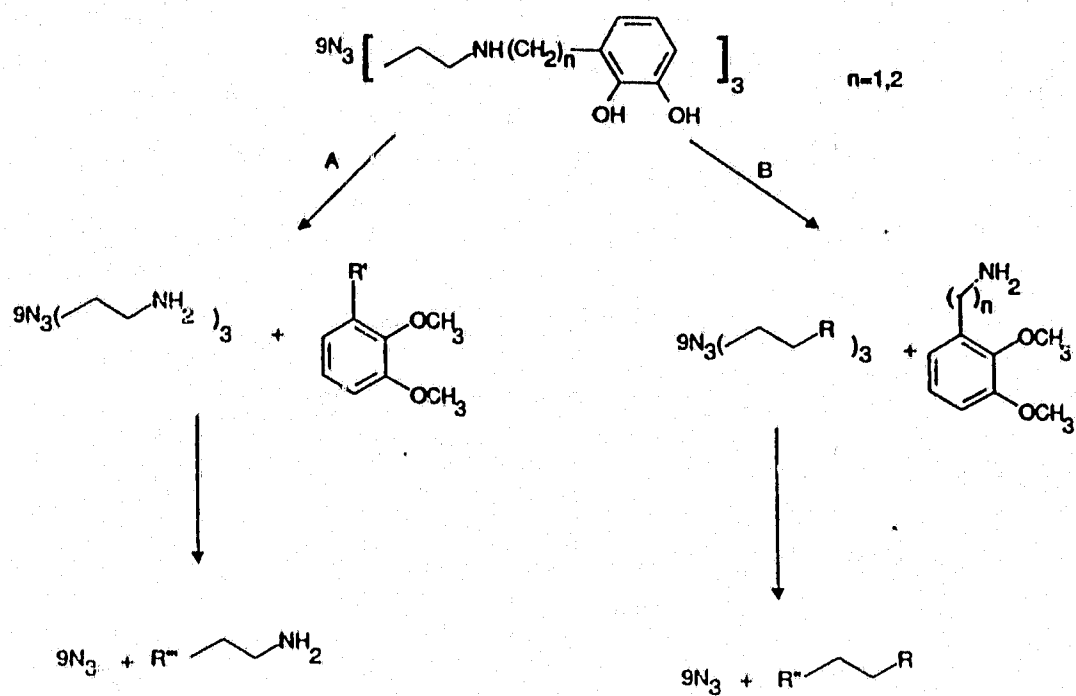


Figure 4.2 Retrosynthetic analysis of target molecule



represents a retrosynthetic analysis of the target molecule.

Route A was the initial approach taken in the synthesis. However, problems arose in obtaining free taetacn as discussed above. In route B, the reactive functional group (R=acyl halide, aldehyde, etc.) is present on the pendant arms attached to the [9]-aneN₃ ring and the amine functionality comes from the catechol moiety.

There exist numerous ways to functionalize the pendant arm (R) in route B. These include acyl halides, esters, tosylated alcohols and halides. Each of these techniques was investigated (Figure 4.3).

The preparation of 1,4,7-triazacyclononane-1,4,7-triacetic acid⁹³⁻⁹⁵ (**28**) was successful following the method of Wieghardt *et al*⁹⁵, and formed in good yields. The problem arose in the next step, the preparation of the acid chloride from the acid. The acid did not dissolve in organic solvents, since it exists as a zwitterion and thus a suitable material for reaction with thionyl chloride could not be isolated.

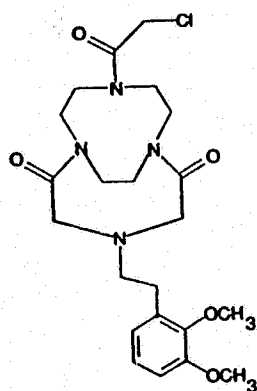
The reaction of [9]-aneN₃ with bromoethyl ester and purification by silica gel chromatography (CH₂Cl₂/MeOH) produced the di-armed species, (1,4-diacetyl ethylester-1,4,7-triazacyclononane), characterized by nmr spectroscopy and mass spectrometry, as the major product. A small amount of the mono-armed adduct was also formed during the reaction. Even with a 10-fold excess of the bromoethyl ester the tri-armed product was not formed during the reaction.

Ethylene oxide is a good candidate for the synthesis of 1,4,7-tri(hydroxyethyl)-1,4,7-triazacyclononane. The procedure has been reported earlier with [9]-aneN₃⁹⁶ and with cyclam^{97,98}. In each of these reported procedures, the compounds were purified as the metal complexes. All attempts at isolation of the free ligand, 1,4,7-trihydroxyethyl-1,4,7-triazacyclononane, were unsuccessful.

This led the synthesis to the preparation of halide derivatives. The reaction of chloroacetyl chloride with [9]-aneN₃, following a similar procedure to that of Bradshaw et al.⁹⁹, resulted in 92% yield of pure 1,4,7-(trioxoethylchloro)-1,4,7-triazacyclononane (29).

4.1.2 Synthesis of Taetacn-Catecholates

The first approach taken was to react the α -chloroamide adduct of tacn with 2,3-dimethoxyphenethylamine. A small amount of the target molecule was detected in the mass spec. The major product obtained was probably the result of a cyclization between two α -chloroamide arms and one amine;



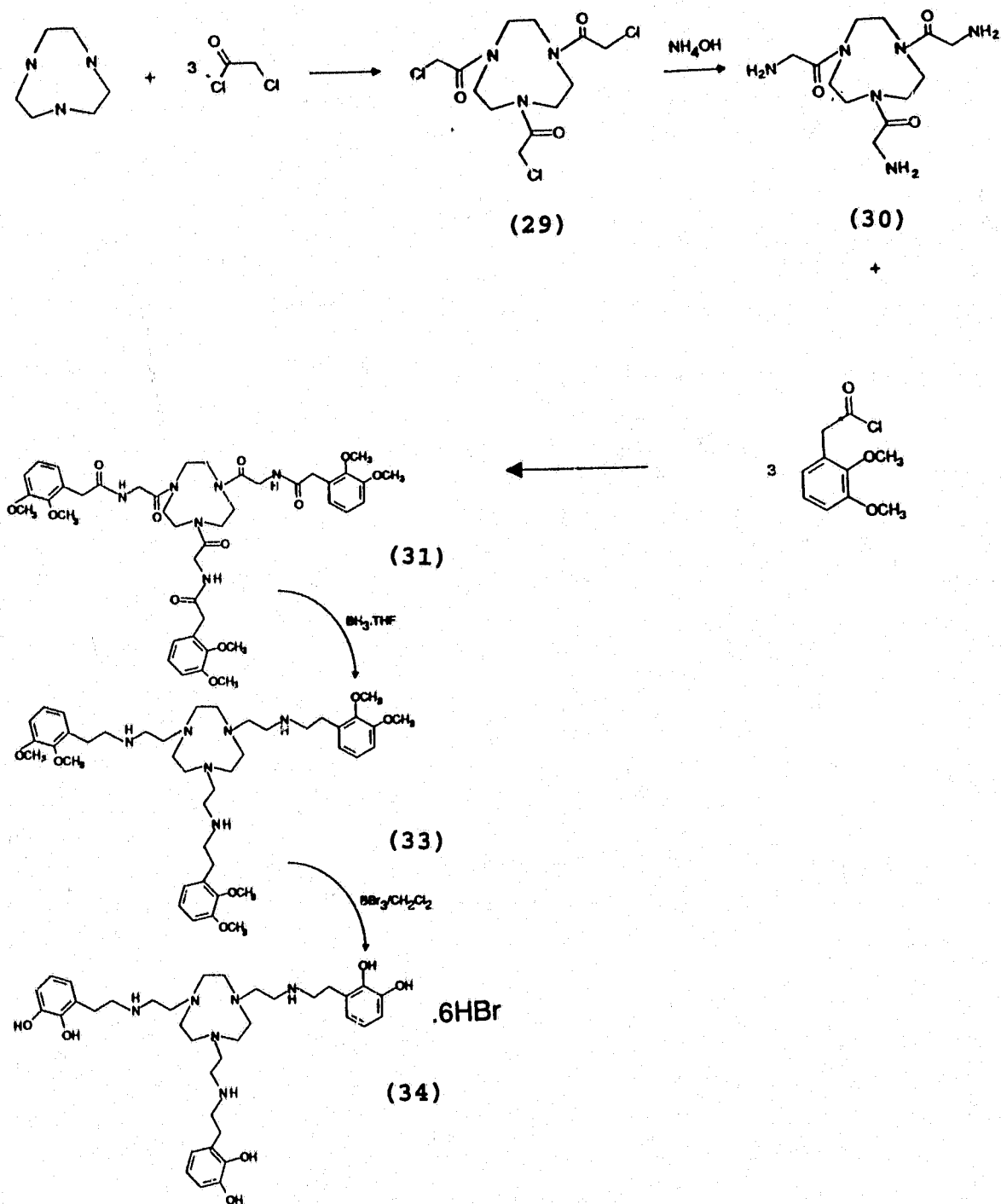
This was determined from the amount of 2,3-dimethoxyphenethylamine hydrochloride salt isolated from the reaction mixture (an excess of the amine was used to mop up the HCl formed during the reaction).

This product may be expected based on results of Bradshaw et al.¹⁰⁰⁻¹⁰² where the authors successfully cyclized several amines with the α -chloroamide route. The α -chloroamides are "crab-like" and are positioned with the atoms suitable for cyclization with the appropriate amine.

The reaction of the pendant α -chloroamide (29) with conc. NH_4OH resulted in quantitative yield of the 1,4,7-(trioxoaminoethyl)-1,4,7-triazacyclononane (30). This finding led to a reconsideration of route A of the retrosynthetic

analysis (Figure 4.2), with the pendant arm of the macrocycle functionalized as the amine, so reaction with the acid chloride of the catechol moiety was appropriate. This reaction was successful with yields on the order of 60-70%, for both tris-1,4,7-(N-(2,3-dimethoxyphenylacetyl)-1-oxo-2-aminoethyl)-1,4,7-triazacyclononane (31) and tris-1,4,7-(N-(2,3-dimethoxybenzoyl)-1-oxo-2-aminoethyl)-1,4,7-triazacyclononane (32). These hexa-amide compounds were reduced with BH_3 .THF complex and the methylated catechols were deprotected by use of BBr_3 in CF_2Cl_2 solution. Recrystallization from MeOH/EtOAc resulted in an off-white powder, each compound analysing with one molecule of ethyl acetate (also evident in the NMR spectra). The ^{13}C NMR spectra for both compounds are shown in Figure 4.4. The synthetic routes are outlined in Scheme 4.3 (compound 34) and Scheme 4.4 (compound 36).

Scheme 4.3 Synthetic route to compound 34.



Scheme 4.4 Synthetic route to compound 36.

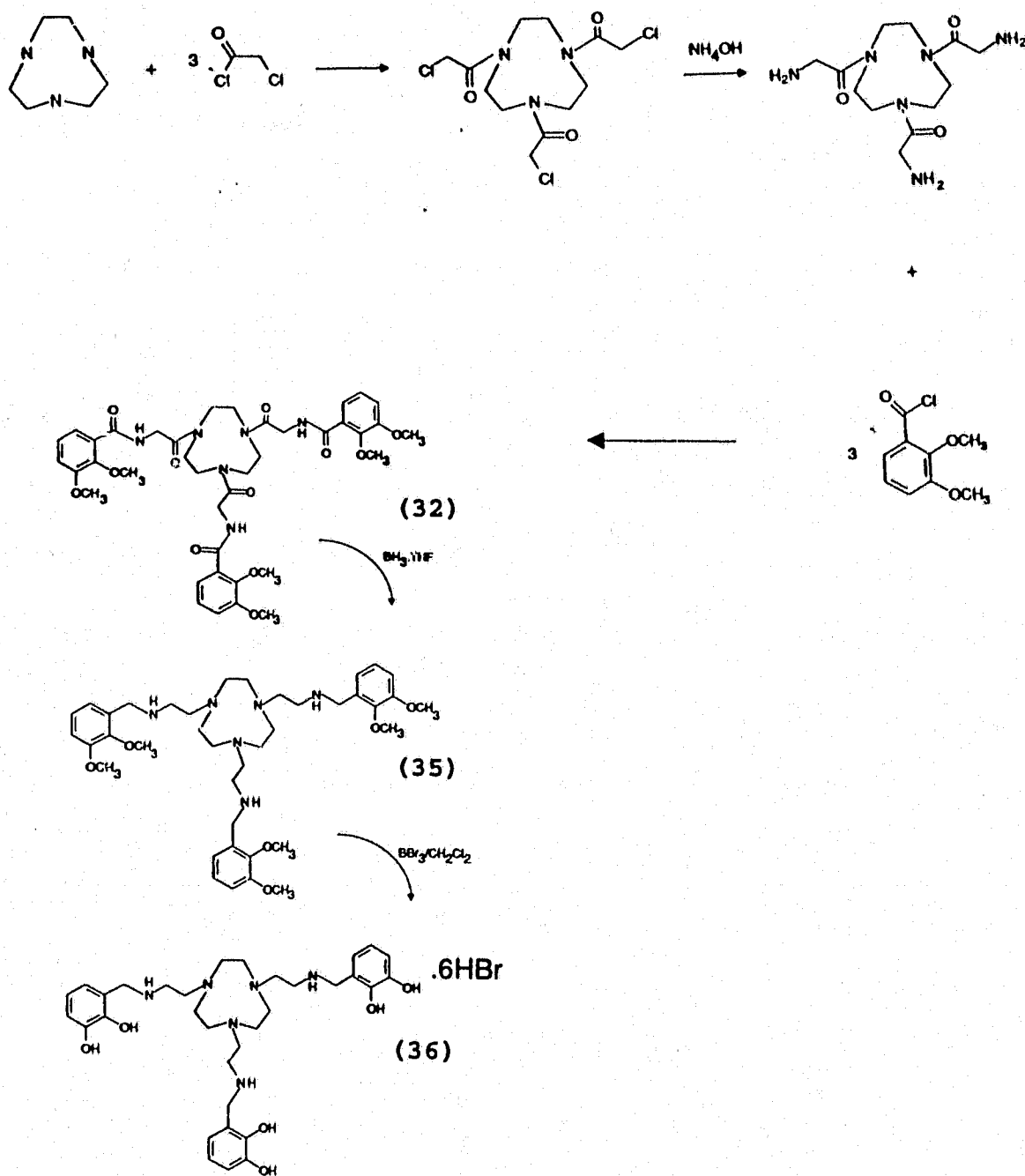
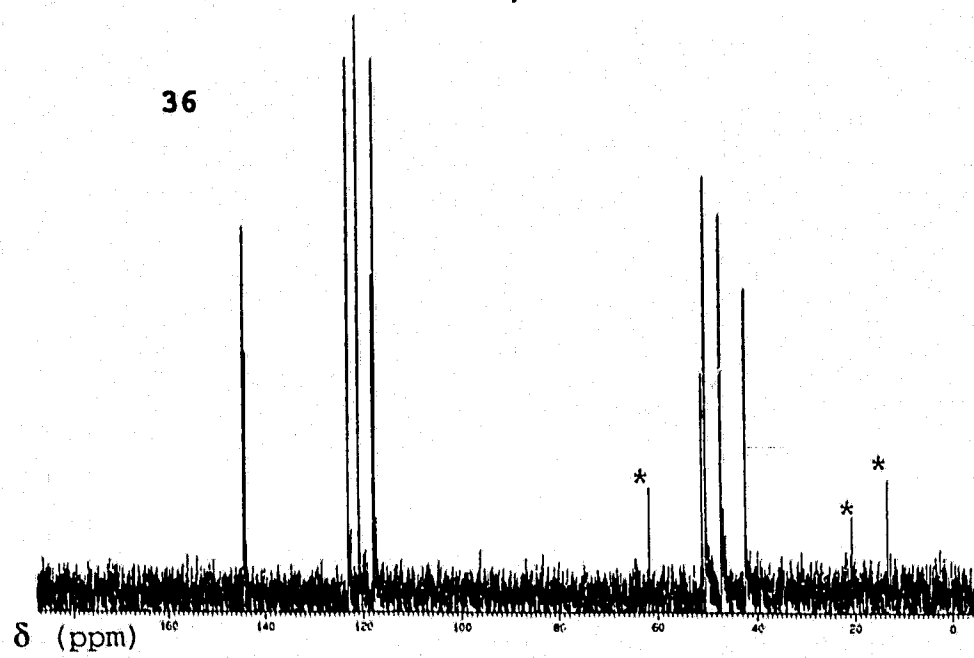
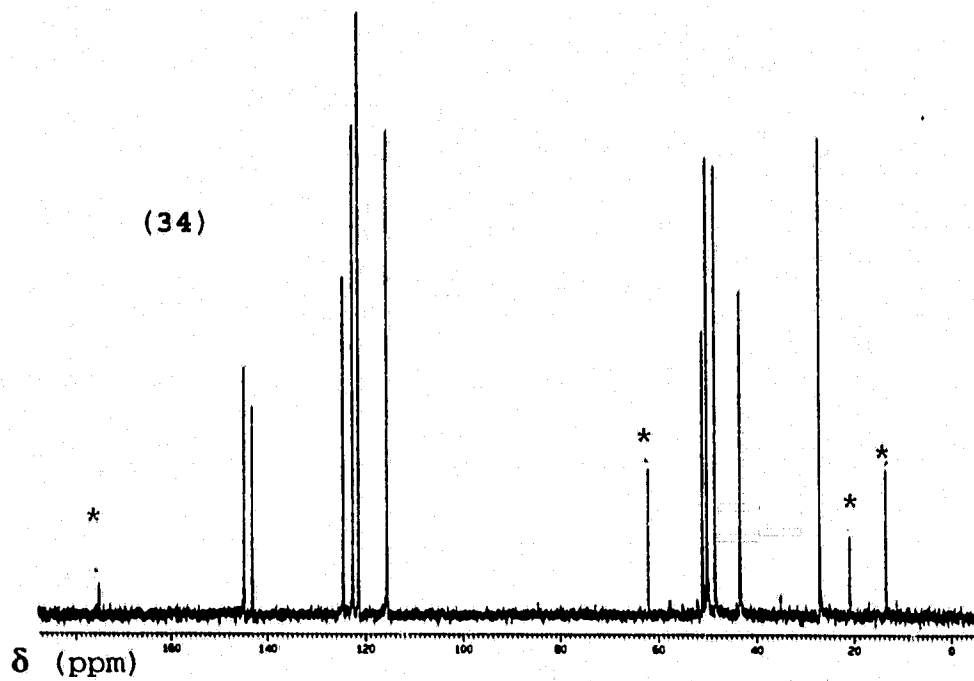


Figure 4.4 ^{13}C nmr spectra of compounds **34** and **36** (*=EtOAc peaks)



4.2 Mononuclear transition metal complexes

4.2.1 Ferric complexes of 34 and 36

The ferric complexes of the pendant tris-catecholates were prepared under high dilution conditions with the slow dropwise addition of Fe(acac), to a basic solution (KOH) of the ligand in MeOH. Purification on Sephadex LH20 gel column (MeOH as eluent) resulted in the pure complexes.

The electronic spectra for the two complex species, Fe(34)³⁺ and Fe(36)³⁺ are shown in Figure 4.5. These complexes show typical spectra for ferric tris-catecholate complexes, with a broad intense band (LMCT) centered around the 500 nm region.

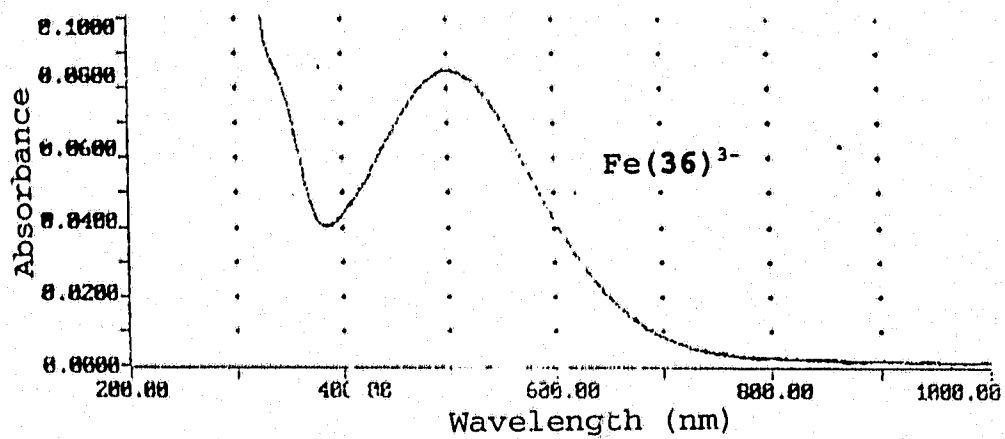
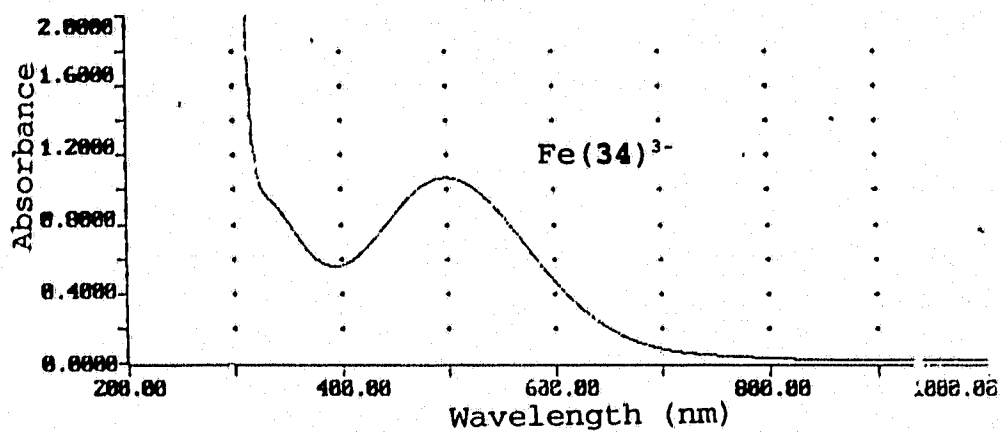
4.2.2 Nitrogen coordinated transition metal complexes of the taetacn-catecholates

The nickel (II) complexes of both the protected catechol ligands and the unprotected ligands were prepared in a methanol solution. The preparations of the Ni(34)²⁺ ion and Ni(36)²⁺ ion were carried out in a deficiency of base (4 equivalents, NaHCO₃).

The electronic spectra of the nickel complexes synthesized are shown in Figure 4.6, and the results are tabulated in Table 4.1 together with other selected Ni(N_c)²⁺ chromophores.

The purple compounds are consistent with a Ni(N_c)²⁺

Figure 4.5 Electronic absorption spectra of Fe(34)^{3-} and Fe(36)^{3-} .



chromophore in solution. The molar absorption coefficients (ϵ) of the d-d transitions are slightly higher than those of other NiN_6 systems. This has been attributed previously¹⁰⁴ to a trigonal twist (see Figure 4.7) enforced on the triazacyclononane moieties of $\text{Co}(\text{dtne})^{3+}$ (dtne=1,2-bis(1,4,7-triaza-1-cyclononyl)-ethane) and a similar force may be acting on the Ni-taetacn catecholate systems.

Figure 4.6 Electronic absorption spectra of $\text{Ni}(33)^{2+}$ and $\text{Ni}(34)^{2+}$.

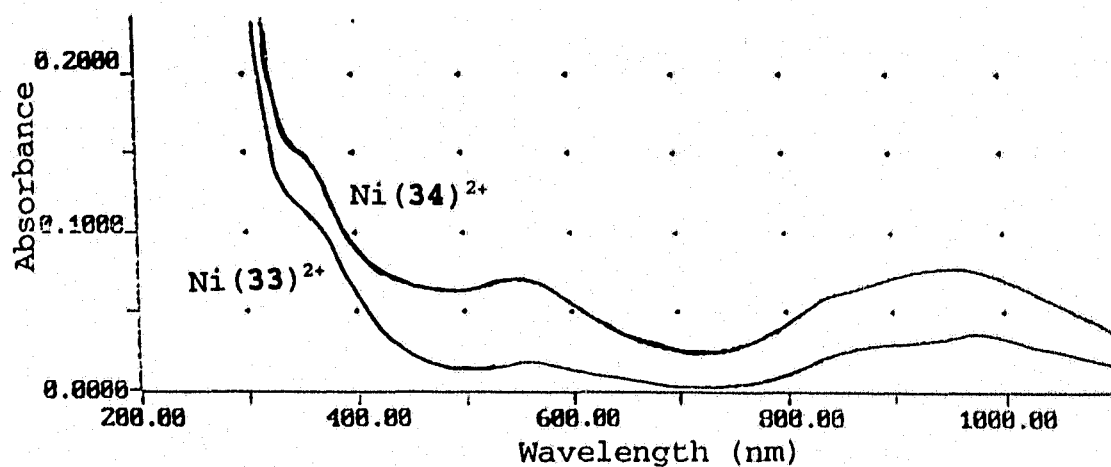


Table 4.1 Electronic spectra of NiN_6^{2+} chromophores

Complex	λ_{max} (nm) (ϵ , $\text{M}^{-1}\text{cm}^{-1}$)	Ref
$\text{Ni}(\text{taptacn})^{2+}$	340 (10), 538 (7.9), 815 (sh, 7.7), 860 (7.8)	72
$\text{Ni}(\text{tacn})_2^{2+}$	308 (12), 505 (7), 800 (7), 870 (sh)	103
$\text{Ni}(\text{dtne})^{2+,a}$	363 (16), 516 (18), 848 (31), 917 (31)	104
$\text{Ni}(\text{2ON}_6)^{2+}$	340, 526, 819, 877	105
$\text{Ni}(\mathbf{34})^{2+}$	354 (86), 550 (44), 843 (35), 959 (45)	b
$\text{Ni}(\mathbf{33})^{2+}$	359, 557, 851, 969	b
$\text{Ni}(\mathbf{36})^{2+}$	573 (48), 827 (sh), 929 (84)	b

a. dtne = 1,2-bis-(1,4,7-triaza-1-cyclononyl)ethane

b. this work

The cobalt complex of compound **34** was prepared in the same manner as the nickel complex. The amines were deprotonated in a deficiency of base with the addition of either NaHCO_3 or aqueous KOH , permitting coordination to the Co^{2+} ion. The preparation of the complex was carried out under an inert atmosphere to prevent oxidation of the catechol

moieties to the quinones.

The low energy absorption bands at 410 nm ($\epsilon=20 \text{ M}^{-1}\text{cm}^{-1}$) and 570 nm ($\epsilon= 11 \text{ M}^{-1}\text{cm}^{-1}$) suggest that the cobalt ion remains in the 2+ oxidation state. However, if the solution is left to stand for 2-3 days the transitions shift to higher energies and exhibit higher extinction coefficients, 386 nm ($\epsilon=167 \text{ M}^{-1}\text{cm}^{-1}$) and 470 nm ($\epsilon=113 \text{ M}^{-1}\text{cm}^{-1}$). This is indicative of a Co^{3+} ion in an N_6 coordinating environment; as compared to other $\text{CoN}_6^{3+/2+}$ chromophores in Table 4.2. These transitions, namely ${}^1\text{T}_{1g} \leftarrow {}^1\text{A}_{1g}$ and ${}^1\text{T}_{2g} \leftarrow {}^1\text{A}_{1g}$, are characteristic of a low spin Co^{3+} ion in an octahedral environment. If the solution is left to stand at room temperature for longer than 3-4 days, a dark colored solution results, indicating oxidation of the catecholate moieties, after which time no distinct d-d transitions are identifiable. For this reason the mononuclear transition metal complexes of these ligand systems have not been isolated, and the binuclear complexes (Fe^{3+} or Al^{3+}) were prepared immediately following the identification of the mononuclear complex (uv-visible spectroscopy).

Figure 4.7 Definition of twist angle

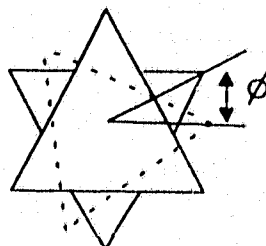


Table 4.2 Electronic spectra of Co and Cu taetacn-catecholates

Complex	λ_{\max} (nm) (ϵ , $M^{-1}cm^{-1}$)	Ref
Co(dtne) ³⁺	346 (230), 495 (323)	104
Co(sep) ³⁺	340 (116), 472 (109)	72
Co(taetacn) ³⁺	347 (198), 480 (242)	87
Co(taptacn) ³⁺	358 (93), 497 (77)	72
Co(34) ³⁺	386 (167), 470 (113)	a
Co(34) ²⁺	410 (20), 570 sh (11)	a
Co(sep) ²⁺	467 (8.2), 539 (1.9), 545 (2), 552 (1.8), 664 (0.8), 910 (5)	72
Co(taptacn) ²⁺	482 (12.7), 541 (sh, 4.4), 985 (10.3)	72
Co(20N ₆) ²⁺	485 (13.2), 538 (sh, 5.6), 980 (8.3)	72
Co(9N ₃) ²⁺	462 (5.9), 545 (sh), 630 (1.4), 850 (2.4)	72
Cu(daptacn) ²⁺	578 (106), 869 (35)	72
Cu(bicycloN ₅) ²⁺	276 (5700), 567 (145), 859 (42)	72
Cu(taptacn) ²⁺	278 (5300), 581 (98), 867 (39)	a
Cu(bicycloN ₆) ²⁺	280 (5500), 558 (135)	a
Cu(33) ²⁺	456 (208), 585 (135)	a
Cu(34) ²⁺	461 (210), 591 (150)	a

a. This work.

The Cu²⁺ complex of compounds 33 and 34 were also prepared. The methylated complex (ligand 33) shows a similar coordination environment as the deprotected ligand (34), as exemplified by the uv-visible spectrum (Table 4.2).

4.3 Binuclear transition metal complexes

Binuclear tris-catecholate complexes are of interest

because of an earlier study¹⁰⁶ where the binding of Ca^{2+} to ferric enterobactin was investigated. The authors report an association constant of $4 \times 10^4 \text{ M}^{-1}$ for Ca^{2+} to the enterobactin complex in 95% methanol. The synthetic analogue, MECAM, showed no affinity for the Ca^{2+} ion and thus they conclude the likely site of coordination in the enterobactin complex is in the molecular backbone, such that the Ca^{2+} ion is coordinated to six oxygen atoms.

In a more recent study, Raymond et al.¹⁰⁷ investigated the K^+ ion coordination to the vanadium enterobactin complex, $\text{K}_2[\text{V}(\text{ent})] \cdot 3\text{DMF}$. The authors found that one K^+ ion is six coordinate (pseudo-trigonal prism) and the other is five coordinate (square pyramidal). The most basic oxygen atoms in the enterobactin complex are the catecholate oxygen atoms, followed by the amide carbonyl oxygen atoms. Indeed, the K^+ ions coordinate to the accessible catecholate oxygens, the amide carbonyl oxygen, and the oxygen atoms of DMF.

Since K^+ is significantly larger than Ca^{2+} , it was not expected to show "cavity coordination" in the enterobactin complex. The authors examined Ca^{2+} coordination in the $\text{V}(\text{ent})^{2-}$ anion by molecular visualization software and found that in order for the Ca^{2+} ion to be located in the cavity the amide groups would have to rotate, causing considerable strain on the molecule. They suggest that coordination is more likely to occur at the accessible catecholate oxygen atoms. However, this does not explain the results obtained previously

with MECAM.

4.3.1 Synthesis of binuclear transition metal complexes of taetacn-catecholate systems

Following coordination of the appropriate metal ion into the N_6 environment of the ligand systems, the binuclear complex was prepared by a high dilution route, with the simultaneous dropwise addition of base (NaHCO_3). The preparation involved a metathesis reaction of $\text{Fe}(\text{acac})_3$ and the mononuclear complex. The complexes precipitated out of solution on formation and were removed by filtration. The purple solid of the $[\text{NiFe}(34)]^{1-}$ complex showed satisfactory microanalysis; calc. (found) for $\text{NaNiFe}(34) \cdot 2\text{H}_2\text{O} \cdot 0.1.5\text{NaHCO}_3$, C 48.65% (48.22%), H 5.83% (5.68%) and N 9.08% (8.59%).

4.3.2 Electronic absorption spectra of NiFe taetacn-catecholates

Owing to the high intensity of the LMCT bands in the ferric tris-catecholate complexes, any d-d transitions are obscured. The electronic spectra of the mononuclear, $[\text{Fe}(34)]^{3-}$ and $[\text{Fe}(36)]^{3-}$, and the binuclear $[\text{NiFe}(34)]^{1-}$ and $[\text{NiFe}(36)]^{1-}$ anions are presented in Table 4.3.

There is a significant shift of the LMCT bands in the binuclear complexes to a lower energy, indicating that the coordinated nickel ion does have an effect on the ferric ion in the catecholate environment. However, there is no evidence

of intervalence bands in the spectra, although this could again be due to the lower extinction coefficients associated with these bands.

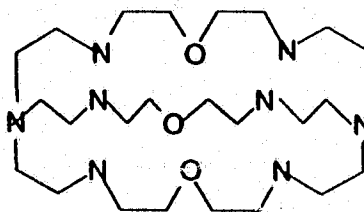
Table 4.3 Electronic absorption spectra of Fe(34)^{3-} , Fe(36)^{3-} , $[\text{NiFe(34)}]^{1-}$ and $[\text{NiFe(36)}]^{1-}$

Complex	λ_{max} (nm) (ϵ , $\text{M}^{-1}\text{cm}^{-1}$)
Fe(34)^{3-}	339 (sh), 498 (5100)
Fe(36)^{3-}	340 (sh), 499 (4200)
$[\text{NiFe(34)}]^{1-}$	415 (sh), 565 (5400)
$[\text{NiFe(36)}]^{1-}$	555 (4600)

CHAPTER 5
TREN-CATECHOLATE SYSTEMS

5.1 Introduction

The coordination of tripodal ligands towards transition metal cations have been extensively studied¹⁰⁸. Tris-(2-aminoethyl)amine (tren) exhibits remarkable complexation properties towards transition metals¹⁰⁹ and has led to the development of numerous derivatives of this ligand, which include the cryptand type ligands of Lehn and coworkers¹¹⁰⁻¹¹²;



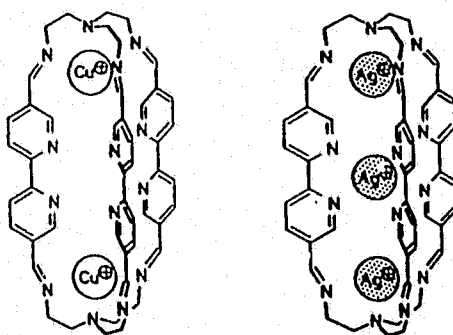
Utilizing these aza-based macrobicycles, Lehn has investigated the incorporation of anions¹¹³ into the hexa-protonated form of the ligand.

More recently¹¹⁴, tren-based cryptates with furan and pyridine linkages have been shown to complex group I cations such as the sodium ion. In the case of the furan system the Na⁺ ion is five coordinate, however, it is six coordinate in

the pyridine linked macrobicycles.

The Schiff base condensation of tren with salicylaldehyde¹¹⁵ or acetylacetone or hydroxyacetophenone¹¹⁶ leads to tripodal ligands designed for lanthanide complexation, where the amines may or may not be involved in coordination to the metal ion.

The condensation of tren with suitable dicarbonyl pyridine moieties¹¹⁷ leads to the formation of macrobicyclic ligands which complex Cu(I) or Ag(I) ions, in binuclear or trinuclear fashions. The two Cu(I) ions coordinate in the tren portion of the ligand, while two of the three Ag(I) ions coordinate at the tren ends of the ligand, and the other Ag(I) ion is six coordinate, with all nitrogen atoms of the bipyridine functionalities coordinating the metal ion;



A pentanuclear system, a macrobicycle based on tren and

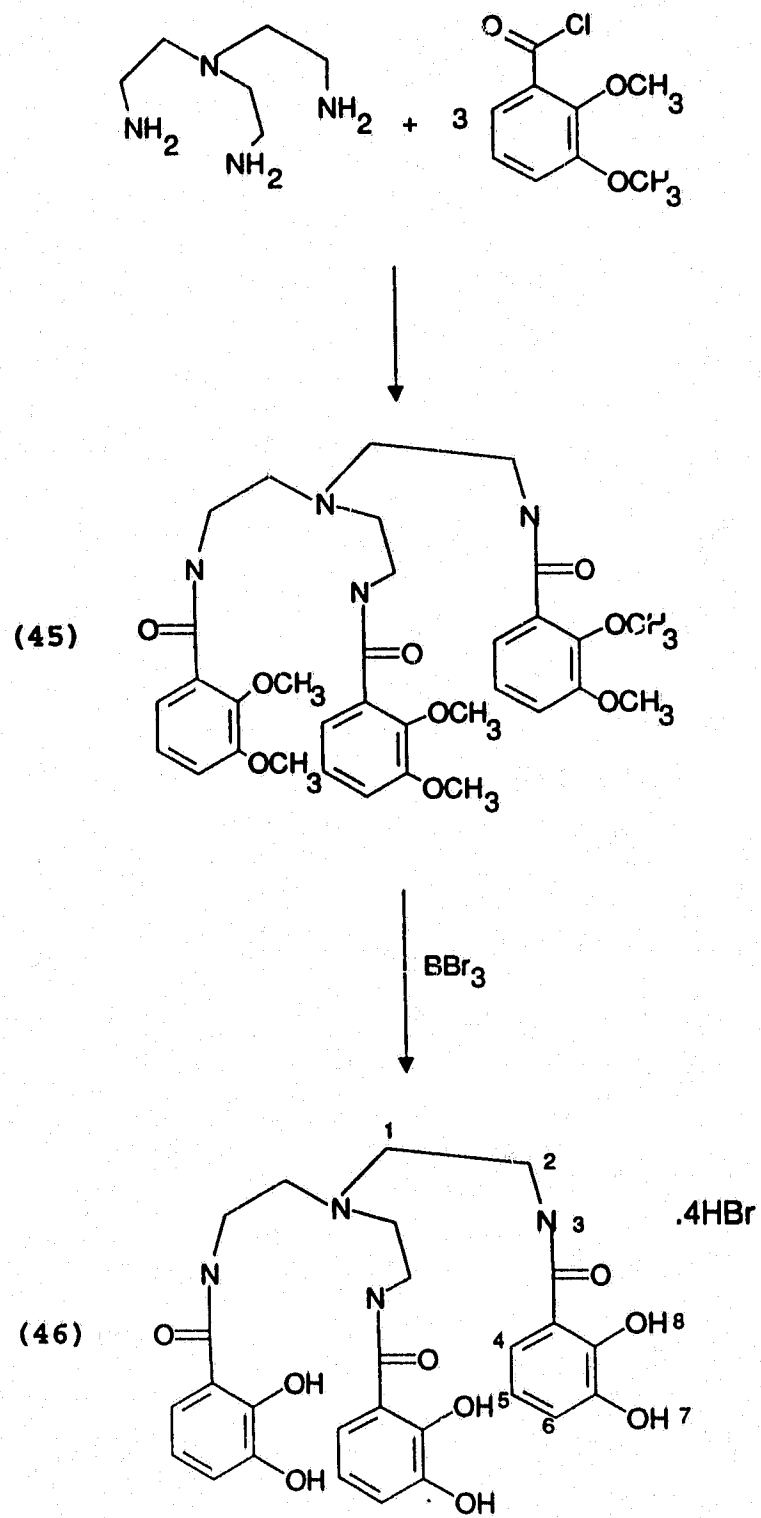
benzene linkages, containing two Cu(I) ions and three arene tricarbonyl chromium substituents has been characterized¹¹⁸. The Cu(I) ions coordinate inside the cavity to the nitrogen atoms at each end of the macrobicycle, whereas the Cr atoms are situated outside the cavity, each being complexed to one of the arene rings and three carbonyls.

The ability of the tren based macrobicycles to form multinuclear entities raised an interest in extending this type of complexation to the tren based enterobactin analogues (trenam) of Raymond and coworkers^{119,120}.

5.2 Ligand syntheses

The procedure of Raymond *et al.*¹²⁰ was successfully carried out to synthesize Me₆trenam (45) and deprotection with BBr₃ in CH₂Cl₂ solution resulted in ~ 93% trenam.4HBr. The synthetic procedure is outlined in Scheme 5.1. The amide was synthesized by using a modified Schotten-Bauman approach, and recrystallization from a cyclohexane/EtOAc mixture resulted in ~ 50% of the desired product.

Scheme 5.1 Synthetic route to the preparation of trencam (46).



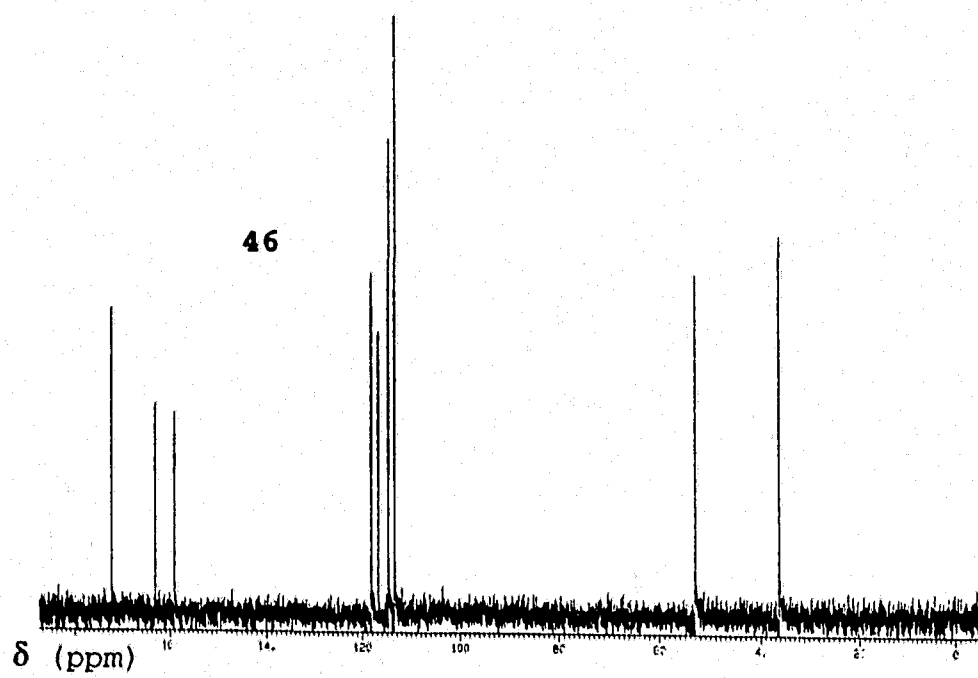
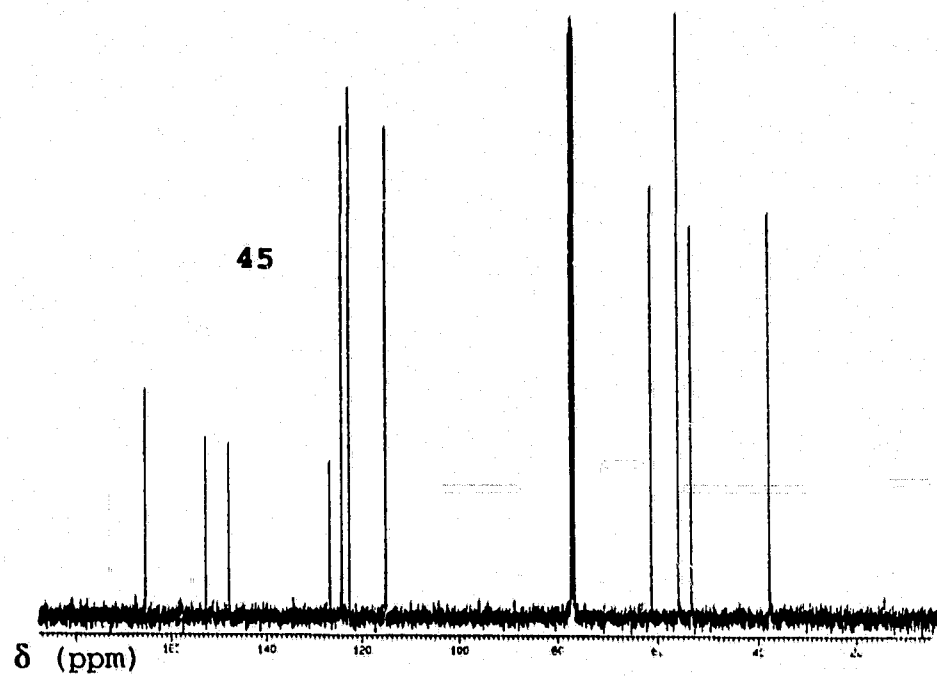
The ^{13}C NMR spectra of the protected (45) and deprotected (46) compounds are shown in Figure 5.1. The disappearance of the $-\text{OCH}_3$ resonances at $\delta 61.2$ and $\delta 55.9$ indicates that the demethylation reaction went to completion. There are significant shifts of the aromatic and amide carbon atoms on deprotection. The amide carbon and the two aromatic carbons next to the hydroxyl groups are shifted further downfield, while the remaining aromatic carbons are shifted slightly upfield. This is probably due to solvent effects since the NMR spectrum of the unprotected ligand (46) was determined in $\text{D}_2\text{O}/\text{NaOD}$.

Similar results are obtained with the ^1H nmr, the data are presented in Table 5.1.

Table 5.1 ^1H nmr data for compounds 45 and 46.

	Compound 45	Compound 46
H^a	δ (ppm)	δ (ppm)
3	8.16 (t)	-
4^b	7.58 (dd)	6.31 (dd)
5	7.07 (t)	5.66 (t)
6^b	6.97 (dd)	5.89 (dd)
7^c	3.83 (s)	-
8^c	3.82 (s)	-
2	3.57 (q)	2.87 (t) ^d
1	2.85 (t)	2.21 (t) ^d

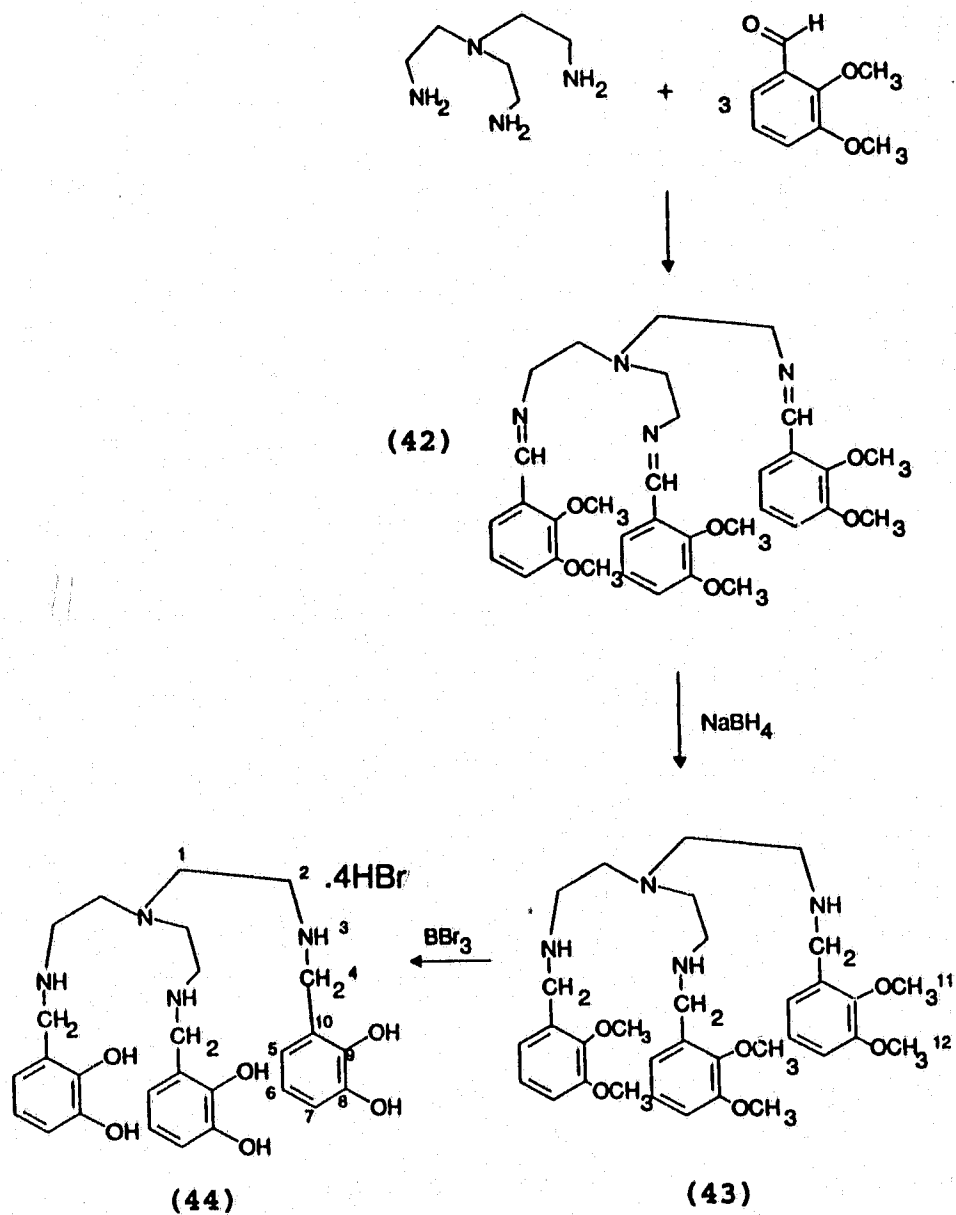
a. See scheme 5.1 for numbering system.
 b, c, d. ^1H 's may be interchanged.

Figure 5.1 ^{13}C NMR spectra of 45 and 46.

Again, the absence of sharp singlets at $\delta 3.83$ and $\delta 3.82$ indicate complete demethylation. The amide protons and the hydroxyl protons are not observed, since they undergo exchange in the solvent system used ($D_2O/NaOD$).

Attempts at reducing the amide with $LiAlH_4$ in THF solution resulted in extremely low yields of crude product, that could not be purified by conventional methods, so other methods of preparing the reduced product (compound **44**) were used. The best approach was to use a Schiff-base condensation reaction of tris-(2-aminoethyl)amine (tren) and 2,3-dimethoxybenzaldehyde following a procedure of Orvig et al.¹²¹ for the preparation of tripodal pyridinones for lanthanide complexation. The yields were on the order of 90%. Demethylation of the protected catechols was again achieved with BBr_3 in CH_2Cl_2 solution (~ 80% yield). Scheme 5.2 shows the procedure for the preparation of tris-(2-(2,3-dihydroxybenzylamino)ethyl)amine (**44**).

Scheme 5.2 Synthetic route to compound 44.



The results of the ^{13}C NMR spectra are tabulated in Table 5.2 and the ^1H NMR data are given in Table 5.3.

Table 5.2 ^{13}C NMR data for compounds 42-44.

	42 (CDCl_3)	43 (CDCl_3)	44 ($\text{D}_2\text{O}/\text{NaOD}$)
C^{a}	δ (ppm)	δ (ppm)	δ (ppm)
4	157.7	54.3	48.6
9 ^b	152.7	152.5	144.2
8 ^b	149.1	147.2	143.7
10	129.9	133.6	118.0
5 ^c	124.1	123.8	122.9
6 ^c	118.7	121.5	120.8
7 ^c	114.0	111.2	117.5
11 ^d	61.6	60.6	-
2	60.4	46.9	46.7
12 ^d	55.7	55.6	-
1	55.6	48.1	43.3

a. See scheme 5.2 for numbering system.
b, c, d. Carbons may be exchanged.

Table 5.3 ^1H NMR data for compounds 42-44.

	42 (CDCl_3)	43 (CDCl_3)	44 ($\text{D}_2\text{O}/\text{NaOD}$)
H^a	δ (ppm)	δ (ppm)	δ (ppm)
4	8.61 (s)	3.73 (s)	4.04 (s)
5 ^b	7.46 (dd)	6.84 (dd)	6.68 (m)
6	7.00 (t)	6.94 (t)	6.79 (dd)
7 ^b	6.88 (dd)	6.76 (dd)	6.68 (m)
11 ^c	3.81 (s)	3.79 (s)	-
12 ^c	3.80 (s)	3.77 (s)	-
2	3.74 (t)	2.60 (t) ^d	2.95 (t) ^d
1	2.94 (t)	2.52 (t) ^d	2.69 (t) ^d
3	-	-	3.15 (q)

a. See scheme 5.2 for numbering system

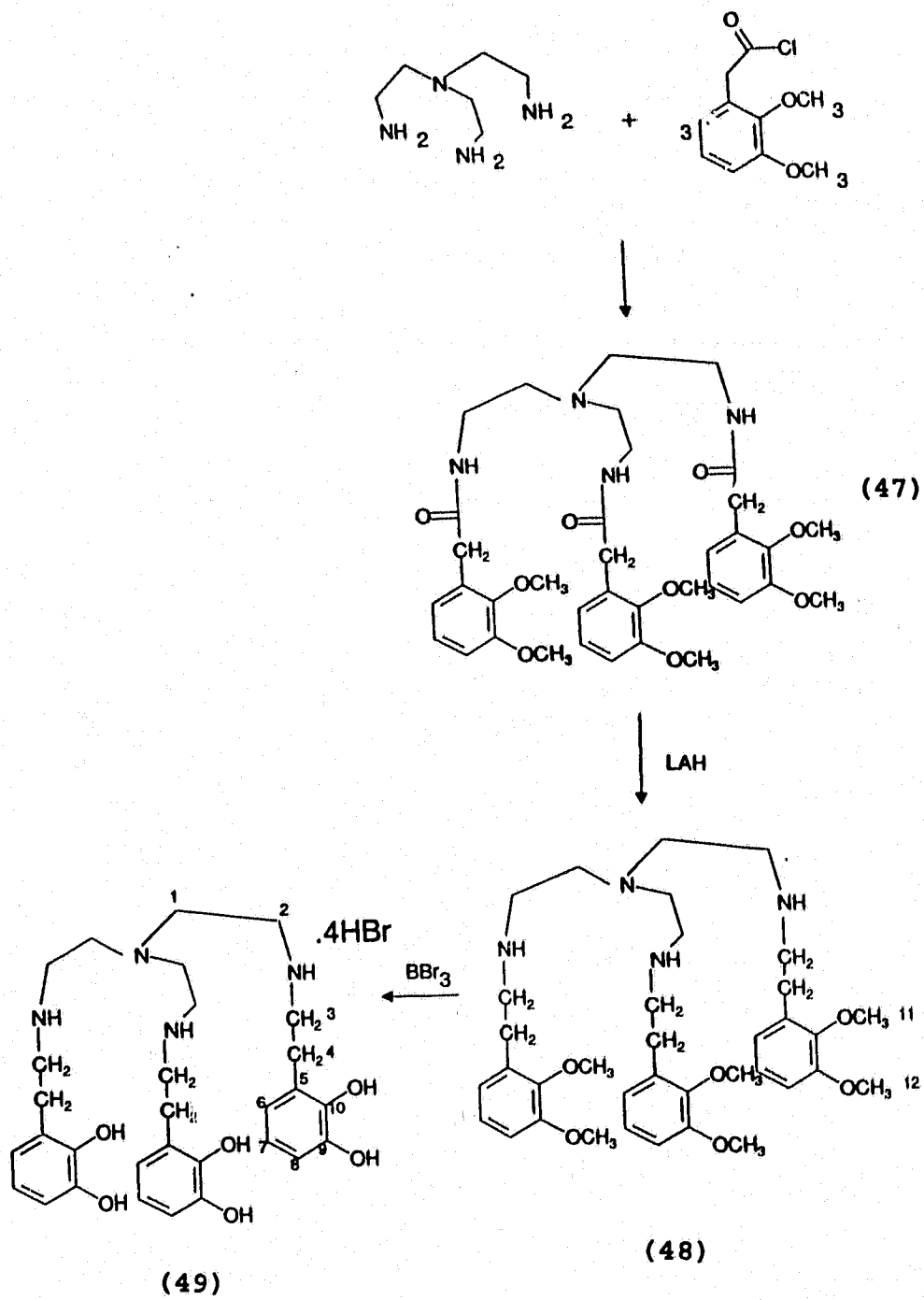
b, c, d. H's are interchangeable.

The NMR data confirm the complete reduction of the imine with NaBH_4 ; the disappearance of $\text{N}=\text{CH}$ resonances ($^{13}\text{C}\sim\delta 158$, $^1\text{H}\sim\delta 8.6$) and the appearance of benzylic resonances ($^{13}\text{C}\sim\delta 54$, $^1\text{H}\sim\delta 3.7$) also confirm this process.

Complete demethylation is also verified by the absence of $-\text{OCH}_3$ resonances ($^{13}\text{C}\sim\delta 61$, 56 and $^1\text{H}\sim\delta 3.8$) in the NMR spectra of the deprotected ligand (44).

A procedure similar to that used for the preparation of compound 45 was used to prepare tris-((2,3-dimethoxyphenylacetyl)amino)ethyl)amine (47). The reaction of three mole equivalents of 2,3-dimethoxyphenylacetyl chloride with one mole equivalent of tren under Schotten-Bauman conditions resulted in 75% yield of the desired product (see

Scheme 5.3 Synthetic route to compound 49.



Scheme 5.3). Reduction of the amide was successful utilizing LiAlH_4 in THF, after purification on a Sephadex LH20 gel column. Deprotection of the catechol moieties with BBr_3 yielded 78% of compound 49. The ^{13}C NMR data are presented in Table 5.4.

Table 5.4 ^{13}C NMR data for compounds 47-49.

	47 (CDCl_3)	48 (CDCl_3)	49 ($\text{D}_2\text{O}/\text{NaOD}$)
C^a	δ (ppm)	δ (ppm)	δ (ppm)
3	171.2	50.6	51.0
10 ^b	152.7	152.8	155.5
9 ^b	146.8	147.4	151.5
5	129.4	133.9	127.9
6 ^c	124.3	123.8	120.0
8 ^c	122.6	122.2	119.6
7 ^c	111.5	110.5	116.6
11 ^d	60.5	60.6	-
12 ^d	55.6	55.6	-
4	54.0	54.6	55.7
2	38.0	47.6	47.9
1	37.9	30.7	32.2

a. See scheme 5.3 for numbering system.

b, c, d. C's may be interchanged.

The ^{13}C NMR data confirms the complete reduction of the amide by the absence of the resonance at $\delta 171$ and the presence of a $-\text{NHCH}_2$ peak at $\delta 51$. Also demethylation of the catechol moieties is verified by the absence of the $-\text{OCH}_3$ resonances at $\delta 61$ and $\delta 56$.

5.3 Fe^{III} and Al^{III} complexes of tren-catecholate ligands

The iron and aluminum complexes were prepared by the following method. The ligand was dissolved in methanol and ten equivalents of base was added (aqueous KOH or NaOH). A methanol solution of FeCl₃ or Fe(acac)₃, or Al(NO₃)₃ or Al(acac)₃ was added dropwise to the ligand solution at room temperature. On formation, the complexes precipitated out of solution. In some instances it was possible to purify the complex on a Sephadex LH20 gel column (MeOH as eluent).

5.3.1 Electronic absorption spectra of Fe^{III} complexes

The uv-visible spectra of the ferric complexes of ligands 44, 46, or 49 are consistent with previously prepared ferric tris-catecholates. The complexes absorb strongly in the 500 nm region of the spectrum, which is assigned as a LMCT band. The data are tabulated in Table 5.5.

Table 5.5 Electronic absorption data of Fe(44)³⁻, Fe(46)³⁻, and Fe(49)³⁻.

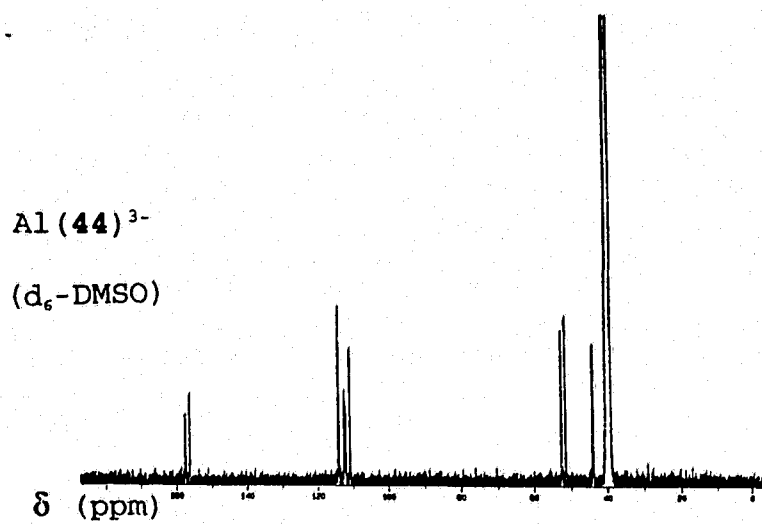
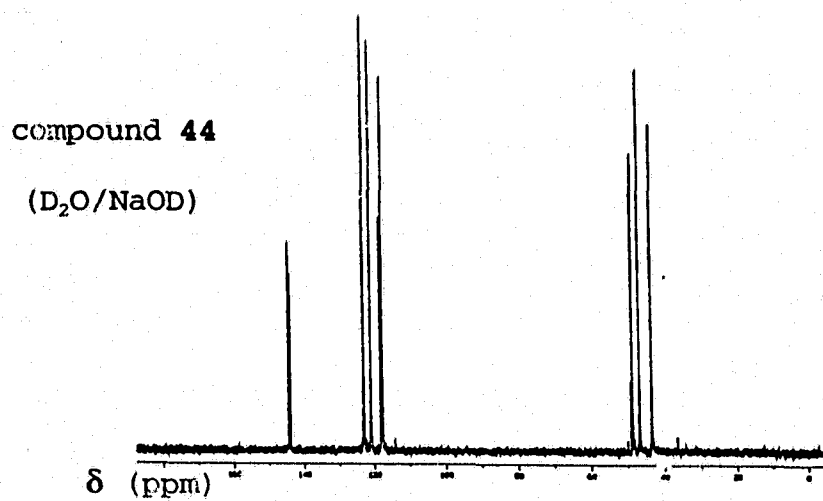
Complex	λ_{\max} (nm) (ϵ , M ⁻¹ cm ⁻¹)	Ref.
Fe(ent) ³⁻	495 (5600)	122
Fe(eta) ³⁻	437 (4800) 538 (4600)	123
Fe(44) ³⁻	456 (4500) 521 (sh)	a
Fe(46) ³⁻ Fe(trencam)	496 (4900)	122, a
Fe(49) ³⁻	401 (4600) 529 (sh)	a

a. This work

It is interesting to note that Fe(eta)³⁻, Fe(44)³⁻, and Fe(49)³⁻ show some resolution of the LMCT band into its two components¹⁶.

5.3.2 Al(44)³⁻

The ¹³C NMR spectra of compound 44 and its aluminum complex are shown in Figure 5.2. The spectra reflect the maintenance of the symmetry of the molecule on coordination to the metal ion.

Figure 5.2 ^{13}C NMR of compound **44** and $\text{Al}(\mathbf{44})^{3-}$.

It is likely that the molecule would maintain this symmetry in the ferric complex as well.

The upfield shift of the aromatic carbons next to the hydroxyl groups in the Al^{3+} complex shows the deshielding effect of coordination to a metal ion.

5.4 Nitrogen coordinated transition metal complexes

The nickel, copper, and cobalt complexes of compound 43 were prepared prior to deprotection of the ligand precursor to be sure that complexation would occur in these systems. The complexes were synthesized in a methanol solution, however isolation of these complexes as solids was unsuccessful.

It is evident from the uv-visible spectra (Table 5.6) that complexation does indeed occur. It is not possible at present to provide a definite assignment to the coordination geometries of these metal complexes based on the electronic absorption spectra data alone. The Ni^{2+} ion may be in a six coordinate environment with two solvent molecules coordinated as well as the tren end of the ligand, or it could also be five coordinate with only one solvent molecule. The most likely geometry would be that of a trigonal bipyramid (tbp) with this type of tripodal ligand¹²⁵.

The Cu^{2+} ion is extremely flexible in its stereochemistry, and the absorption spectra vary considerably depending on geometry¹²⁴. This is mainly due to Jahn-Teller effects which arise because of the d^9 configuration. The uv-visible data

are consistent those of other five-coordinate Cu^{2+} complexes based on the tren ligand.

Table 5.6 Electronic absorption data of $\text{Ni}(\mathbf{43})^{2+}$, $\text{Cu}(\mathbf{43})^{2+}$ and $\text{Co}(\mathbf{43})^{3+}$ complexes.

Complex	λ_{max} (nm)	Ref.
$\text{Ni}(\text{im})_4(\text{OH}_2)_2^{2+}$	353, 571, 674, 845, 1070	124
$\text{Ni}(\text{NH}_3)_4(\text{NCS})_2$	358, 571, 930	124
$\text{Ni}(\text{Me}_6\text{tren})\text{I}^+$	411, 724, 961, 1388	124
$\text{Ni}(\mathbf{43})^{2+}$	357, 556, 818 (sh), 924	a
$\text{Cu}(\text{tren})(\text{NCS})^+$	340, 680, 840	124
$\text{Cu}(\text{tren})\text{Br}^+$	892	124
$\text{Cu}(\text{tren})\text{NH}_3^+$	877	124
$\text{Cu}(\mathbf{43})^{2+}$	836	a
$\text{t-Co}(\text{en})_2(\text{OH}_2)_2^{3+}$	344, 444, 549	124
$\text{c-Co}(\text{cyclen})\text{Cl}_2^+$	390, 559	124
$\text{Co}(\mathbf{43})^{3+}$	380 (sh), 532	a

a. This work

The Co^{3+} ion invariably exists in a six coordinate environment (octahedral) although a few examples of tetrahedral and square antiprismatic are known in the solid state¹²⁵. In the complex described here, the two solvent molecules (H_2O) must be in a *cis* configuration because the ligand does not permit the *trans* configuration. The spectral data are consistent with other *cis*- $\text{Co}^{\text{III}}\text{N}_4\text{X}_2$ complexes¹²⁴.

In any event, the metal ions, Ni^{2+} , Cu^{2+} , and Co^{3+} , do coordinate to the tren portion of the ligand, showing promise to form binuclear complexes in the case of the unprotected ligand.

CHAPTER 6**BASE HYDROLYSIS AND ANATION REACTIONS OF Co(III) PENTAAMMINES**

6.1 INTRODUCTION

Inorganic reaction mechanisms are interesting to study as they often form the basis for biological, catalytic, and environmental processes. Ligand substitution reactions can be defined as those reactions in which the inner coordination sphere of the metal ion is changed.¹²⁶ Taube¹²⁷ has classified these reactions according to their lability. Those reactions with $t_{1/2} > 30\text{sec}$ are considered substitution inert (usually represented by complexes with high ligand field stabilization energies), and those with $t_{1/2} < 30\text{sec}$ are termed substitution labile (complexes with low ligand field stabilization energies). Conventional methods such as uv-vis and nmr spectroscopy may be used to monitor substitution inert complexes, while labile complexes require the use of stopped-flow and relaxation (e.g. T-jump, P-jump) methods.

Extensive studies have been carried out on the substitution reactions of square planar and octahedral complexes¹²⁸, however only those of octahedral complexes will be discussed here. Inorganic substitution reaction mechanisms are divided into three categories:

- (1) Associative (A) - an intermediate with an increase in coordination number can be detected;
- (2) Dissociative (D) - an intermediate with a decrease in coordination number can be detected;

(3) Interchange (I) - if **A** or **D** are not detected. This is further subdivided into **I_a** if there are important entering group effects, and **I_d** if there are none.

This classification is dependent upon the degree of bonding of the leaving group, X^{n-} , and the incoming ligand, Y^{n-} ;



Figure 6.1¹²⁹ gives a pictorial view of these reaction mechanisms.

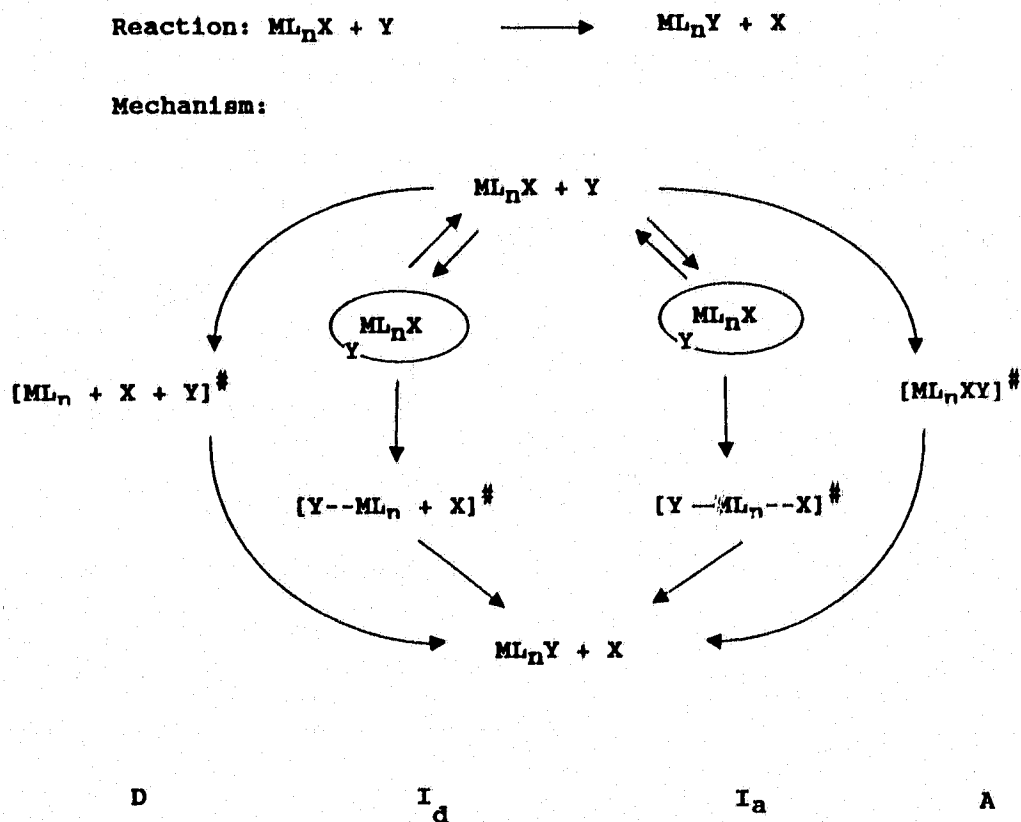


Figure 6.1 Inorganic Substitution Reaction Mechanisms

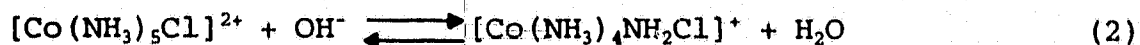
Generally, substitution reactions on octahedral Co^{III} (d^6) complexes occur via D or I_a pathways and several techniques have been used to distinguish between the two mechanisms. The measure of the volumes of activation (ΔV^\ddagger) from the pressure dependence of the rate constants¹³⁰ potentially provides such a resolution. Those reactions with a large and positive ΔV^\ddagger are indicative of a D mechanism and those with a large and negative ΔV^\ddagger pertain to an A mechanism. If ΔV^\ddagger is only slightly negative or slightly positive an I_a or I_d mechanism is assumed, respectively. Table 6.1¹³¹ lists the volumes of activation for the base hydrolysis of various Co^{III} pentaammine complexes. The data support a dissociative mechanism (thus, the existence of a five-coordinate intermediate).

COMPLEX	ΔV^\ddagger (cm^3/mol)
$\text{cis-Co}(\text{NH}_3)_4(\text{CH}_3\text{NH}_2)\text{Cl}^{2+}$	29.4 ± 0.4
$\text{trans-Co}(\text{NH}_3)_4(\text{CH}_3\text{NH}_2)\text{Cl}^{2+}$	28.6 ± 1.3
$\text{trans-Co}(\text{NH}_3)_4(\text{C}_2\text{H}_5\text{NH}_2)\text{Cl}^{2+}$	28.3 ± 1.4
$\text{cis-Co}(\text{NH}_3)_4(n\text{-C}_3\text{H}_7\text{NH}_2)\text{Cl}^{2+}$	26.4 ± 1.5
$\text{trans-Co}(\text{NH}_3)_4(n\text{-C}_3\text{H}_7\text{NH}_2)\text{Cl}^{2+}$	29.9 ± 1.2
$\text{trans-Co}(\text{NH}_3)_4(n\text{-C}_4\text{H}_9\text{NH}_2)\text{Cl}^{2+}$	28.7 ± 0.7
$\text{trans-Co}(\text{NH}_3)_4(i\text{-C}_4\text{H}_9\text{NH}_2)\text{Cl}^{2+}$	28.5 ± 1.2

Table 6.1 Volumes of Activation for the Base Hydrolysis of Co^{III} pentaammine Cl^{2+} Complexes.

Although the proposal for the mechanism of base hydrolysis of cobalt(III) ammine complexes was presented over fifty years ago,¹³² and the π -donor behaviour of the amido group

responsible for its lability was recognized some twenty years later,¹³³ there is still considerable interest in such reactions.¹³⁴ The mechanism first proposed by Garrick is as follows;



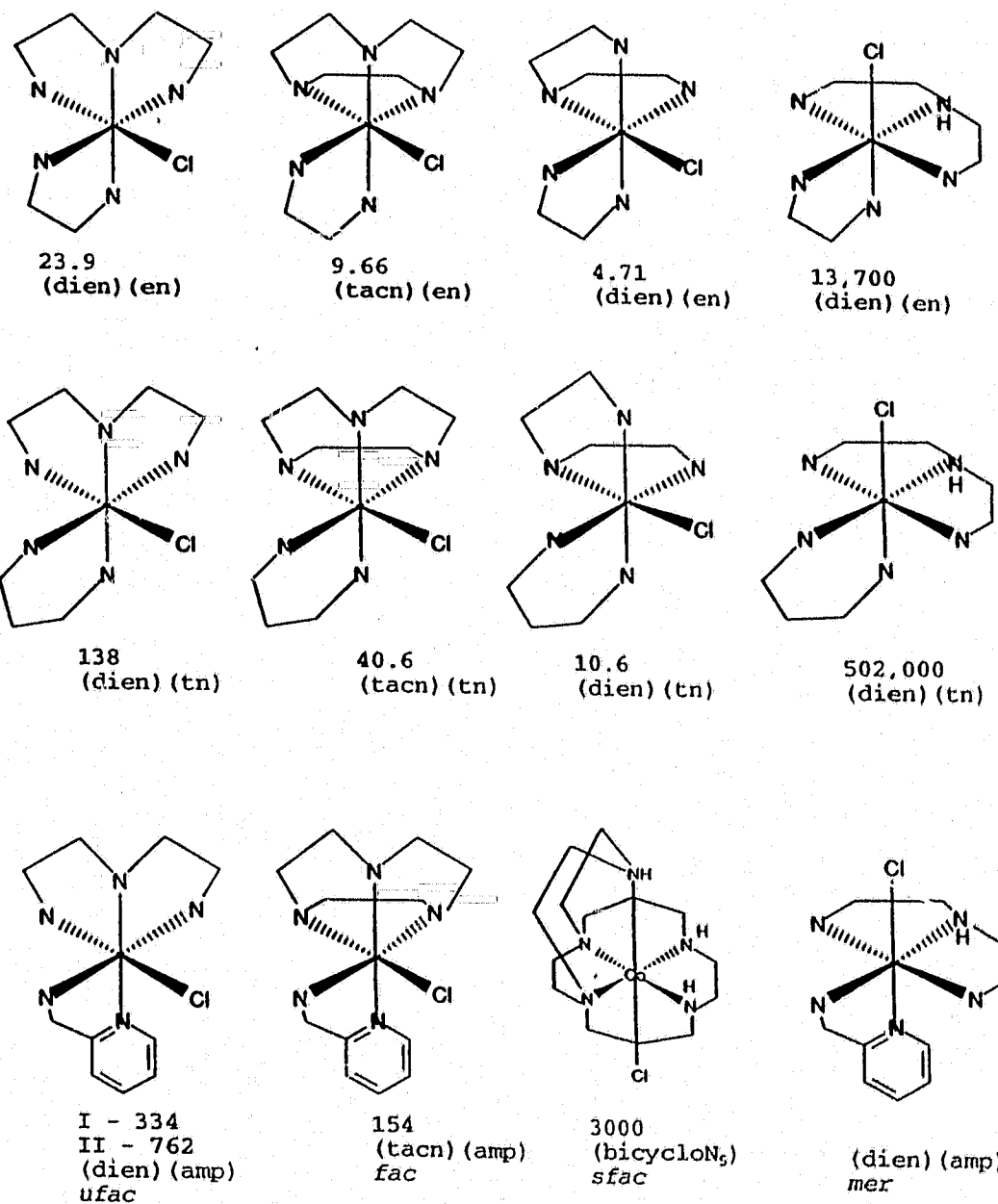
This internal conjugate base mechanism is most commonly referred to as the $S_N1\text{CB}$ mechanism.¹²⁶ The reaction occurs via deprotonation of one of the amines in a rapid acid-base pre-equilibrium (2). The lower charged complex ion can more easily lose the Cl^- ligand (3) and this is the rate determining step. Step (4), involving the incorporation of H_2O is relatively fast. Following work by Tobe¹³⁴⁻¹³⁷, and others¹³⁸⁻¹⁴², on the base hydrolysis kinetics of $[\text{CoCl}(\text{pentaammine})]^{2+}$ complexes, it is considered that the incorporation of a "flat" secondary nitrogen¹³⁵ (i.e., the central atom in a group of three linked donors occupying meridional sites in a coordinated polyamine skeleton) *cis* to the coordinated chloro ligand induces a marked lability of the leaving group. The incorporation of pyridine directly coordinated to the Co^{III} centre also causes an increase in the rate of base hydrolysis when compared with an aliphatic monoamine.¹³⁹ The combination of both effects exhibits an extraordinary lability, and base hydrolysis rate constants of $\sim 10^7 \text{ M}^{-1} \text{ s}^{-1}$ (25°) have been recorded.¹³¹ Henderson and Tobe¹³⁵

have listed the requirements for high lability towards base hydrolysis;

- (i) there should be a "flat" secondary nitrogen to form the amido group
- (ii) the amido group must be cis to the leaving group
- (iii) the plane of the amido group in the intermediate should be able to lie perpendicular to the trigonal plane of the cobalt
- (iv) there should be five-membered rings on either side of this group to hold it in position, and
- (v) there should be monodentate amines or a six-membered chelate occupying the remaining equatorial site in the intermediate, so that there is minimal strain.

In order to provide further insight into the geometrical influences on these effects we have measured the base hydrolysis rate constants for a series of $[\text{CoCl}(\text{triamine})(\text{diamine})]^{2+}$ complexes where the triamines are tacn or dien and the diamines are en, tn, or amp. The former triamine coordinates exclusively facially and the latter diamine allows the incorporation of a coordinated pyridine ligand in a diamine chelate, (Fig. 6.2).

Figure 6.2 Base hydrolysis rate constants ($M^{-1}s^{-1}$) for various Co(III) Pentaammines



Anation reactions are those in which a coordinated water molecule is replaced by an anion. The usual order of reactivity of $[\text{Co}^{\text{III}}(\text{pentaammine})\text{X}]^{\text{n+}}$ complexes is $\text{Br}^- > \text{Cl}^- > \text{H}_2\text{O} > \text{N}_3^- > \text{OH}^-$ ^{140,141}, and unusual results are reported herein.

In the current investigation two aspects of the labilization of the axial ligand are explored, the base hydrolysis of the $[\text{Co}^{\text{III}}\text{chloropentaammine}]^{2+}$ complex ions, and some preliminary data on the anation reactions of the corresponding $[\text{Co}^{\text{III}}\text{aquapentaammine}]^{3+}$ complex is also provided. Although much attention has been paid to the substitution and anation reactions of these inert metal complexes¹⁴⁵⁻¹⁴⁷, controversy over the mechanism, be it dissociative (D) or interchange dissociative (I_d), still remains. Elegant mixed-anion competition studies of Jackson *et al*¹⁴⁸ on the reaction of $(\text{NH}_3)_5\text{CoX}^{\text{n+}}$ have emphasized the existence of the five-coordinate intermediate $[(\text{NH}_3)_5\text{Co}]^{3+}$ in these substitution reactions.

Owing to the stability of these complexes in both acidic and basic media we have been able to examine the reaction of $[\text{Co}(\text{OH}_2)(\text{bicycloN}_5)]^{3+}$ (bicycloN₅ = 1,5,8,12,15-pentaazabicyclo[10.5.2]nonadecane) with SCN^- and $[\text{Co}(\text{OH}_2)(\text{tacn})(\text{en})]^{3+}$ with SCN^- and Br^- as a function of pH. Thiocyanate ion was chosen because of the large change in the absorption spectrum in the 300nm region associated with the formation of these complexes.

Very little information is available for even simple

[Co^{III}aquapentammine]³⁺ complexes, and most studies on anation reactions have been made under conditions below pH-3 to ensure the aqua and not the hydroxo complex is the predominant form of the reactant. To our knowledge there are no well documented data for the pH dependence of such anation reactions.¹⁴⁵⁻¹⁴⁷

6.2 Results and Discussion

6.2.1 Electronic Absorption Spectra

Six-coordinate Co^{III} complexes are invariably low spin and diamagnetic (¹A_{1g} ground term) with the exception of some fluorides¹⁴⁹.

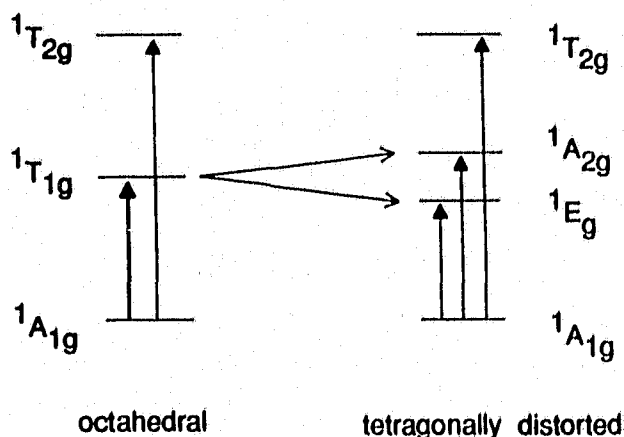


Figure 6.5 Splitting of energy levels for Co^{III} complexes

In general, for octahedral Co^{III}pentaammine complexes there exist two main ligand-field transitions, ¹T_{1g} ← ¹A_{1g} and ¹T_{2g} ← ¹A_{1g} at ca. 500nm and 350nm respectively. In some instances the lower energy transition is split by the tetragonal distortion of the complex¹⁵⁰ (Figure 6.5). The electronic absorption data for various Co^{III}pentaammine

complexes are given in Table 6.2.

For each of the complexes listed in Table 6.2, the shifts to higher energies of the ${}^1T_{1g} \leftarrow {}^1A_{1g}$ transition, in general, follow the expected trend of the spectrochemical series of the changing ligand. Increasing energies are in the order $Cl^- < Br^- < OH^- < NCS^- < OH_2$.

COMPLEX	${}^1T_{1g} \leftarrow {}^1A_{1g}$	${}^1T_{2g} \leftarrow {}^1A_{1g}$	Ref.
<i>mer</i> -exo(H) - Co(dien)(dapo)Cl ²⁺	540(61); 486(82)	375(75)	a
<i>mer</i> -exo(H) - Co(dien)(dapo)OH ²⁺	490(106)	350(91)	a
<i>mer</i> -exo(H) - Co(dien)(dapo)NCS ²⁺	485(254)	-	a
<i>mer</i> -exo(H) - Co(dien)(dapo)(OH ₂) ³⁺	473(91)	352(74)	a
Co(tacn)(en)Cl ²⁺	523(80); 480(sh)	362(78)	b
Co(tacn)(en)OH ²⁺	494(82)	362(76)	b
Co(tacn)(en)Br ²⁺	510(57) 460(sh)	316(sh)	b
Co(tacn)(en)NCS ²⁺	491(119)	307(sh)	b
Co(tacn)(en)OH ₂ ³⁺	493(135)	354(sh)	b
Co(bicycloN ₅)Cl ²⁺	553(80) 484(sh)	377(106)	b
Co(bicycloN ₅)OH ²⁺	506(126)	342(235)	b
Co(bicycloN ₅)Br ²⁺	515(68)	348(sh)	b
Co(bicycloN ₅)NCS ²⁺	506(214)	318(sh)	b
Co(bicycloN ₅)OH ₂ ³⁺	513(75); 469(sh)	353(102)	b

Table 6.2 Electronic absorption data for Co^{II}pentaammine complexes. a=Ref.140, b=this work. All spectra were recorded in aqueous solution (I=1.0M NaClO₄).

6.2.2 Stereochemical Assignments

Only one isomer is expected (and found) for each of $[\text{CoCl}(\text{tacn})(\text{diammine})]^{2+}$, diammine = en, tn, amp. Although amp is an unsymmetrical bidentate ligand, the symmetry of the facially coordinated tacn requires that the end-for-end isomers are equivalent (Figure 6.2).

This is not the case for $[\text{CoCl}(\text{dien})(\text{amp})]^{2+}$ since there are three topological forms for the (dien)(bidentate) combination sfac, ufac, and mer, and non-equivalent, end-for-end isomers of amp in the ufac and mer situations. Within the two mer combinations, the secondary N-H proton can be either adjacent to, or remote from the coordinated chloro ligand (Figure 6.3). In the present study two isomeric forms have been isolated where the dien is in the ufac configuration, but it was not possible to make an absolute assignment. Similarly in the mer series, the isomers with the secondary N-H proton remote from the coordinated chloro ligand are most likely, but a more definite assignment is awaited. The mer isomer shown in Figure 6.3 would be of considerable interest since Co^{III} complexes with pyridine coordinated trans to a chloro leaving group are rare.¹⁴⁷

In the case of the cobalt(III)bicyclopentaamine complex, while there is no crystallographic evidence for the structure, the ^{13}C NMR spectrum (Figure 6.4) displaying seven lines is consistent with a single isomeric form of square pyramidal conformation of the ligand identified. This structure has

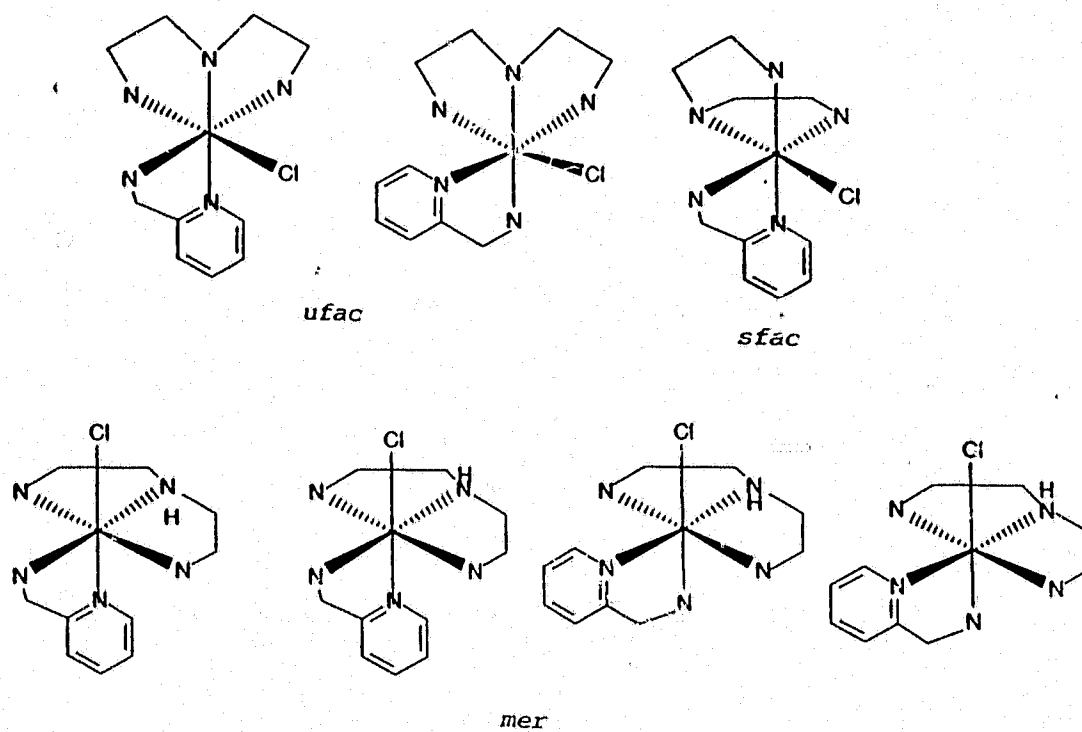
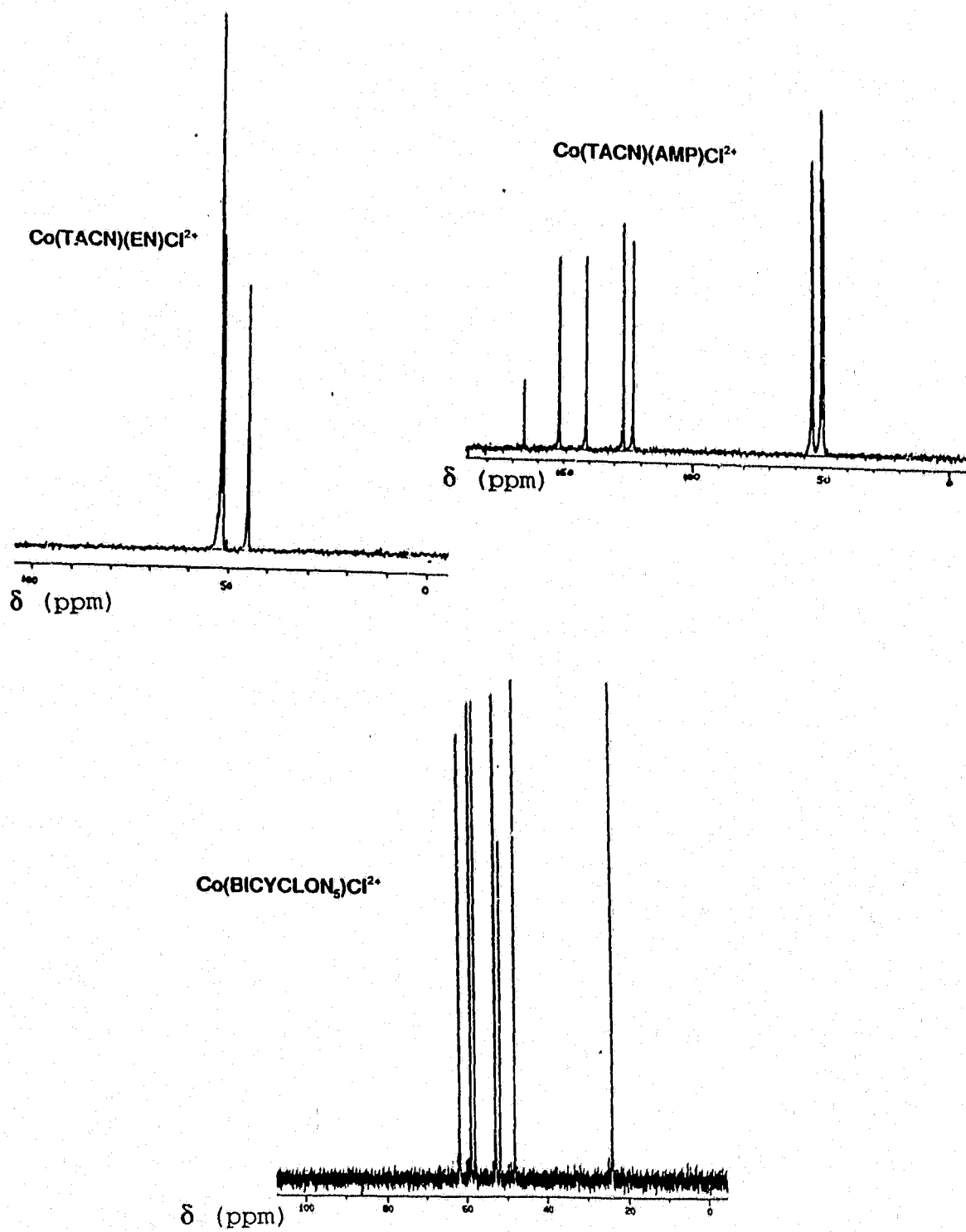
Figure 6.3 Possible isomers of $[\text{Co}(\text{dien})(\text{amp})\text{Cl}]^{2+}$ 

Figure 6.4 ^{13}C NMR spectra of $[\text{Co}(\text{diammine})(\text{triammine})\text{Cl}]^{2+}$ complex ions in D_2O .



been observed previously for the corresponding copper(II) complex. In the present instance, the conformation of the cyclam ring is *trans I* (Figure 6.2). Previous studies have shown a different geometry for the cobalt(III) complex of the precursor ligand to the macrobicyclic,¹⁵¹ but in this case there is a flexibility of the pendant arms to coordinate such that the chloro ligand is located *trans* to a tertiary amine. In the fully developed macrobicyclic the geometry is consistent with the chloro ligand being adjacent to two secondary amines and *trans* to the third.

6.2.3 Base Hydrolysis

In order to avoid the problems of converting pH to $[\text{OH}^-]$ in high ionic strength media¹⁵² that are inherent in the use of buffers or a pH-stat, the base hydrolysis rates were measured using stopped flow techniques in the $[\text{OH}^-]$ range of 5 - 250 mM ($I=1.0 \text{ M}$, NaClO_4), $[\text{Co}^{\text{III}}] \sim 0.1 \text{ mM}$. With the present apparatus reactions with halflives of $< 5 \text{ ms}$ may be measured easily, so that k_{OH} values of $> 1.4 \times 10^5 \text{ M}^{-1}\text{s}^{-1}$, may be evaluated using the most dilute OH^- solution. Where possible, a range of $[\text{OH}^-]$ concentrations was used to check the linearity and zero intercept of the $[\text{OH}^-]$ vs. k_{obs} plot, and the plot for $\text{Co}(\text{tacn})(\text{en})(\text{Cl})^{2+}$ is shown in Figure 6.6. These data are presented in Table 6.3. Activation parameters (Table 6.4) were evaluated from the temperature variation of k_{OH} .

The base hydrolysis reaction (5) is a reaction between



two ions of different charge and is thus expected to exhibit a negative salt effect¹⁵³. Since it is frequently useful to compare values of k_{OH} from one N_5 system to another¹³², it is important to take this effect into consideration. Ionic strengths of 0.1 and 1.0 M (NaClO_4) are often used and for a number of the systems described here we have measured k_{OH} under both conditions. The relationship of k_{OH} ($I=0.1$ M) $\sim 2.2k_{\text{OH}}$ ($I=1.0$ M) appears to hold quite well (Table 6.4).

Although in complex ions such as $[\text{CoCl}(\text{tacn})(\text{en})]^{2+}$ or $[\text{CoCl}(\text{tacn})(\text{tn})]^{2+}$, the facial geometry of the macrocycle provides two secondary amine centres *cis* to the chloro group, a feature known to promote reaction, they cannot readily become "flat" in the trigonal plane of the intermediate. For this reason, these species display few of the acceleratory influences outlined in the introduction. The observed base hydrolysis rates of less than $50 \text{ M}^{-1} \text{ s}^{-1}$ ¹³⁵ are consistent with this consideration. The *tn* complex reacts about four times faster than the *en* analogue, a ratio similar to that found for other systems¹³⁶ where the replacement of a five membered ring by a six membered unit (i.e. *tn* for *en*) induced increases of about ten-fold in base hydrolysis rates, (Figure 6.2). The incorporation of the pyridine ligand in the five membered chelate ring does cause a 16-fold increase in rate relative to

Figure 6.6 Base hydrolysis of $[\text{Co}(\text{tacn})(\text{en})\text{Cl}]^{2+}$ as a function of $[\text{OH}^-]$.

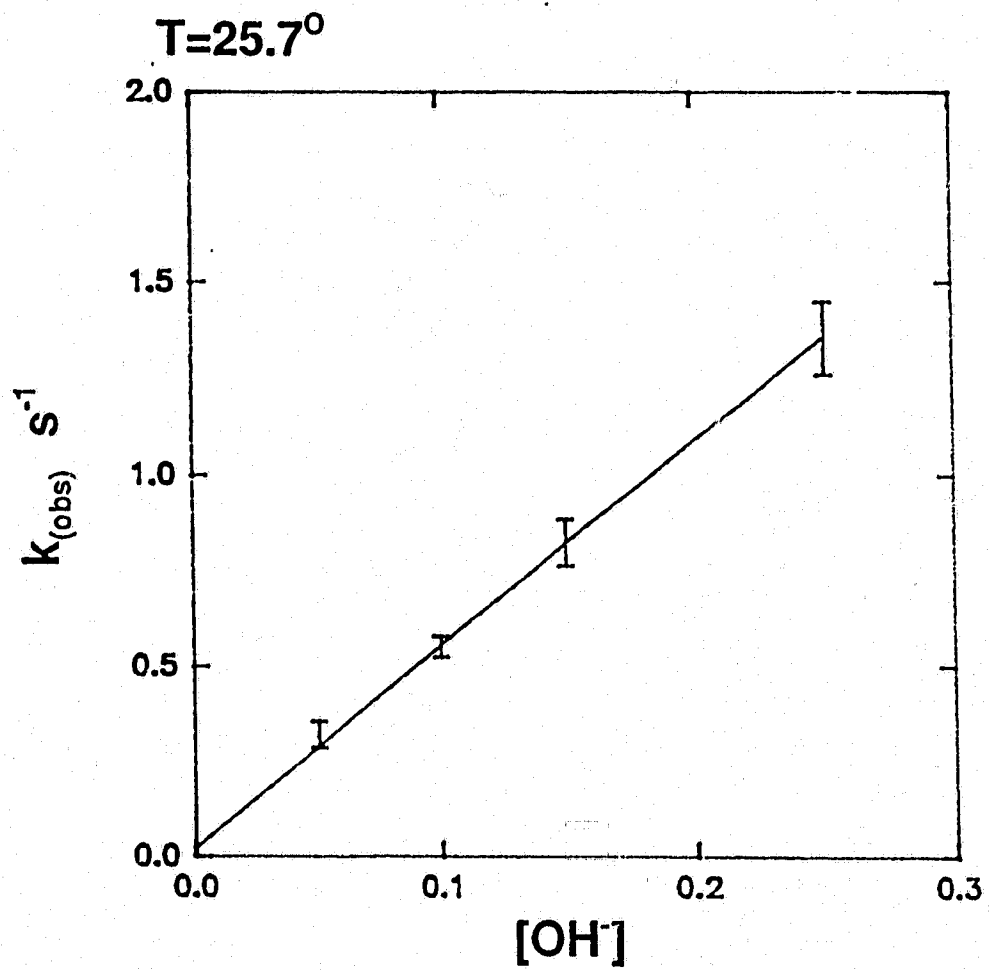


Table 6.3 Observed Rate Constants for the Base Hydrolysis of [Co(III)chloropentaammine]²⁺ Complexes at I = 1.0 M NaClO₄.

(triammine) / (diammine)	T (°C)	[NaOH] (M)	k _{obs} (s ⁻¹)	k _{OH} (M ⁻¹ s ⁻¹)
(tacn) (en)	39.0	0.25	5.93±0.3	23.7±1.2
		0.15	3.40±0.07	22.6±0.4
		0.10	2.24±0.1	22.4±1.0
			Mean	22.9±1.0
	25.0	0.05 ^a	0.483±0.013	9.66±0.26
	24.6	0.25	0.874±0.02	3.50±0.08
		0.15	0.497±0.012	3.31±0.08
		0.10	0.361±0.013	3.61±0.13
			Mean	3.47±0.1
	11.4	0.25	0.142±0.006	0.568±0.02
		0.15	0.0841±0.006	0.561±0.04
		0.10	0.0565±0.003	0.565±0.03
		Mean	0.564±0.03	
(tacn) (tn)	39.0	0.25	20.5±0.5	82.0±2
		0.15	14.7±0.8	98.0±5
		0.10	9.70±0.2	97.0±2
		0.05	4.16±0.2	83.2±4
			Mean	90.0±5

Table 6.3 (cont'd)

	25.0	0.05 ^a	2.03±0.12	40.6±2.4
	24.7	0.15	2.23±0.08	14.8±0.5
		0.10	1.57±0.07	15.7±0.7
		Mean		15.2±0.4
	11.4	0.25	0.595±0.01	2.38±0.04
		0.15	0.360±0.01	2.40±0.07
		0.10	0.240±0.01	2.40±0.10
		0.04	0.0970±0.005	2.42±0.12
		Mean		2.40±0.01
(tacn) (amp)	39.0	0.15	45.5±1.0	303±7
		0.10	31.4±1.0	314±10
		Mean		308±5
	25.0	0.05 ^a	7.69±0.26	154±5
		0.10	6.33±0.31	63.3±3
		0.05	3.54±0.07	70.8±1
		Mean		66.7±2
	11.2	0.15	1.85±0.09	12.3±0.6
		0.10	1.21±0.04	12.1±0.4
		Mean		12.2±0.4
I- (dien) (amp)	38.6	0.15	129±8	860±53
	25.0	0.05 ^a	16.7±0.54	334±11
		0.15	27.7±1.2	184±8
		0.10	18.1±1.2	181±12
		Mean		183±3

Table 6.3 (cont'd)

	11.2	0.25	9.26±0.7	37.0±3
		0.15	6.09±0.6	40.6±4
		0.10	4.02±0.3	40.2±3
			Mean	39.3±1
II-(dien) (amp)	38.6	0.15	196±14	1310±93
	25.0	0.05 ^a	38.1±0.75	762±15
		0.15	53.8±1.2	359±8
	11.2	0.15	11.4±0.3	76.0±2
		0.10	8.18±0.2	81.8±2
			Mean	78.9±1
bicycloN ₅	25.0	0.005	15.0	3000

^a I=0.1M (NaClO₄)

en in the $[\text{CoCl}(\text{tacn})(\text{diamine})]^{2+}$ pair, but this is not as great as found for $\text{cis-}[\text{CoCl}(\text{en})_2\text{py}]^{2+}$ relative to $\text{cis-}[\text{CoCl}(\text{en})_2(\text{MeNH}_2)]^{2+}$ (30-fold)¹³⁹. However, in the $\text{ufac-}[\text{CoCl}(\text{dien})(\text{diamine})]^{2+}$ (en, amp) pair (Figure 6.2), the relative rate increase is again 30-fold. If folding to a five-coordinate intermediate is important in base hydrolysis, then tacn is less flexible than dien and consequently somewhat less reactive. Nevertheless, the nature of the diamine also contributes to the distortion since the (tacn)(diamine):(dien)(diamine) rate ratios increase in the order en, tn, amp (Figure 6.2).

The two $\text{ufac-}[\text{CoCl}(\text{dien})(\text{amp})]^{2+}$ isomers base hydrolyse relatively rapidly, one about twice as fast as the other (Table 6.4) and end-for-end interchange in this system (py trans to secondary N-H / py trans to NH_2 , Figure 6.3) appears to have little influence.

The activation parameters obtained (Table 6.4) are normal for this type of reaction¹⁵⁴, with ΔH^\ddagger in the 70-90 kJ mol^{-1} range and large positive entropies of activation ($\Delta S^\ddagger = +50$ to $+95 \text{ J K}^{-1} \text{ mol}^{-1}$). This positive entropy change is in contrast to the large negative ΔS^\ddagger usually observed for acid hydrolysis¹⁵³, and has been used as evidence to support the concept of a hydroxide ion dependent pre-equilibrium process in the mechanism.¹⁵⁴

Table 6.4

Second Order Rate Constants for the Base Hydrolysis of some [Co(III)chloropentaammine]²⁺ Complexes at 25.0°C.

(triamine)/ (diamine)	I ^a	k _{OH} ^b	ΔH ^{†c}	ΔS ^{†d}	Ref.
sfac-(dien)(en)	0.1	4.71	87.0	+72	4
ufac-(dien)(en)	0.1	23.9	86.3	+62	4
mer-(dien)(en)	0.1	18,700	93.2	+149	4
(tacn)(en)	0.1	9.66			
	1.0	3.66	96.6±0.8	+90±2.4	e
(tacn)(tn)	0.1	40.6			
	1.0	15.8	94.4±1.2	+94±4	e
(tacn)(amp)	0.1	154			
	1.0	66.7	83.3±1.2	+69±4	e
ufac-I-(dien)	0.1	334			
(amp)	1.0	183	79.6±1.7	66±6	e
ufac-II-(dien)	0.1	762			
(amp)	1.0	359	73.3±1.3	+50±5	e
bicycloN ₅	1.0	3000			e

^a = [NaClO₄]/M ^b = M⁻¹ s⁻¹ ^c = kJ mol⁻¹

^d = J K⁻¹ mol⁻¹ ^e = present study.

An interesting result is that obtained for the macrobicyclic complex which appears to conform to almost all the requirements for ready hydrolysis¹⁴⁷. However, despite the presence of two secondary amines *cis* to the leaving chloro ligand with the ability to become planar, the rate is only about an order of magnitude greater than for the *ufac*-(dien)(amp) isomers. This may be the result of failure to achieve the optimum geometry with respect to the five coordinate intermediate. In the most favourable circumstances, second order rate constants ranging from 3×10^4 to $5 \times 10^5 \text{ M}^{-1} \text{ s}^{-1}$ have been determined¹³⁵. The rearrangement from a square pyramidal configuration is accompanied by some steric strain which is exhibited in the lower rate observed in the present study. Although it is possible to construct a model of a trigonal bipyramidal intermediate, there is strong evidence for hydrogen-hydrogen interactions and overall strain especially around the Co - N amido linkage which is somewhat shorter than other metal -nitrogen bonds.^{155,156} Further examples of such effects may be available through the use of other macrobicycles now being synthesised in this laboratory and elsewhere.

6.2.4 Anation Reactions

Split cell reactions were performed in each case; $[\text{Co}(\text{tacn})(\text{en})(\text{OH}_2)]^{3+} + [\text{SCN}^-]$ or $[\text{Br}^-]$ and $[\text{Co}(\text{bicycloN}_5)(\text{OH}_2)]^{3+} + [\text{SCN}^-]$ or $[\text{Br}^-]$, at pH ~ 2 to determine

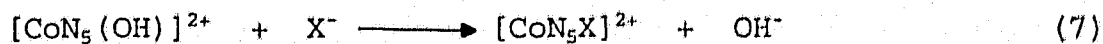
the wavelength to monitor the reactions. In the case of the $[\text{Co}(\text{bicycloN}_5)(\text{OH}_2)]^{3+} + [\text{Br}^-]$ reaction there was no significant change in the uv-visible spectrum at the concentrations being used so no further experiments were carried out. The split cell reaction of $[\text{Co}(\text{bicycloN}_5)(\text{OH}_2)]^{3+} + [\text{SCN}^-]$ showed three isosbestic points at 542, 476, and 407nm with the largest change in the spectrum occurring at $\sim 320\text{nm}$. The $[\text{Co}(\text{tacn})(\text{en})(\text{OH}_2)]^{3+}$ showed one isosbestic point at 425 nm with thiocyanate and with bromide ion there were two isosbestic points at 557 and 370nm. The largest change in the absorption spectrum in both instances occurred at $\sim 300\text{nm}$.

The rates of anation with thiocyanate ion were measured at varying pH's (in the range of pH-2 - pH-10) for both complexes studied, $[\text{Co}(\text{tacn})(\text{en})(\text{OH}_2)]^{3+}$ and $[\text{Co}(\text{bicycloN}_5)(\text{OH}_2)]^{3+}$. The pH dependence on the rate of anation with bromide ion was also measured for the $[\text{Co}(\text{tacn})(\text{en})(\text{OH}_2)]^{3+}$ complex.

At low pH (below the pK_a of the coordinated water), the anation reaction is a reaction between:



and at higher pH (above the pK_a of the coordinated water), it is a reaction of the hydroxo complex:



To avoid any back reaction low Co^{III} concentrations ($\sim 10^{-4}$ M) and high anion concentrations (0.6 M) were used (pseudo-first order conditions).

It is considered intuitive that the rate of reaction (6) should proceed much faster than reaction (7). A kinetic-titration plot of the type shown in Figure 6.7 is expected, with the typical sigmoidal curve.

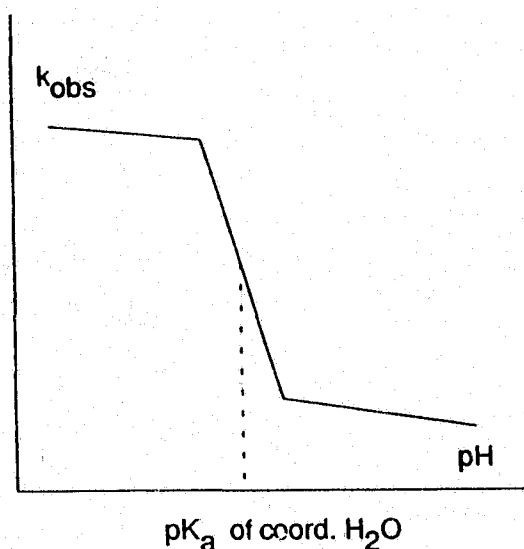


Figure 6.7. Expected shape of the kinetic-titration of the Co^{III} pentaamine complexes studied.

Surprisingly, this is not what is observed in either of the two complexes studied here as is shown in Figures 6.8 and 6.9.

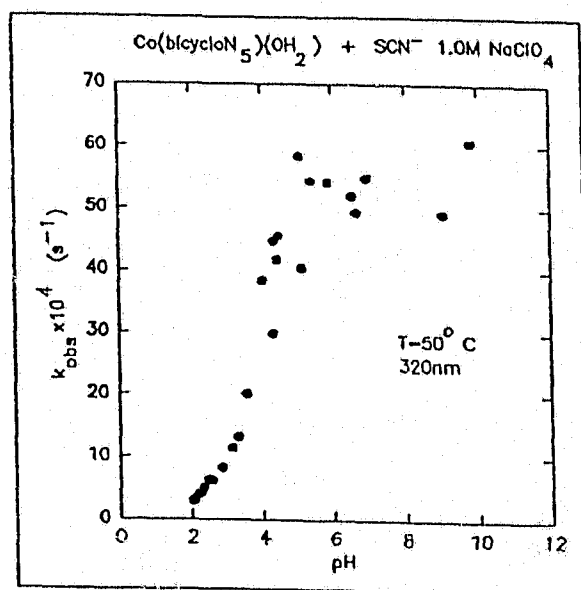


Figure 6.8 Kinetic Titration plot Co(bicycloN₅)(OH₂)³⁺

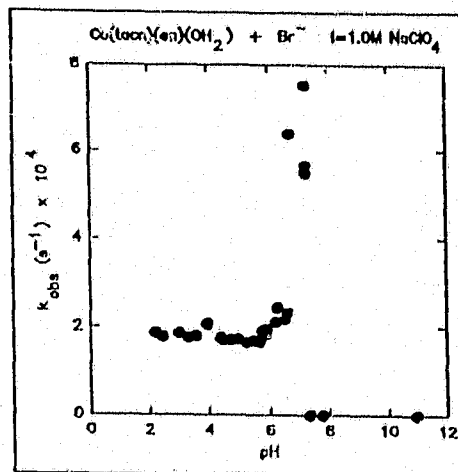
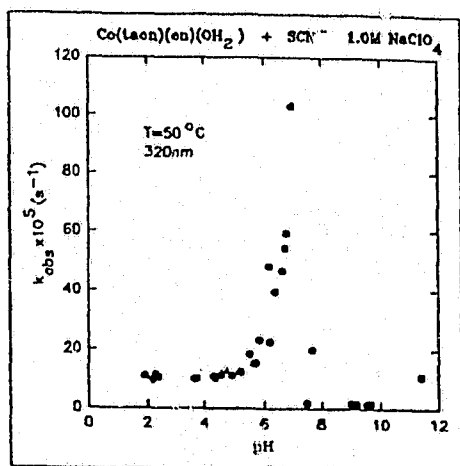


Figure 6.9 Kinetic titration of Co(tacn)(en)(OH₂)³⁺ a) + NCS⁻
b) + Br⁻

Rather, the opposite occurs in which the rate of reaction (7) is faster than the rate of reaction (6). Although the kinetic titration plot for $[\text{Co}(\text{bicycloN}_5)(\text{OH}_2)]^{3+}$ is the reverse of that expected, it does represent the sigmoidal shape (the scatter at high pH is unexplainable). This is not the case however with the $[\text{Co}(\text{tacn})(\text{en})(\text{OH}_2)]^{3+}$ complex, where the observed reaction rate reaches a maximum (at pH=6.97 (SCN^-) and at pH=7.22 (Br^-)) and falls abruptly to a negligible reaction rate at higher pH.

A recent report¹⁴¹ has shown a similar result to that of the macrobicycle complex on the azide-anation of *mer*- $\text{Co}(\text{dien})(\text{dapo})(\text{OH}_2)^{3+}$ where *dien* = N-(2-aminoethyl)ethane-1,2-diamine and *dapo* = 1,3-diaminopropan-2-ol. The results for the *mer*-*exo*(H) isomer are shown graphically in Figure 6.10. Through the azide-anation and racemization of pure *mer*-*exo*(H) and *mer*-*endo*(H), the authors interpreted this phenomenon as an internal conjugate base mechanism involving an amino-hydroxo/aminato-aqua tautomerism. The reaction mechanism given is shown in Scheme 6.2.

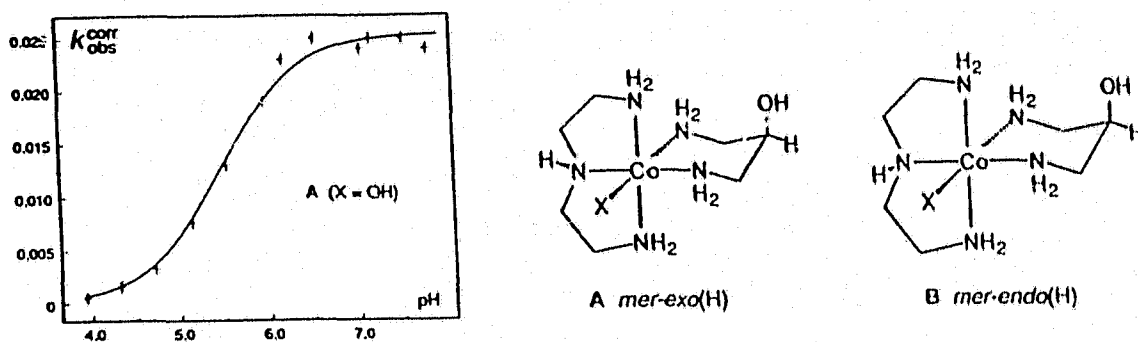
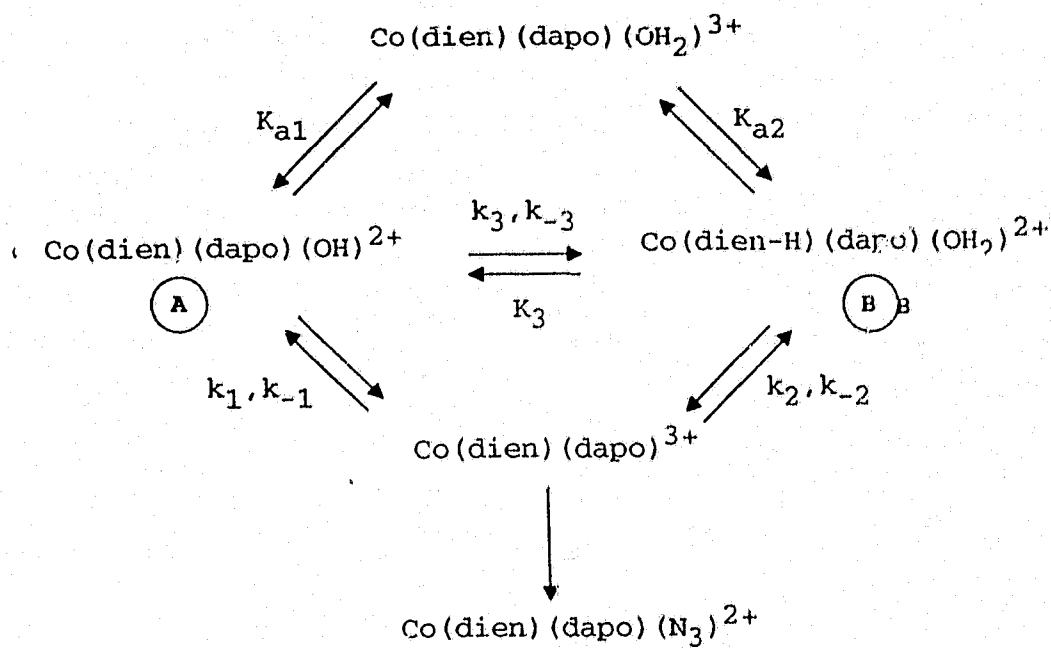


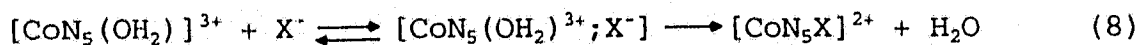
Figure 6.10 Rate data for the azide-ation of $\text{Co(dien)(dapo)(OH}_2\text{)}^{3+}$



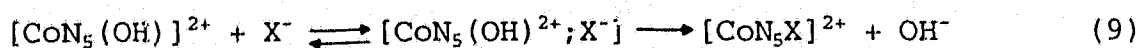
Scheme 6.2 Reaction Mechanism for Azide Anation of $\text{Co(dien)(dapo)(OH}_2\text{)}^{3+}$

As shown, the reaction is a base catalysed substitution of $[\text{Co}(\text{dien})(\text{dapo})(\text{OH}_2)]^{3+}$ where deprotonation occurs predominately at the secondary amine N-H of dien.

The $[\text{SCN}^-]$ dependence on the observed rate of reaction is non-linear (linearity results when $1/k_{\text{obs}}$ vs. $1/[\text{SCN}^-]$ is plotted; see Figure 6.11) in the case of $[\text{Co}(\text{bicycloN}_5)(\text{OH}_2)]^{3+}$. The usual implication of this type of result is that there is a fast pre-equilibrium before the substitution step. Inherently, this is considered to be an ion-pair forming equilibrium:



and consequently, the same pre-equilibrium for the hydroxo complex will result in the same mechanism:



This mechanism does not account for the enhanced reactivity of the hydroxo complex however, but the internal conjugate base mechanism is feasible.

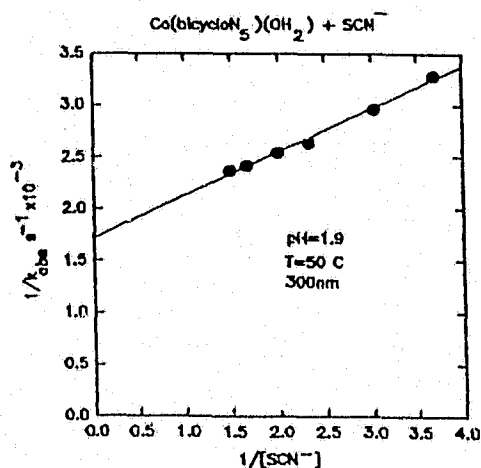
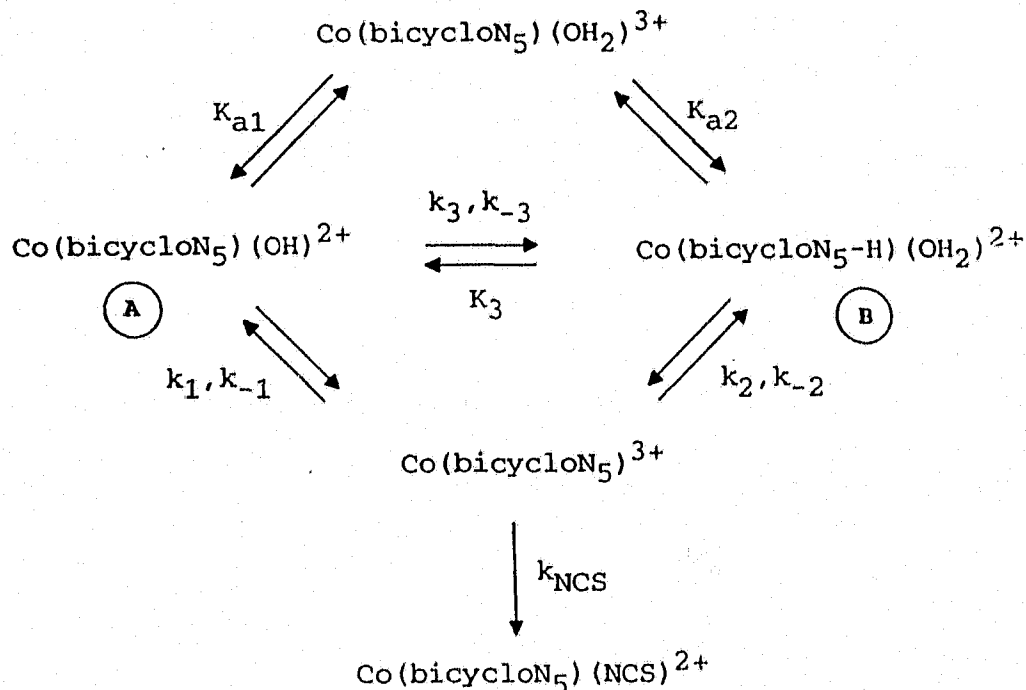


Figure 6.11 $[\text{SCN}^-]$ Dependence on rate of the $\text{Co}(\text{bicycloN}_5)(\text{OH}_2)^{3+}$ Anation

As demonstrated by Comba et al.¹⁴¹ a similar reaction scheme involving a deprotonated secondary N-H amine can be drawn for the $[\text{Co}(\text{bicycloN}_5)(\text{OH}_2)]^{3+}$ anation reaction.



Scheme 6.3 Reaction Mechanism for $[\text{NCS}]^-$ Anation of $\text{Co}(\text{bicycloN}_5)(\text{OH}_2)^{3+}$.

The site of deprotonation is the main issue in Schemes 6.2 and 6.3. The two possible sites of deprotonation are at the coordinated H_2O ($\text{p}K_a=3.8$ for $[\text{Co}(\text{bicycloN}_5)(\text{OH}_2)]^{3+}$ based on spectrophotometric titration and kinetic titration plot; $\text{p}K_a=5.5$ for $[\text{Co}(\text{dien})(\text{dapo})(\text{OH}_2)]^{3+}$) or at the coordinated secondary amine ($\text{p}K_a\sim 15$)¹⁵⁷. The equilibrium, K_3 , is estimated for $[\text{Co}(\text{bicycloN}_5)(\text{OH}_2)]^{3+}$ as

$$K_3 = K_{a2}/K_{a1} \sim 10^{-12}$$

The rate law for the hydroxo complex is in the form

$k_{\text{obs}} = k_1 + k_2K_3$ where k_1 is the slow substitution of the hydroxo complex (A) ($\sim 10^{-6}\text{s}^{-1}$) and k_2K_3 represents reaction from the tautomer (B). Although (B) is in extremely low concentration ($K \sim 10^{12}$) it must be sufficiently reactive to overcome the k_1 term. This is demonstrated in the fact that the observed rate of anation is $\sim 5 \times 10^{-3}\text{s}^{-1}$. Thus, the internal conjugate base mechanism is a viable reaction pathway.

Again, as is shown in Figure 6.12 the inverse plot of k_{obs} vs. $[\text{SCN}^-]$ is linear for the reaction with $[\text{Co}(\text{tacn})(\text{en})(\text{OH}_2)]^{3+}$.

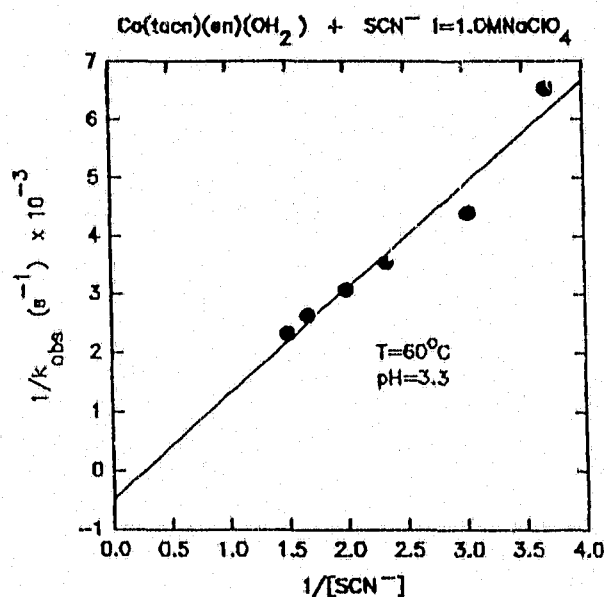
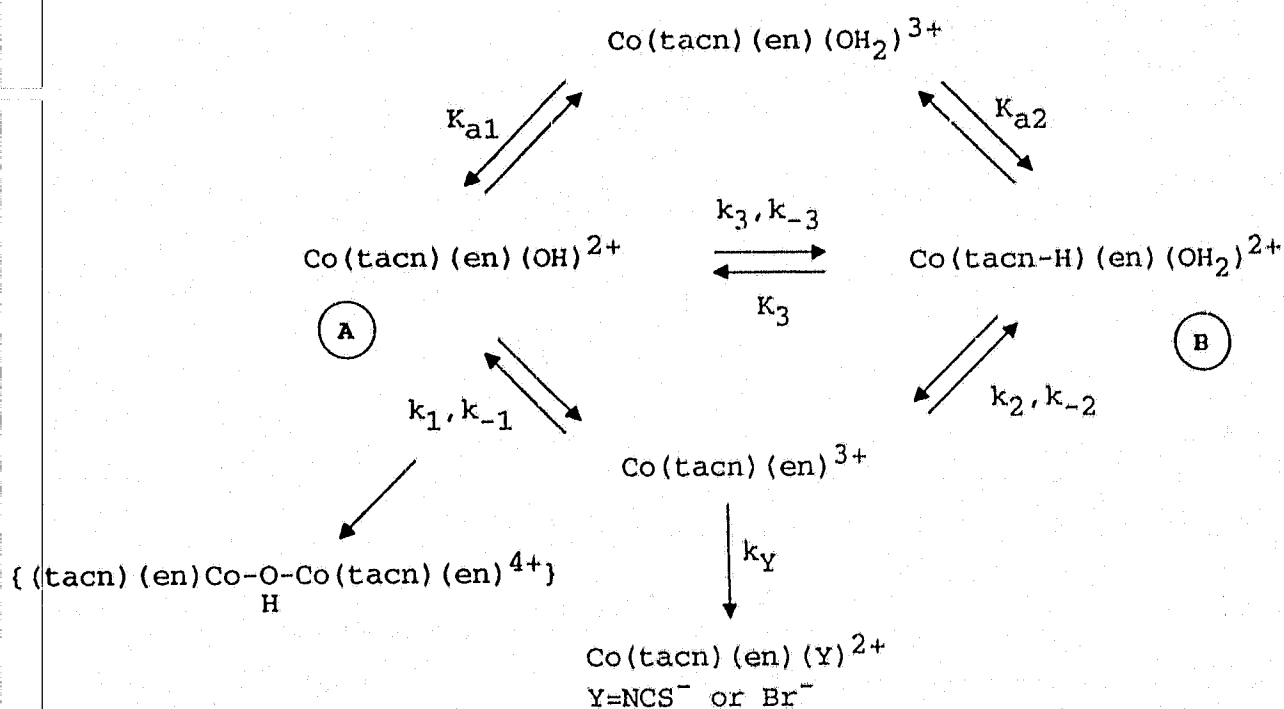


Figure 6.12 $[\text{SCN}^-]$ Dependence on Rate of Anation of $\text{Co}(\text{tacn})(\text{en})(\text{OH}_2)^{3+}$.

The kinetic titration results show an initial increase of the rate of anation with increasing pH, however above a certain

hydroxide ion concentration the reaction is no longer observed.

This can be argued in terms of an internal conjugate base mechanism, reflecting the initial increase in the observed rate. There must also be an alternate path for the reaction intermediate so that the site of anation is blocked. Of course one can only speculate as to the origin of this pathway, however one possibility is the formation of a hydroxo-bridged dimer. A possible reaction pathway is given in Scheme 6.4.



Scheme 6.4 Possible reaction mechanism for the anation of $[\text{Co}(\text{tacn})(\text{en})(\text{OH}_2)]^{3+}$ complex.

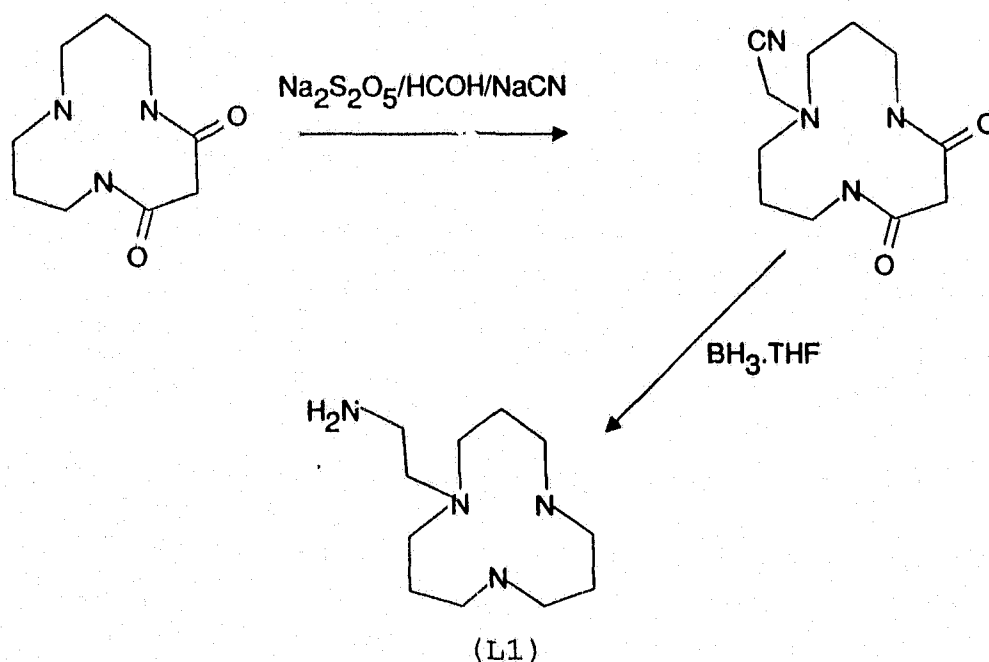
The fact that there is no substantial increase in the rate of base hydrolysis of this complex leads one to the conclusion that there is little stabilization of the five-coordinate intermediate, $[\text{Co}(\text{tacn})(\text{en})]^{3+}$. Once past the pK_a of the coordinated water, the complex essentially exists as the hydroxo complex, and any of the five-coordinate intermediate either reacts in the back reaction to form the hydroxo complex or combines with a molecule of the hydroxo complex to form the dimer.

This mechanism is speculative and is by no means to be taken as the only possibility. However, it just represents a possible pathway indicating a "blockage" of the site of anation by formation of a dimer. It does, also, leave the door open for further interesting investigations to be undertaken.

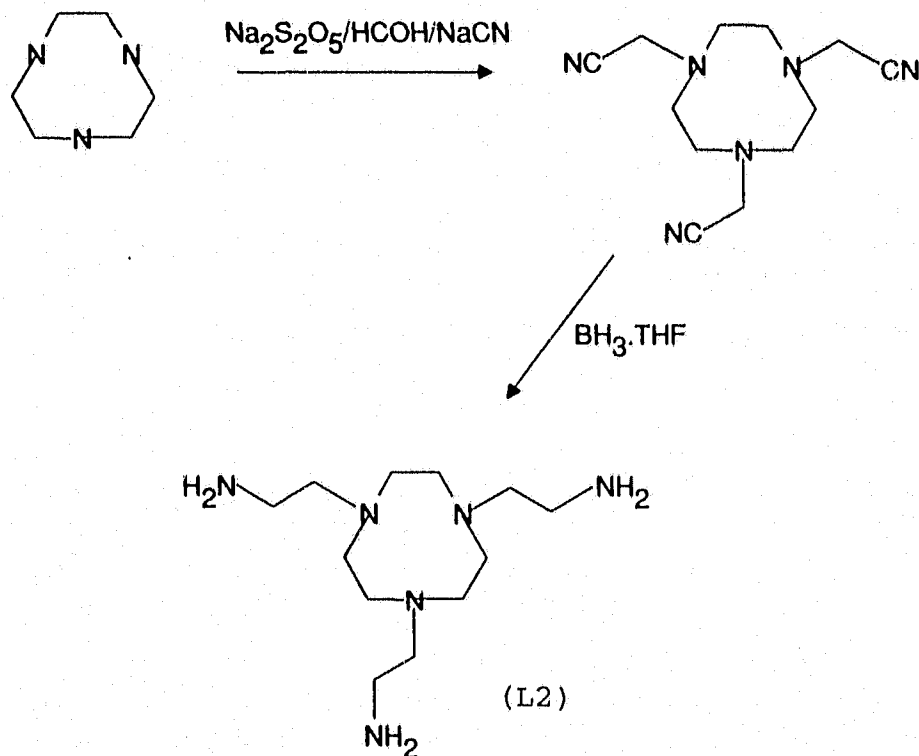
CHAPTER 7
CONCLUSIONS AND SUGGESTIONS FOR FUTURE STUDIES

The series of taptacn-catecholate ligands were successfully synthesized and serve as models for the naturally occurring enterobactin. The use of these compounds as binucleating ligands appears to be unsuccessful. This led to the preparation of the taetacn-catecholate ligands where there is one less methylene in the pendant arm of the tacn ring.

The synthetic route used to obtain these ligands opens the door for the preparation of a multitude of pendant arm aza-macrocycles with an ethylene bridge between the donor atoms. The synthesis is simple and the products are easily purified by conventional methods. At the time this work was near completion, an article appeared on the mono-functionalization of 1,5,9-triazacyclododecane¹⁵⁸. The authors report the synthesis of L1 by the following reaction;



It would be worthwhile to try and use this same procedure to prepare taetacn (L2),



which should again be an improvement on the Strecker synthesis used by Sargeson.

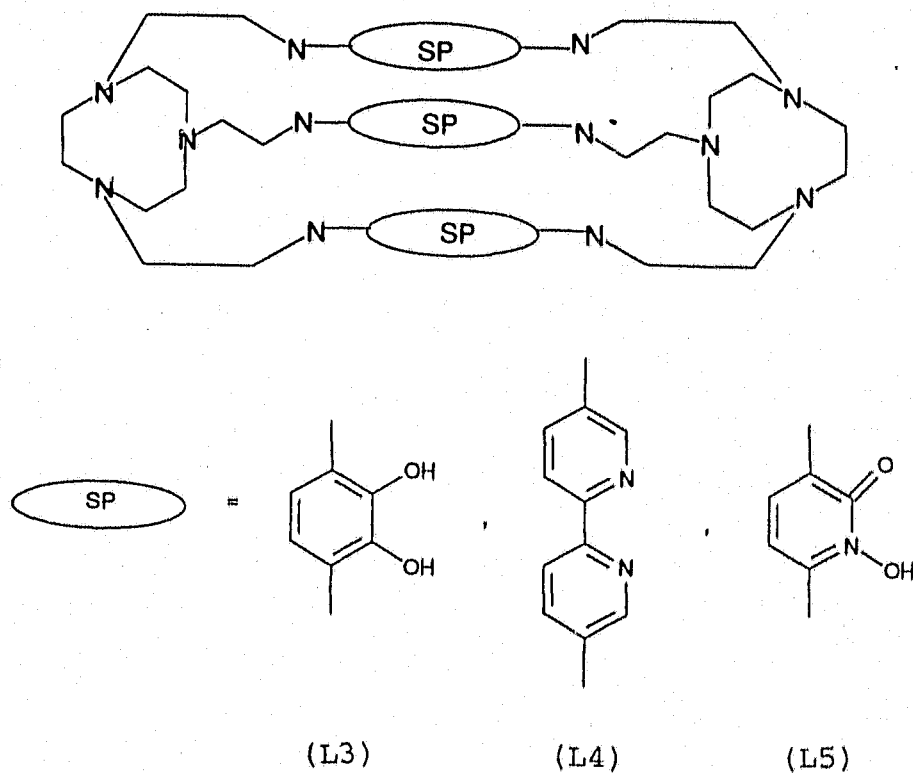
The taetacn-catecholate ligands also serve as models for enterobactin. Future studies should include the measurement of formation constants via spectrophotometric and potentiometric methods. These compounds do form binuclear complexes with first row transition metal ions. Owing to the low solubility of these compounds they are extremely difficult to characterize. Perhaps future work should lead to the preparation of similar compounds, where instead of using tris-

catechol moieties to coordinate the second transition metal, groups such as bipyridine or hydroxypyridinone should be incorporated into these systems. This would eliminate the need for deprotection of the methylated catechols (using BBr_3), consequently permitting complex formation without the presence of a base.

The ligands described in this work contain 10-12 donor atoms with a highly negative charge (6-). Their use as lanthanide complexing agents should be investigated, since the lanthanides are known to have high coordination numbers. The search for these types of reagents has increased because of their use as MRI (magnetic resonance imaging) agents and their use as lanthanide shift reagents.

The tren-based catecholate ligands show promise for binucleating ability. Future studies should include the isolation of these binuclear complexes, although limitations will be encountered due to solubility problems. The presence of only four amines as opposed to six, as in the previous systems, may make it easier to develop a method of isolating these compounds. Again, extrapolating these systems with hydroxypyridinones instead of catecholate moieties would be fruitful.

The obvious place to proceed with these ligands would be to "cap" the other end of the catechol moieties, or in general, prepare ligands L3, L4, and L5 shown below;

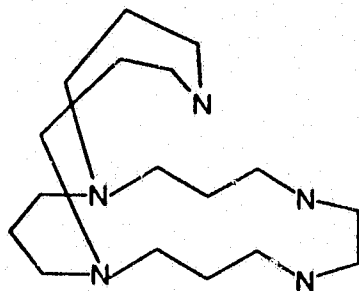


These cage ligands would have the potential of forming trinuclear transition metal complexes.

The base hydrolysis and anation reactions of $[\text{Co}^{\text{III}}(\text{pentammine})(\text{X})]^{n+}$ complexes proceeded as expected. The data provide evidence supporting the formation of a five-coordinate intermediate in the reaction mechanism (thus, a dissociative pathway).

The base hydrolysis of $[\text{Co}^{\text{III}}(\text{bicycloN}_5)(\text{Cl})]^{2+}$ was not as fast as expected, due to strain imparted on the ligand in the formation of the five-coordinate intermediate. Future studies should include the preparation of a similar macrobicyclic (2).

ligand (L6), where the strain on formation of the tbp intermediate would be minimized;



(L6)

REFERENCES

1. J. Huheey in Inorganic Chemistry 3rd Ed., Harper & Row, Publishers, Inc., New York, 1983
2. B. Douglas, D. H. McDaniel, and J. J. Alexander in Concepts and Models of Inorganic Chemistry 2nd Ed., John Wiley & Sons, Inc., USA, 1983
3. J. C. Bailar in Coordination Chemistry, Vol. 1, ACS Monograph 168, A. E. Martell, Ed., Van Nostrand Reinhold Co., 1971, ix.
4. L. Pauling in The Nature of the Chemical Bond, 3rd Ed., Cornell University Press, New York, 1960
5. H. Bethe, *Ann. Physik.*, 1929, 5, 135
- 6a. J. H. Van Vleck, *Phys. Rev.*, 1932, 41, 208
b. J. H. Van Vleck, *J. Chem. Phys.*, 1935, 3, 803, 807
7. R. S. Mulliken, *Phys. Rev.*, 1932, 40, 55
8. S. Ahrland, J. Chatt, N. R. Davies, *Quart. Rev.*, 1958, 12, 265
9. R. G. Pearson, *J. Am. Chem. Soc.*, 1963, 85, 3533
10. G. Schwarzenbach, *Helv. Chem. Acta*, 1952, 35, 2344
11. D. K. Cabbiness, D. W. Margerum, *J. Am. Chem. Soc.*, 1969, 91, 6540
12. J. M. Lehn, *Acc. Chem. Res.*, 1978, 11, 49
13. R. D. Hancock, A. E. Martell, *Comments Inorg. Chem.*, 1988, 6, 237
14. A. W. Adamson, *J. Am. Chem. Soc.*, 1954, 76, 1578
15. D. J. Cram, T. Kaneda, R. C. Helgeson, S. B. Brown, C. B. Knobler, E. Maverick, K. N. Trueblood, *J. Am. Chem. Soc.*, 1985, 107, 3645
16. D. H. Busch, K. Farmery, V. Goedken, V. Katovik, A. C. Melnyk, C. R. Sperati, N. Tokel, *Adv. Chem. Ser.*, 1971, 100, 44
17. G. A. Melson in Coordination Chemistry of Macrocyclic Compounds, Plenum Press, New York, 1979
18. N. F. Curtis, *J. Chem. Soc.*, 1960, 4409
19. M. C. Thompson, D. H. Busch, *Chem. Eng. News*, 1962, 57

20. B. Bosnich, C. K. Poon, M. L. Tobe, *Inorg. Chem.*, 1965, **4**, 1102
21. E. K. Barefield, F. Wagner, A. W. Herlinger, A. R. Dahl, *Inorg. Synth.*, 1975, **16**, 210
22. T. J. Atkins, J. E. Richman, W. F. Oettle, *Org. Synth.*, 1978, **58**, 86
23. J. E. Richman, T. J. Atkins, *J. Am. Chem. Soc.*, 1974, **96**, 2268
24. J. S. Bradshaw, K. E. Krakowiak, R. M. Izatt, *J. Heterocyclic Chem.*, 1989, **26**, 1431
25. J. S. Bradshaw, K. E. Krakowiak, R. M. Izatt, D. J. Zamecka-Krakowiak, *Tet. Lett.*, 1990, **31**, 1077
26. K. E. Krakowiak, J. S. Bradshaw, R. M. Izatt, *J. Org. Chem.*, 1990, **55**, 3364
27. K. E. Krakowiak, J. S. Bradshaw, W. Jiang, N. Kent Dalley, G. Wu, R. M. Izatt, *J. Org. Chem.*, 1991, **56**, 2675
28. L. F. Lindoy in The Chemistry of Macrocyclic Ligand Complexes, Cambridge University Press, 1989
29. J. P. Collman, R. A. Gagne, C. A. Reed, T. H. Halbert, G. Lang, W. T. Robinson, *J. Am. Chem. Soc.*, 1975, **97**, 1427
30. a) C. Gueutin, D. Lexa, M. Momenteau, J.-M. Savéant, F. Xu, *Inorg. Chem.*, 1986, **25**, 4294
b) J. Almoy, J. E. Baldwin, R. L. Dyer, M. Peters, *J. Am. Chem. Soc.*, 1975, **97**, 226, 227
31. N. F. Curtis, D. F. Cook, *J. Chem. Soc. Chem. Comm.*, 1967, 962
32. D. C. Olson, J. Vasilevskis, *Inorg. Chem.*, 1969, **8**, 1611
33. *ibid.*, 1971, **10**, 463
34. *ibid.*, 1971, **10**, 1228
35. A. J. Blake, R. O. Gould, A. J. Holder, T. I. Hyde, A. J. Lavery, M. O. Odulate, M. Schröder, *J. Chem. Soc. Chem. Comm.*, 1987, 118
36. A. McAuley, T. W. Whitcombe, *Inorg. Chem.*, 1988, **27**, 3090
37. B. L. Vallee, R. J. P. Williams, *Prog. Nat. Acad. Sci.*, 1968, **59**, 498

38. S. J. Rodgers, PhD Dissertation, University of California, Berkeley, 1985
39. M. M. Jones, *Comments Inorg. Chem.*, 1992, **13**, 91
40. P. M. May, R. A. Bulman, *Prog. Med. Chem.*, 1983, **20**, 225
41. K. N. Raymond, G. Müller, B. F. Matzanke, *Curr. Top. Chem.*, 1984, **123**, 49
42. J. B. Neilands, *Nature*, 1952, **74**, 4846
43. K. N. Raymond, *Coord. Chem. Rev.*, 1990, **105**, 135
44. T. M. Garrett, M. E. Cass, K. N. Raymond, *J. Coord. Chem.*, 1992, **25**, 241
45. J. R. Pollack, J. B. Neilands, *Biochem. Biophys. Res. Commun.*, 1970, **38**, 989
46. T. B. Karpishin, K. N. Raymond, *Angew. Chem. Int. Ed. Eng.*, 1992, **31**, 466
47. T. B. Karpishin, T. M. Dewey, K. N. Raymond, *J. Am. Chem. Soc.*, 1993, **115**, 1842
48. A. E. Martell, R. J. Motekaitis, I. Murase, L. F. Sala, R. Stoldt, C. Y. Ng, H. Rosenkrantz, J. J. Metterville, *Inorg. Chim. Acta*, 1987, **138**, 215
49. K. N. Raymond, G. E. Freeman, M. J. Kappel, *Inorg. Chim. Acta*, 1984, **94**, 193
50. F. L. Weitzl, K. N. Raymond, W. L. Smith, T. R. Howard, *J. Am. Chem. Soc.*, 1978, **100**, 1170
51. J. Xu, T. D. P. Stack, K. N. Raymond, *Inorg. Chem.*, 1992, **31**, 4903
52. Y. Tor, J. Libman, A. Shanzer, S. Lifson, *J. Am. Chem. Soc.*, 1987, **109**, 6517
53. A. W. Coleman, C-C. Ling, M. Miocque, *Angew. Chem. Int. Ed. Eng.*, 1992, **31**, 1381
54. J. Kiggen, F. Vögtle, S. Franken, H. Puffé, *Tetrahedron*, 1986, **42**, 1959
55. T. M. Garrett, T. J. McMurray, M. W. Hosseini, Z. E. Reyes, F. E. Hahn, K. N. Raymond, *J. Am. Chem. Soc.*, 1991, **113**, 2965

56. S. J. Rodgers, C-W. Lee, C. Y. Ng, K. N. Raymond, *Inorg. Chem.*, 1987, **26**, 1622
57. C. Seel, F. Vögtle, *Angew. Chem. Int. Ed. Eng.*, 1992, **31**, 528
58. L. D. Loomis, K. N. Raymond, *Inorg. Chem.*, 1991, **30**, 906
59. W. R. Harris, F. L. Weitzl, K. N. Raymond, *J. Chem. Soc. Chem. Comm.*, 1979, 177
60. T. M. Garrett, T. J. McMurray, M. W. Hosseini, Z. E. Reyes, F. E. Hahn, K. N. Raymond, *J. Am. Chem. Soc.*, 1991, **113**, 2965
61. T. B. Karpishin, T. D. P. Stack, K. N. Raymond, *J. Am. Chem. Soc.*, 1993, **115**, 182
62. T. J. McMurray, M. W. Hosseini, T. M. Garrett, F. E. Hahn, Z. E. Reyes, K. N. Raymond, *J. Am. Chem. Soc.*, 1987, **109**, 7196
63. G. H. Searle, R. J. Geue, *Aust. J. Chem.*, 1984, **37**, 959
64. G. W. Bushnell, D. G. Fortier, A. McAuley, *Inorg. Chem.*, 1988, **27**, 2626
65. F. L. Weitzl, K. N. Raymond, W. L. Smith, T. R. Howard, *J. Am. Chem. Soc.*, 1978, **100**, 1170
66. W. Siedel, H. Nahn, *Chem. Abstr.*, 1958, **52**, 5471
67. A. Hammershoi, A. M. Sargeson, *Inorg. Chem.*, 1983, **22**, 3554
68. S. J. Rodgers, C. W. Lee, C. Y. Ng, K. N. Raymond, *Inorg. Chem.*, 1987, **26**, 1622
69. D. G. Fortier, A. McAuley, *J. Am. Chem. Soc.*, 1990, **112**, 2640
70. T. J. Atkins, J. E. Richman, W. F. Oettle, *Org. Synthesis*, 1978, **58**, 86
71. G. H. Searle, R. J. Geue, *Aust. J. Chem.*, 1984, **37**, 959
72. D. G. Fortier, Ph.D Dissertation, University of Victoria, 1988
73. G. W. Bushnell, D. G. Fortier, A. McAuley, *Inorg. Chem.*, 1988, **27**, 2626
74. S. J. Rodgers, C. W. Lee, C. Y. Ng, K. N. Raymond, *Inorg.*

Chem., 1987, **26**, 1622

75. T. W. Greene, Protective Groups in Organic Synthesis, John Wiley & Sons, Inc., 1981

76.a) M. Node, K. Nishide, K. Fuji, E. Fujita, *J. Org. Chem.*, 1980, **45**, 4275

b) M. Node, K. Nishide, M. Sai, K. Ichikawa, K. Fuji, E. Fujita, *Chem. Lett.*, 1979, 97

77. E. J. Corey, S. Bhattacharyya, *Tet. Lett.*, 1977, **45**, 3919

78. A. Avdeef, S. R. Sofen, T. L. Bregante, K. N. Raymond, *J. Am. Chem. Soc.*, 1978, **100**, 5362

79. B. F. Anderson, D. A. Buckingham, G. B. Robertson, J. Webb, K. S. Murray, P. E. Clark, *Nature*, 1976, **262**, 722

80. R. C. Hider, A. R. Mohd-Nor, J. Silver, I. E. G. Morrison, L. V. C. Rees, *J. Chem. Soc. Dalton Trans.*, 1981, 609

81. D. J. Gordon, R. F. Fenske, *Inorg. Chem.*, 1982, **21**, 2916

82. M. D. Hall, R. F. Fenske, *Inorg. Chem.*, 1972, **11**, 768

83. T. B. Karpishin, M. S. Gebhard, E. I. Solomon, K. N. Raymond, *J. Am. Chem. Soc.*, 1991, **113**, 2977

84. R. J. Geue, T. W. Hambley, J. M. Harrowfield, A. M. Sargeson, *J. Am. Chem. Soc.*, 1984, **106**, 5478

85. I. I. Creaser, J. M. Harrowfield, A. J. Herlt, A. M. Sargeson, J. Springborg, R. J. Geue, M. R. Snow, *J. Am. Chem. Soc.*, 1977, **99**, 3181

86. N. Sutin, *Acc. Chem. Res.*, 1982, **15**, 275 and *Prog. Inorg. Chem.*, 1983, **30**, 441

87. A. Hammershoi, A. M. Sargeson, *Inorg. Chem.*, 1983, **22**, 3554

88. A. M. Sargeson, *Pure & Appl. Chem.*, 1986, **58**, 15

89. S. J. Rodgers, C. W. Lee, C. Y. Ng, K. N. Raymond, *Inorg. Chem.*, 1987, **26**, 1622

90. T. B. Karpishin, M. S. Gebhard, E. I. Solomon, K. N. Raymond, *J. Am. Chem. Soc.*, 1991, **113**, 2977

91. T. M. Garrett, T. J. McMurray, M. W. Hosseini, Z. E. Reyes, F. E. Hahn, K. N. Raymond, *J. Am. Chem. Soc.*, 1991, **113**, 2965

92. A. Hammershoi, A. M. Sargeson, *Inorg. Chem.*, 1983, **22**, 3554
93. M. Takahashi, S. Takamoto, *Bull. Chem. Soc. Japan*, 1977, **50**, 3413
94. A. Bevilacqua, R. I. Gelb, W. B. Hebard, L. J. Zompa, *Inorg. Chem.*, 1987, **26**, 2699
95. K. Wieghardt, U. Bossek, P. Chaudhuri, W. Herrmann, B. C. Menke, J. Weiss, *Inorg. Chem.*, 1982, **21**, 4308
96. B. A. Sayer, J. P. Michael, R. D. Hancock, *Inorg. Chim. Acta*, 1983, **77**, L63
97. S. Buoen, J. Dale, P. Groth, J. Crane, *J. Chem. Soc. Chem. Comm.*, 1977, 1172
98. R. W. Hay, M. P. Pujari, W. T. Moodie, S. Craig, D. T. Richens, A. Perotti, M. Ungaretti, *J. Chem. Soc. Dalton Trans.*, 1987, 2605
99. M. Bochenska, J. F. Biernat, J. S. Bradshaw, *J. Incl. Phen. and Mol. Recog. Chem.*, 1991, **10**, 19
100. J. S. Bradshaw, K. E. Krakowiak, R. M. Izatt, *Tet. Lett.*, 1989, **30**, 803
101. K. E. Krakowiak, J. S. Bradshaw, N. K. Dalley, W. Jiang, R. M. Izatt, *Tet. Lett.*, 1989, **30**, 2897
102. K. E. Krakowiak, J. S. Bradshaw, R. M. Izatt, *J. Org. Chem.*, 1990, **55**, 3364
103. K. Wieghardt, W. Schmidt, W. Herrmann, H. J. Küppers, *Inorg. Chem.*, 1983, **22**, 2953
104. K. Wieghardt, I. Tolksdorf, W. Herrmann, *Inorg. Chem.*, 1985, **24**, 1230
105. T. N. Margulis, L. J. Zompa, *J. Chem. Soc. Chem. Comm.*, 1979, 430
106. R. C. Hider, A. R. Mohd-Nor, J. Silver, J. B. Neilands, *J. Inorg. Chem.*, 1982, **17**, 205
107. T. B. Karpishin, T. M. Dewey, K. N. Raymond, *J. Am. Chem. Soc.*, 1993, **115**, 1842
108. G. A. Melson, B. N. Figgis, Eds., Transition Metal Chemistry Vol. 8, Marcel Dekker, Inc., New York, 1982

109. J. E. Pure, G. Schwarzenbach, *Helv. Chem. Acta*, 1950, **33**, 963
110. J. M. Lehn, *Pure & Appl. Chem.*, 1980, **52**, 2441
111. J. M. Lehn, *Pure & Appl. Chem.*, 1977, **49**, 857
112. R. J. Motekaitis, A. E. Martell, J. M. Lehn, E. Watanabe, *Inorg. Chem.*, 1982, **21**, 4253
113. B. Dietrich, J. Guilhem, J. M. Lehn, C. Pascard, E. Sonveaux, *Helv. Chem. Acta*, 1984, **67**, 91
114. V. McKee, M. R. J. Dorrity, J. F. Malone, D. Marrs, J. Nelson, *J. Chem. Soc. Chem. Comm.*, 1992, 383
115. S. Lui, L. Gelmini, S. J. Rettig, R. C. Thompson, C. Orvig, *J. Am. Chem. Soc.*, 1992, **114**, 6081
116. A. Smith, S. J. Rettig, C. Orvig, *Inorg. Chem.*, 1988, **27**, 3929
117. J. de Mendoza, E. Mesa, J.-C. Rodríguez-Ubis, P. Vazquez, F. Vögtle, P.-M. Windscheif, K. Rissanen, J. M. Lehn, D. Lilienbaum, R. Ziessel, *Angew. Chem. Int. Ed. Eng.*, 1991, **30**, 1331
118. M.-T. Youinou, J. Suffert, R. Ziessel, *Angew. Chem. Int. Ed. Eng.*, 1992, **31**, 775
119. T. J. McMurray, S. J. Rodgers, K. N. Raymond, *J. Am. Chem. Soc.*, 1987, **109**, 3451
120. S. J. Rodgers, C. W. Lee, C. Y. Ng, K. N. Raymond, *Inorg. Chem.*, 1987, **26**, 1622
121. S. Lui, L. Gelmini, S. J. Rettig, R. C. Thompson, C. Orvig, *J. Am. Chem. Soc.*, 1992, **114**, 6081
122. *Inorg. Chem.*, 1987, **26**, 1622
123. T. B. Karpishin, M. S. Gebhard, E. I. Soloman, K. N. Raymond, *J. Am. Chem. Soc.*, 1991, **113**, 2977
124. A. B. P. Lever in Inorganic Electronic Spectroscopy 2ndEd., Elsevier Science Publishers, The Netherlands, 1984
125. F. A. Cotton and G. Wilkinson in Advanced Inorganic Chemistry 3rdEd., John Wiley & Sons, Inc., USA, 1972
126. B. Douglas, D.H. McDaniel, J.J. Alexander Concepts and Models of Inorganic Chemistry 2ndEd., John Wiley & Sons,

Inc., 1983

127. H. Taube, *Chem. Rev.*, 1952, **50**, 69

128. J. Atwood, *Inorganic and Organometallic Reaction Mechanisms* Brooks/Cole, Monterey, Calif., 1985

129. R. van Eldik, *Comments Inorg. Chem.*, 1986, **5**(3), 135

130. D. R. Stranks, *Pure and Appl. Chem.*, 1974, **38**, 303

131. R. van Eldik, Y. Kitamura, C.P.P. Mac-Coll, *Inorg. Chem.*, 1986, **25**, 4252

132. F. J. Garrick, *Nature*, 1937, **109**, 507

133. R. G. Pearson and F. Basolo, *J. Amer. Chem. Soc.*, 1956, **78**, 4878

134. M. L. Tobe, *Advances in Inorganic and Bioinorganic Mechanisms* ed. A. G. Sykes, 1983, **2**, 1

135. R. A. Henderson and M. L. Tobe, *Inorg. Chem.* 1977, **16**, 2576

136. D. A. House and M. L. Tobe, *J. Chem. Soc., Dalton Trans.*, 1989, 853

137. E. Ahmed, C. Chatterjee, C. J. Cooksey, M. L. Tobe, G. Williams, M. Humanes, *J. Chem. Soc. Dalton Trans.*, 1989, 645

138. D.A.House, P.R.Norman, and R.W.Hay, *Inorg. Chim. Acta*, 1980, **45**, L117

139. J. McKenzie and D. A. House, *J. Inorg. Nucl. Chem.*, 1977, **39**, 1843

140. P. Comba, W.G. Jackson, W. Marty, L. Zipper, *Helv. Chem. Acta*, 1992, **75**, 1147

141. *ibid.*, *Helv. Chem. Acta*, 1992, **75**, 1172

142. A. A. Watson, M. Prinsep, and D. A. House, *Inorg. Chim. Acta*, 1986, **115**, 95

143. P. D. Ford, K.B.Nolan, and D.C.Povey, *Inorg. Chim. Acta*, 1982, **61**, 189

144. Lim Say Dong and D. A. House, *Inorg. Chim. Acta*, 1976, **19**, 23,

145. M. C. Ghosh, P. Bhattacharya and P. Banerjee, *Coord.*

Chem. Rev., 1988, 91, 1

146. P. A. Lay, *Comments Inorg. Chem.*, 1991, 11, 235

147. M. L. Tobe, *Comprehensive Coordination Chemistry*, eds. G. Wilkinson, R.D.Gillard and J.McCleverty, 1986, 1, 281

148. W. G. Jackson, B. C. McGregor and S. S. Jurrison, *Inorg. Chem.*, 1990, 29, 4677

149. A.B.P. Lever, "Inorganic Electronic Spectroscopy" 2ndEd. Elsevier Science Publishing Company, Inc., copyright 1984

150. F.A. Cotton and G. Wilkinson, "Advances in Inorganic Chemistry" 5thEd.

151. D.G.Fortier and A.McAuley, *J.Chem. Soc., Dalton Trans.*, 1991, 101

152. D. A. House *Coord. Chem. Rev.*, 1992, 114, 249

153. D. A. House, *Coord. Chem. Rev.*, 1977, 23, 223

154. R.J.Geue, T.W.Hambley, J.McB.Harrowfield, A.M.Sargeson, M.R.Snow, *J. Am. Chem. Soc.*, 1984, 106, 5478

155. H. B. Bürgi in Perspectives in Coordination Chemistry, eds. A. F. Williams, C. Floriani and A. Merbach, Verlag Helvetica Chimica Acta, Basel, 1992, 1-31 esp. p26

156. J. O. Edwards, F. Monacelli, G. Ortaggi, *Inorg. Chim. Acta*, 1974, 11, 47 (section 8)

157. D.M. Goodall, M.H. Hardy, *J. Chem. Soc. Chem. Comm.*, 1975, 919

158. S. C. Rawle, A. J. Clarke, P. Moore, N. A. Alcock, *J. Chem. Soc. Dalton Trans.*, 1992, 2755